

INFLUENCE OF RICE BRAN WAX AND POLICOSANOL ORGANOGELS ON
PHYSICOCHEMICAL PROPERTIES OF WATER-IN-OIL EMULSION



A Dissertation Submitted in Partial Fulfillment of the Requirements
for the Degree of Doctor of Philosophy in Food Technology

Department of Food Technology

Faculty of Science

Chulalongkorn University

Academic Year 2018

Copyright of Chulalongkorn University

อิทธิพลของออร์แกโนเจลจากไคร์ข้าวและออร์แกโนเจลจากพอลิโคซานอลต่อสมบัติทางเคมีกายภาพ
ของอิมัลชันชนิดน้ำในน้ำมัน



วิทยานิพนธ์นี้เป็นส่วนหนึ่งของการศึกษาตามหลักสูตรปริญญาวิทยาศาสตรดุษฎีบัณฑิต
สาขาวิชาเทคโนโลยีทางอาหาร ภาควิชาเทคโนโลยีทางอาหาร
คณะวิทยาศาสตร์ จุฬาลงกรณ์มหาวิทยาลัย
ปีการศึกษา 2561
ลิขสิทธิ์ของจุฬาลงกรณ์มหาวิทยาลัย

ศวรรษญา ปั่นตลสุข : อิทธิพลของออร์แกนเจลจากไขรำข้าวและออร์แกนเจลจากพอลิโคซานอลต่อสมบัติทางเคมีกายภาพของอิมัลชันชนิดน้ำในน้ำมัน. (

INFLUENCE OF RICE BRAN WAX AND POLICOSANOL ORGANOGELS ON PHYSICO-CHEMICAL PROPERTIES OF WATER-IN-OIL EMULSION) อ.ที่ปรึกษาหลัก : ผศ. ดร.ศศิกานต์ กู้พงษ์ศักดิ์

ไขรำข้าวพอกสี (BRX) เป็นผลพลอยได้จากกระบวนการทำบริสุทธิ์น้ำมันรำข้าว ซึ่งสามารถใช้ประโยชน์สำหรับอุตสาหกรรมอาหารได้หลากหลาย และสามารถนำมาใช้เพื่อเป็นสารก่อเจลในอาหารได้ งานวิจัยนี้มีวัตถุประสงค์ที่จะศึกษาการผลิตออร์แกนเจล และอิมัลชันชนิดน้ำในน้ำมัน (W/O emulsion) จาก BRX และพอลิโคซานอล (PC) ที่สกัดได้จาก BRX ศึกษาคุณสมบัติทางเคมีกายภาพ และการเปลี่ยนแปลงสมบัติระหว่างการเก็บรักษาที่อุณหภูมิ 4 และ 30°C นาน 90 วัน ลักษณะผลึกของ BRX มีลักษณะแบบรูปร่างคล้ายเข็ม (needle-like) และมีการจัดเรียงตัวแบบ beta prime- และ beta-form BRX มีอุณหภูมิในการเกิดผลึก (T_c) และอุณหภูมิในการหลอมเหลว (T_m) สูง เท่ากับ 71.47 และ 73.99°C ตามลำดับ ออร์แกนเจลจากไขรำข้าวพอกสี (BRXOs) ผลิตโดยผสมน้ำมันรำข้าวกับ BRX ที่ระดับความเข้มข้นของไขร้อยละ 3, 5, 7 และ 9 โดยน้ำหนัก BRXO สามารถเกิดเจลได้ที่ระดับความเข้มข้นของไขต่ำสุดเท่ากับ ร้อยละ 5 โดยระดับความเข้มข้นของไขที่เดิมมีอิทธิพลต่อคุณสมบัติทางเคมีกายภาพของ BRXO ได้แก่ ระยะเวลาในการเกิดเจล ความสามารถในการกักเก็บน้ำมัน สี ปริมาณไขมันแข็ง (SFC) ลักษณะเนื้อสัมผัส ลักษณะผลึก และพฤติกรรมทางความร้อน ($p < 0.05$) เมื่อนำ BRXO ที่ระดับความเข้มข้นไข ร้อยละ 9 มาผลิตอิมัลชัน (EO) พบว่า EO มีความคงตัวที่ดี ระหว่างการเก็บรักษาตัวอย่าง BRXO และ EO มีความคงตัวต่อการเปลี่ยนแปลงคุณภาพทางเคมีกายภาพ และแสดงให้เห็นถึงความคงตัวต่อการเกิดออกซิเดชัน เมื่อพิจารณาค่าเปอร์ออกไซด์ (PV) และค่า Thiobarbituric acid reactive substances (TBARS) พบว่า BRXO และ EO มีความคงตัวต่อการเกิดออกซิเดชันมากกว่าน้ำมันรำข้าว (RO) และอิมัลชันที่ไม่มีการเติมออร์แกนเจล (E) ตามลำดับ ปริมาณพอลิโคซานอล (PC) ที่สกัดจาก BRX เท่ากับร้อยละ 31.21 โดยน้ำหนัก องค์ประกอบของ PC ที่สกัดได้ ประกอบด้วย tetracosanol (C24), hexacosanol (C26), octacosanol (C28), และ triacosanol (C30) เท่ากับ 58.63, 75.93, 125.50 และ 143.24 มิลลิกรัม/กรัม ตัวอย่าง ตามลำดับ PC มีค่า T_c และ T_m เท่ากับ 79.53 และ 78.15°C ผลึกของ PC มีลักษณะคล้ายเข็ม และจัดเรียงตัวแบบ beta prime- และ beta-form ผลิตออร์แกนเจลจาก PC (PCOs) โดยผสมน้ำมันรำข้าวกับสารสกัด PC ที่ระดับความเข้มข้นร้อยละ 12.5, 13 และ 15 โดยน้ำหนัก พบว่า ที่ความเข้มข้นของ PC ร้อยละ 15 ให้ออร์แกนเจลที่มีคุณภาพทางเคมีกายภาพที่ดีที่สุด คุณลักษณะของ PCOs เปลี่ยนแปลงตามความเข้มข้นของ PC ($p < 0.05$) เช่นเดียวกับลักษณะของ BRXO ลักษณะผลึกของ PCOs เป็นแบบ dendrite-like และเปลี่ยนเป็นแบบ spherulite เมื่อระยะเวลาการเก็บรักษาเพิ่มขึ้น อิมัลชันที่ผลิตจาก PCO ที่ความเข้มข้น PC ร้อยละ 15 (PCE) และอิมัลชันที่ผสม PCO และ BRXO ในอัตราส่วน 50:50 (PCM) แสดงให้เห็นว่าอิมัลชันมีความคงตัว และมีโครงสร้างที่แข็งแรง ตัวอย่าง PCO, PCE และ PCM มีความคงตัวต่อการเกิดออกซิเดชันสูง โดยพบว่าค่า PV ของ PCE และ PCM สูงกว่า EO ขณะที่ TBARS มีค่าที่ใกล้เคียงกัน

สาขาวิชา เทคโนโลยีทางอาหาร
ปีการศึกษา 2561

ลายมือชื่อนิสิต
ลายมือชื่อ อ.ที่ปรึกษาหลัก

5672907023 : MAJOR FOOD TECHNOLOGY

KEYWORD: BLEACHED RICE BRAN WAX, POLICOSANOL, ORGANOGEL, WATER-IN-OIL EMULSION

Sawanya Pandolsook :

INFLUENCE OF RICE BRAN WAX AND POLICOSANOL ORGANOGELS ON PHYSICOCHEMICAL PROPERTIES OF WATER-IN-OIL EMULSION. Advisor: Asst. Prof. Sasikan Kupongsak, Ph.D.

Bleached rice bran wax (BRX) is a by-product of rice bran oil purification. It has a variety of uses in the food industry and can also be utilized as a gelling agent in food. This research aims to study the production of organogels and water-in-oil emulsion (W/O emulsion) from BRX and policosanol (PC) extracted from BRX. Physicochemical properties and changes in properties during storage at 4°C and 30°C for 90 days were evaluated. Regarding morphology, BRX appeared to have a needle-like shape and an arrangement with beta prime- and beta- form formations. BRX had a high crystalline temperature (T_c) and melting temperature (T_m) of 71.47°C and 73.99°C, respectively. Bleached rice bran wax organogels (BRXO) were prepared by mixing rice bran oil with BRX at wax concentrations of 3, 5, 7 and 9 wt%. BRXO formed gels at a minimum concentration of 5 wt%. The concentration of added wax influenced physicochemical properties of BRXO, including gelation time, oil binding capacity, colour, solid fat content, textural characteristics, crystal morphology and thermal behaviour ($p < 0.05$). The BRXO with a 9% wax concentration was used to produce an emulsion (EO). It was found that the EO showed good stability. During storage, the BRXO and EO were stable with respect to changes in physicochemical properties and exhibited oxidative stability. When peroxide (PV) and thiobarbituric acid reactive substances (TBARS) were considered, it was found that the BRXO and EO had higher oxidation stabilities than the rice bran oil (RO) and emulsion without added organogel (E), respectively. The yield of PC extracted from BRX was 31.21 wt%. Regarding the composition of PC extract, tetracosanol (C24), hexacosanol (C26), octacosanol (C28), and triacosanol (C30) accounted for 58.63, 75.93, 125.50 and 143.24 mg / g of sample, respectively. PC had T_c and T_m values of 79.53°C and 78.15°C. PC crystals had a needle-like shape and an arrangement with beta prime- and beta-form formations. Policosanol organogels (PCOs) were prepared by mixing rice bran oil with PC extract at concentrations of 12.5, 13 and 15 wt%. It was found that the PCO prepared using a 15% concentration of PC exhibited the best properties. The characteristics of PCOs were altered by PC concentration ($p < 0.05$) in the same manner as the characteristics of BRXO. With respect to crystal morphology, PCO showed dendrite-like crystals, changing to spherulite crystals as storage time increased. The emulsion produced from the PCO at a 15% concentration of PC (PCE) and the emulsion produced from PCO mixed with BRXO at a 50:50 ratio (PCM) showed emulsion stability and strong structure. The PCO, PCE and PCM were stable to oxidation. The PV of PCE and PCM had higher values than the EO but similar values to those of TBARS.

Field of Study: Food Technology

Student's Signature

Academic Year: 2018

Advisor's Signature

ACKNOWLEDGEMENTS

I would like to express my deepest gratitude to my advisor, Assistant Professor Dr. Sasikan Kupongsak, for valuable suggestions and great kindness throughout my doctoral degree pursuit. I am also deeply grateful to Dr. Daris Kuakpetoon, Assistant Professor Dr. Chidphong Pradititsuwan, Dr. Sirima Puangpraphant and Associate Professor Dr. Wanna Tungjaroenchai for their valuable suggestions.

I am grateful to Suan Dusit University for allowing me to pursue and providing a scholarship for my Ph.D. research in Food Technology in the Faculty of Science of Chulalongkorn University. I also wish to thank the Graduate School of Chulalongkorn University for providing a scholarship (the Overseas Academic Presentation Scholarship for Graduate Students) and financial support for this research from the 90th Anniversary of Chulalongkorn University Fund (the Ratchadaphiseksomphot Endowment Fund).

I am grateful to Mr. Pravit Santiwattana for providing support with respect to raw materials, and I also wish to thank Miss Tida Sirisukpornchai from Thai Edible Oil Co., Ltd., Thailand, for her assistance. I would additionally like to thank all staff members and friends in the Food Technology Department of Chulalongkorn University for their help, friendliness and encouragement throughout my studies.

Finally, I am especially grateful to my family and all of my friends for their emotional support and care during my studies.

Sawanya Pandolsook

TABLE OF CONTENTS

	Page
ABSTRACT (THAI).....	iii
ABSTRACT (ENGLISH).....	iv
ACKNOWLEDGEMENTS	v
TABLE OF CONTENTS	vi
LIST OF TABLES	viii
LIST OF FIGURES	x
CHAPTER I INTRODUCTION	1
CHAPTER II LITERATURE REVIEW	3
2.1 Organogels	3
2.2 Emulsion.....	12
2.3 Rice bran wax.....	17
2.4 Policosanol	22
CHAPTER III MATERIALS AND METHODS	27
3.1 Materials.....	27
3.2 Physical and chemical analysis of the raw material.....	27
3.3 Bleached rice bran wax organogels and water-in-oil emulsions.....	30
3.4 Policosanol organogels and water-in-oil emulsions	34
3.5 Statistical analysis.....	37
CHAPTER IV RESULT AND DISSCUSSION	38
4.1 Physical and chemical properties analysis of raw materials.....	38
4.2 Bleached rice bran wax organogels and water-in-oil emulsions.....	44

4.4 Storage stability of bleached rice bran wax organogels and water-in-oil emulsions	56
4.5 Policosanol organogels and water-in-oil emulsions	72
CHAPTER V CONCLUSIONS	95
REFERENCES	97
APPENDICES.....	112
APPENDIX A CHEMICAL ANALYSIS.....	113
APPENDIX B EXPERIMENTAL DATA.....	119
VITA.....	132



LIST OF TABLES

		Page
Table 1	Factors influencing organogels formation	6
Table 2	Physicochemical properties of crude and bleached rice bran wax.....	39
Table 3	Fatty acid composition of crude and bleached rice bran wax.....	44
Table 4	Physical properties of organogels at different concentration of bleached rice bran wax.....	47
Table 5	Thermal properties and solid fat content (%) of bleached rice bran wax organogels (BRXO).....	53
Table 6	properties of emulsion (E) and emulsion prepared from 9% wax concentration organogels (EO)	54
Table 7	Thermal properties of emulsion (E) and emulsion prepared from 9% wax organogels (EO).....	55
Table 8	ESI (%) of E and EO during storage for 90days at 4°C and 30°C	66
Table 9	The physical properties and fatty alcohol composition of policosanol..	74
Table 10	Physical properties of organogels at different concentration of policosanol	78
Table 11	Thermal properties and solid fat content (%) of policosanol	78
Table 12	Physical properties of PCE and PCM	84
Table 13	Thermal properties of PCE and PCM.....	84
Appendix B1	Colour of RO and BRXO during storage for 90 days at 4°C and 30°C	120
Appendix B2	Colour of E and EO during storage for 90 days at 4°C and 30°C.....	121
Appendix B3	Textural properties of BRXO during storage for 90 days at 4°C and 30°C	122

Appendix B4	Textural properties of EO during storage for 90 days at 4°C and 30°C..	123
Appendix B5	PV and TBARS of RO and BRXO during storage for 90 days at 4°C and 30°C	124
Appendix B6	PV and TBARS of E and EO during storage for 90 days at 4°C and 30°C	125
Appendix B7	Colour of PCO during storage for 90 days at 4°C and 30°C	126
Appendix B8	Colour of PCE and PCM during storage for 90 days at 4°C and 30°C	127
Appendix B9	Textural properties of PCO during storage for 90 days at 4°C and 30°C	128
Appendix B10	Textural properties of PCE and PCM during storage for 90 days at 4°C and 30°C	129
Appendix B11	PV and TBARS of PCO during storage for 90 days at 4°C and 30°C....	130
Appendix B12	PV and TBARS of PCE and PCM during storage for 90 days at 4°C and 30°C	131

LIST OF FIGURES

	Page
Figure 1 Classification of organogels.....	4
Figure 2 Schematic illustrations of different strategies of organogels formation; crystalline particles (a), crystalline fibres (b), particle-filled gel (c), liquid crystalline mesophases (d), and polymer strands (e).....	9
Figure 3 Typical behaviour of T_{melt} (melting temperature) evolution at different organogelator concentrations, along with a schematic representation of the sol and gel structures of the organogels	11
Figure 4 The structure of oil-in-water and water-in-oil emulsion.....	13
Figure 5 Schematic of the instability mechanisms responsible for emulsion breakdown	15
Figure 6 Crude rice bran oil refining process.....	18
Figure 7 Policosanol structure.....	23
Figure 8 The character of the CRX (a) and BRX (b).....	38
Figure 9 The polarized light microphotographs of CRX and BRX at magnification 20x and 40x	40
Figure 10 The X-ray diffraction patterns of the samples CRX (a) and BRX (b) in bulk states	41
Figure 11 Cooling (solid line) and heating (dotted line) DSC thermograms of CRX (a) BRX (b) in bulk states.....	42
Figure 12 The polarized light microphotographs of the BRXO at different wax concentration at magnification 20x (a) and 40x (b)	49
Figure 13 The X-ray diffraction patterns of 0% wax (RO) (a) and the BRXO at 3% (b), 5% (c), 7% (e), and 9% (f) wax concentration.....	51

Figure 14	The X-ray diffraction patterns of EO.....	55
Figure 15	Microstructure of the EO using optical microscopy under normal (a) and polarized light (b) at magnification 40x.....	56
Figure 16	The colour L* (a), a* (b) and c* (c) value of RO, BRXO, E and EO storage at 4°C and 30°C for 90 days.....	58
Figure 17	Textural changes in firmness (a), hardness (b) and stickiness (c) during storage in BRXO and EO at 4°C and 30°C for 90 days	61
Figure 18	The polarized light microphotographs of the RO stored at 4°C and 30°C for 0 day, 30 days, 60 days and 90 days at magnification 40x	64
Figure 19	The polarized light microphotographs of the BRXO stored at 4°C and 30°C for 0 day, 30 days, 60 days and 90 days at magnification 40x ...	65
Figure 20	The microphotographs of the E4C during stored for 0 day (a) and 30 days (b) at magnification 40x	67
Figure 21	Polarized light microphotographs of EO stored at 4°C and at 30°C for 0 day, 30 days, 60 days and 90 days at magnification 40x	68
Figure 22	PV (a) and TBARS (b) change of RO and BRXO, E and EO stored at 4°C and 30°C for 90 days during storage time.....	71
Figure 23	Thin layer chromatography of stearyl alcohol (fatty alcohol; FAL) (1), palmitic acid (fatty acid; FA) (2), rice bran oil (triglyceride; TG) (3), purified rice bran wax (wax ester; WE) (4), bleached rice bran wax (5), upper phase (6), and lower phase (7) extracted from policosanol extraction	73
Figure 24	The policosanol extracted from Thai bleached rice bran wax.....	74
Figure 25	The X-ray diffraction patterns of the PC.....	75
Figure 26	DSC patterns taken during cooling (solid line) and heating (dotted line) processes of policosanol.....	76

Figure 27	Polarized light microphotographs of policosanol extracted (PC) (a) and policosanol organogels (PCO) at different policosanol level at 12% (b) 13.5% (c) and 15% (d) at magnification 40x.....	80
Figure 28	The X-ray diffraction patterns of the PCO sample at 12% (a), 13.5% (b) and 15% (c) of PC concentration.....	81
Figure 29	The X-ray diffraction patterns of the PCE (a) and PCM (b).....	85
Figure 30	Colour change in L* (a), a* (b) and b* (c) of PCO, PCE and PCM during storage at 4°C and 30°C for 90 day	86
Figure 31	Textural changes in firmness (a), hardness (b) and stickiness (c) of PCO, PCE and PCM during storage at 4°C and 30°C for 90 days	87
Figure 32	Polarized light microphotographs of PCO stored at 4°C and at 30°C for 0 day, 30 days, 60 days and 90 days at magnification 40x	89
Figure 33	Polarized light microphotographs of PCE stored at 4°C and at 30°C for 0 day, 30 days, 60 days and 90 days at magnification 40x	91
Figure 34	Polarized light microphotographs of PCM stored at 4°C and at 30°C for 0 day, 30 days, 60 days and 90 days at magnification 40x	92
Figure 35	PV (a) and TBARS (b) reactive substances change of PCO, PCE and PCM stored at 4°C and 30°C for 90 days during storage time.....	94

CHAPTER I

INTRODUCTION

A challenge of oil-structured products and emulsions, such as butter, margarine spreads, and margarines, is stability. Thailand has a high average temperature, which causes products to melt, phase separation, oiling off, changes to fat crystals, resulting in a sandy taste, and a decrease in quality during use and storage. Many studies have been conducted to improve the quality of products using various techniques, such as oil blending, hydrogenation, interesterification, and fractionation. However, some techniques use chemicals that can cause toxins in the product or cause difficulty when attempting to control the reaction time, and some techniques require specific equipment, limiting production.

An effective process to possibly improve the consistency of the oil structure and the emulsion products is organogelation. Organogels also inhibit oil mobility and migration. Organogels are prepared by mixing the organogelator with the oil and heating the mixture to an optimum temperature. After cooling, the gel will be formed into a self-assembled three-dimensional structure that holds the liquid within the organogelator molecule. Wax-based organogels are derived from organogelator as wax; some examples are candelilla wax, sugarcane wax, carnauba wax, bayberry wax, beeswax, rice bran wax and shellac wax. Waxes are interesting to use as gelators because they have also been identified as having good organogels functionality, have a relatively low cost, are abundant commercially and are effective at a relatively low concentration. Rice bran wax has the potential to be used in the food industry as an oil-structuring material. Rice bran wax has a relatively high melting point, readily nucleates and crystallizes at room temperature and makes well-dispersed mixtures with oil. Moreover, the important bioactive

compound in rice bran wax has clinical properties for human health. Policosanol is a group of long-chain alcohols with a carbon length of 20-36 atoms. Policosanol can self-assemble and form the three-dimensional structure of an organogels.

Currently, research on organogels and W/O emulsions using bleached rice bran waxes as organogelator is lacking, and many studies have focused only on producing organogels from purified rice bran wax. The objective of this work was to increase the value of rice bran wax and policosanol from Thai rice bran, to use as gel-forming agents of organogels and water-in-oil emulsions and to improve their oil structure and emulsion stabilities. The physicochemical properties of these products were investigated. Moreover, these products were stored at $4\pm 2^{\circ}\text{C}$ and $30\pm 2^{\circ}\text{C}$ for 3 months to observe the changes during storage. The textural, morphological, and oxidative stability of the organogels and the emulsion samples was monitored. The hypothesis of this study was that rice bran wax from Thai rice sources without defatting and/or extracting policosanol can be used as an efficient organogelator.

CHAPTER II

LITERATURE REVIEW

2.1 Organogels

Organogels or oleogels are semi-solid-like gels that are composed of at least two components: the gelling substance (or organogelator) as a solid phase and the organic solvent (or edible oil) at greater than 90 wt% as a liquid phase (Doan, Van de Walle, Dewettinck, & Patel, 2015). These components can lead to a three-dimensional gelation composed of self-assembled crystalline fibres that entrap the liquid phase, which can prevent the liquid from flowing. (Weiss & Terech, 2006) report that organogels have a continuous structure with macroscopic dimensions and is solid-like in its rheological properties. Organogels production is very easy after mixing the organogelator with organic solvent and heating; the organogelator is dissolved in the solution. When cooled, the solubility of the organogelator in the liquid phase decreases, and interactions between the organogelator and solvent are reduced, forming the gel network by entanglement and resulting in a self-supporting bulk gel with well-defined aggregates, such as fibres, rods, and tubules (Jadhav, Patil, Patil, Patil, & Pawar, 2012; Murdan, 2005)

Organogelation does not change the fatty acid composition, and the nutrition remains stable in the organogels. Organogels have numerous potential functionalities in food products, including improving the qualities of food, such as increasing its viscosity and physical stability, resisting microbial contamination and increasing the shelf life. Organogels can also restrict oil mobility and migration, which are important factors in food that can lead to a significant decrease in quality (Rogers, Wright, & Marangoni, 2011). stabilize emulsions (Pandolsook & Kupongsak, 2017), control the rate of nutraceutical release (Garg, Bilandi, Kapoor, Kumar, & Joshi, 2011) and replace

saturated and *trans* fats (H.S. Hwang et al., 2013; Jang, Bae, Hwang, Lee, & Lee, 2015; Mert & Demirkesen, 2016). Currently, organogels have been widely used to develop oil structure systems in alternative-fat products to replace unhealthy fats, such as baking fats (margarine and shortening) or fat-based emulsions, in food products, including baked goods, processed meat, meat sauces, dairy products, ice cream and confections (Boteaga, Marangoni, Smith, & Goff, 2013; H.S. Hwang et al., 2013; H.S. Hwang, Singh, & Lee, 2016; Jang et al., 2015; Lupi, Gabriele, Seta, Baldino, & Cindio, 2014; Mert & Demirkesen, 2016; Patel et al., 2014; Yılmaz & Öğütçü, 2014a, 2014b, 2015).

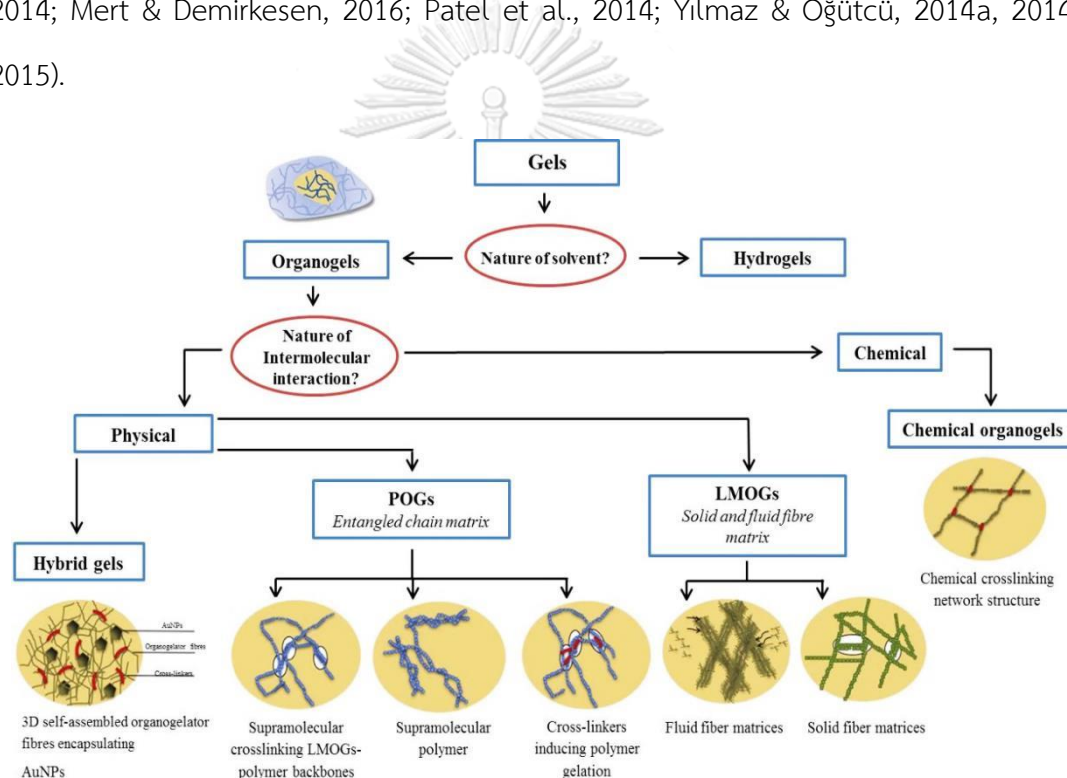


Figure 1 Classification of organogels

Source: Modified from Espositoa, Kirilovb, and Gaëlle Roullina (2018) and Mujawar, Ghatage, and Yeligar (2014)

The various classifications of the gels are based on the nature of the solvents, gelator, and intermolecular interactions (Fig. 1). Organogels can be distinguished from hydrogels by their organic continuous phase and the nature of the gelator molecule,

polymeric organogelators (POGs), and low-molecular-weight organogelators (LMOGs). The nature of the intermolecular interactions can divide organogels into two groups: physical organogels and chemical organogels. Physical organogels have a three-dimensional network that is formed by non-covalent bonds. All LMOGs and most POGs are physical gels (Suzuki & Hanabusa, 2010). Chemical organogels are formed by the entrapment of an organic liquid in a chemical crosslinking network structure. The network is maintained by covalent bonds and is therefore more robust and resistant to physical deformation (Plamen et al., 2015).

Organogels formation is influenced by many factors, and any of them can change the mechanical and physical properties of the organogels. These factors include the type of gelator, type of solvent (polar or apolar), presence of a surfactant, concentration, and the preparation conditions and method (cooling rate, shear rate, stirring conditions) and whether there are any interactions with other components (H. S. Hwang, Singh, Winkler-Moser, Bakota, & Liu, 2014; Lupi, Gabriele, & Cindio, 2011; Mitre, Rueda, Alvarado, Alonso, & Vazquez, 2012; Patel, Schatteema, Vos, Lesaffer, & Dewettinck, 2013; Zetzl & Marangoni, 2011). The temperature and molecular weight of gelators influence the quality of the organogels. The temperature depends on the chemistry of the gelator and the mechanism of the interaction with the medium. If the temperature is reduced once the gel is in solution, the hydration degree will be reduced, and gelation will cause the resulting gel to undergo chemical cross linking such that it is unable to be changed to a liquid by changing the temperature. Low-molecular-weight polymers require a high concentration to build up the viscosity and to set the gel (Mujawar et al., 2014). Esposito et al. (2018) summarized the factors affecting organogels formation, and the data are shown in Table 1. It is difficult to optimize the conditions required to produce organogels that match this requirement, as some modifications of one factor can radically change the organogels.

Table 1 Factors influencing organogels formation

Organogel parameters	Factor	Impact(s)
Solvent	Nature	Morphology
		3-D conformation
		optical properties
Organogelator	Presence of cosolvent	Morphology 3-D conformation
	Presence of water	3-D conformation, stability
	Molecular weight	Mechanical and rheological
	solubility	properties, 3-D conformation
	Concentration	Mechanical and rheological properties, stability
	Charge	Mechanical and rheological properties, 3-D conformation
	Adjuvants	Salt addition
Surfactant addition		Morphology, 3-D conformation
Formulation parameters	Agitation mode	3-D conformation
	Phase transition diagram	Network strength

Source: Esposito et al. (2018)

The organogelator is a material used to assemble organogels, and its major role is to set the gel. Organogelator can be classified into two groups based on their molecular weight: low-molecular-weight organogelators (LMOGs) and polymer organogelators (POGs). LMOGs are a group that can function as network-forming

organogelators with edible oils in food. LMOGs are a group of organic compounds with a molecular weight typically less than 3000 Da (Abdallah & Weiss, 2000). These organogelator efficiently form gels having three-dimensional networks with organic molecules that have molecular weights of less than 2000 g/mol and, more specifically, less than 500 g/mol (Carretti, Dei, & Weiss, 2005). LMOGs are more popular organogelator than POGs because of their lower toxicity, great ability to gel at a low concentration (>1 wt%), and greater flexibility of use and because they are easily prepared and have strong physical stability (Suzuki & Hanabusa, 2010; Vintiloiu & Leroux, 2008). Examples of LMOGs are fatty acids, fatty alcohols, wax esters, phospholipids, monoacylglycerols, sorbitan esters, phytosterols and ceramides. POGs are high molecular-weight molecules, such as polyesters, polycaprolactones, polyethylene glycols, polyolefins, and polycarbonates. POGs can be classified into three categories: (1) supramolecular crosslinkable polymers, (2) polymer-crosslinking agent organogelator and (3) LMOG-incorporated polymer organogelator (Suzuki & Hanabusa, 2010). POGs can form gelling organic solvents via supramolecular cross-linking points and gelation, which are formed by a conformational change in the polymer or by the crosslinking agents added. Supramolecular cross-linking represents an interesting way to improve the π -conjugated polymer performance. When comparing POGs and LMOGs, the gels formed by POGs have a lower maximum gelation temperature (T_{gel}) but a greater gel strength (Garg et al., 2011).

The organogelator, when used at a concentration of approximately <15%, may undergo physical and/or chemical interactions that lead to a gel network formed by the randomize entanglement of fibre-like, tube-like, or plate-like structures, resulting in the formation of a 3-D networked structure (Sahoo et al., 2011; Toro-Vazquez et al., 2007; Toro-Vazquez et al., 2013). The potential applications of organogels in food systems are numerous and offer revolutionary options for nano- and micro-structuring edible oils into functional fats. A number of

organogels systems have the ability to gel edible oils at low concentrations of approximately 0.5 to 2.0 wt%. In general, this network is stable largely due to weak inter-chain interactions, such as hydrogen bonding, dipole-dipole interactions, electron transfer, London dispersion forces, solvophobic effects, Van der Waals forces, and π -stacking (L. Hu, Zhang, & Ramström, 2015; Mujawar et al., 2014). In addition, the organogelator type not only results in the production of different organogels but also differs in the structure that will trap the liquid phase. According to Marangoni & Garti (2011), the organogelator building block for the formation of a three-dimensional network in structured oils can be classified into five different categories:

1) Crystalline particles: A network of crystalline triacylglycerol particles entraps liquid triacylglycerol inside the molecule, causing gel formation (Fig. 2a). The structuring agents in this group are fatty acids, wax esters, sorbitan mono-/triestrate, lecithin and ceramides.

2) Crystalline fibres or self-assembled fibrillar networks (SAFINs): The crystalline fibres from one direction of growth interact with one another, forming a three-dimensional network as the structure forms helical and twisted crystalline ribbons that are hundreds of micrometres long (Fig. 2b). Phytosterols, oryzanol, 12-hydroxystearic acid and ricinoleic acid are the structuring agents in this group.

3) Particle-filled networks or solid particles: The solid or liquid non-fat particles are structuring agents (Fig. 2c). The particles are at a high concentration and are closely packed, which allows mechanical contact between particles to form a gel network.

4) Liquid crystalline mesophases: The orientation of the molecules occurs in mesophases. The molecules assemble into a short- and/or long-structure lattice, which may display 1-D, 2-D, or 3-D order (Fig. 2d). Liquid crystalline mesophases are classified into three groups: thermotropic, metallotropic and lyotropic.

5) Polymer strands: The polymers encourage the gelation of a medium. These gels can be of two types: gels formed by covalent bonding or self-assembly (Fig. 2e). Examples of gelator agents include ethylcellulose, cellulose, starch and gelatin.

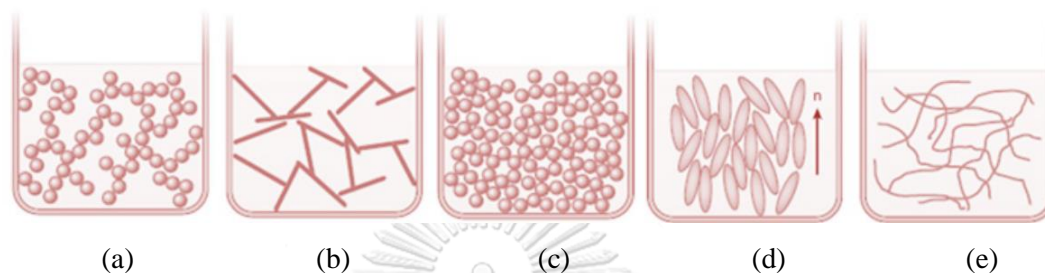


Figure 2 Schematic illustrations of different strategies of organogels formation; crystalline particles (a), crystalline fibres (b), particle-filled gel (c), liquid crystalline mesophases (d), and polymer strands (e)

Source: Kaushik et al. (2017)

Some extensive examples of network-forming edible oil structurants for the food industry include mono-(MAGs), di-(DAGs), triacylglycerols (TAGs), fatty acids, fatty alcohols, derivatives and metal salts of fatty acids, waxes, wax ester, sorbitan mono-stearate, steroids, mixtures of lecithin with sorbitan tri-stearate, phytosterols with oryzanol, oryzanol with sitosterol, fatty acids with fatty alcohols, and steric acid with stearyl alcohol (Bot & Agterof, 2006; Gandolfo, Bot, & Flöter, 2004; Pernetti, van Malsen, Flöter, & Bot, 2007; Schaink, van Malssem, Morgado-Alves, Kalnin, & van der Linden, 2007; Zetzl & Marangoni, 2011).

2.1.1 The physiochemical properties of organogels

The physiochemical properties of organogels depend on the structural features. The isotopic nature and optical clarity can be determined by spectroscopic techniques, such as nuclear magnetic resonance (NMR) spectroscopy

and Fourier- transform infrared spectroscopy (FTIR). The knowledge of the molecular packing within the structure of organogels was obtained using scanning and transmission electron microscopy. Mujawar et al. (2014) reported the specific characteristics of organogels as follows:

1) Viscoelasticity

Organogels are associated with materials having both viscous and elastic properties that generally follow the Maxwell model of viscoelasticity. They behave similar to solid formulations at lower shear rates and present physical cross-linked junctions below the gelator solubility limit. At this point, the organogelator begins self-assembly to form a three-dimensional network and demonstrates an elastic property (Esposito et al., 2018). When the shear stress increases, the physical interacting points amongst the fibre structures begin to weaken until the shear stress is high enough to disrupt the interactions amongst the fibre structures. The organogels being flowing, and the fibre structures begin to weaken until the shear stress is high enough to disrupt the interactions amongst the fibre structures. This behaviour can be explained as plastic flow behaviour (Garg et al., 2011).

2) Non-birefringence

When organogels are viewed under polarized light, they appear as a dark matrix. This is the isotropic nature of organogels: they do not allow polarized light to pass through the system.

3) Thermoreversibility

Organogels can change from liquids to solids to liquids when the temperature changes. At the critical temperature, organogels will lose their semisolid-like structure and begin flowing. The physical interactions of organogelator molecules are disrupted due to the increased thermal energy within the organogels network. When the system is cooled down, the interaction amongst the

organogelator molecules prevails, and the network returns to a more stable system: a solid-like structure.

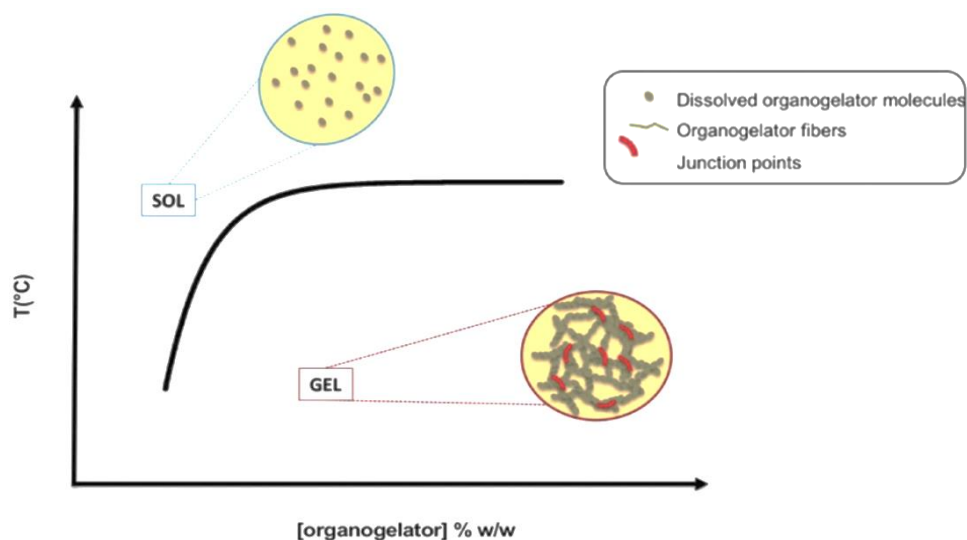


Figure 3 Typical behaviour of T_{melt} (melting temperature) evolution at different organogelator concentrations, along with a schematic representation of the sol and gel structures of the organogels

Source: Espositoa et al. (2018)

4) Thermostability

The organogelators undergo self-assembly, causing the resulting total free energy of the system to decrease, which results in a low-energy thermostable system. The thermodynamically stable nature of organogels has been attributed to the spontaneous formation of a fibrous structure that causes the organogels to remain in a low-energy state. A gel-to-sol transition at room temperature occurs and indicates that external energy has to be supplied to the organogels to break the three-dimensional structure and cause the subsequent transformation of the gelled state to the sol state (Sahoo et al., 2011). The melting temperature corresponding to the gel-sol transition typically increases with the organogelator concentration (Fig. 3). The phase transition temperature (PTT) (i.e., sol-to-gel or gel-

to-sol) gives an understanding into the microstructures that form the cross-linked network. The phase transition temperatures also help optimize the organogels composition (Choudhary, Agrawal, Choukse, & Chaturvedi, 2013).

5) Optical clarity

This property varies depending on the organogels composition and may be transparent or opaque

6) Chirality effects

Low molecular weight organogelator affect the transformation into a solid, the molecular arrangement, the reversibility kinetics and the stability of the solid-fibre networks (Das, Kandaneli, Linnanto, Bose, & Maitra, 2010; Mujawar et al., 2014). The chiral centre location within the organogelator plays an important role in supporting the organization of the molecular packing, which provides kinetic stability and a thermodynamic basis of the organogels system, whereas fluid-filled organogels are far less impacted by chiral organogelator. Additionally, supramolecular gelators form chiral systems through non-covalent interactions, which are independent of the organogelator chirality (Das et al., 2010).

7) Swelling

Organogels can absorb liquids. The gel swells, resulting in a volume increase. When the solvent penetrates the gel system, the gel-gel interaction is replaced by a gel-solvent interaction. Swelling is usually limited by the degree of gel matrix cross-linking that can prevent dissolution.

2.2 Emulsion

An emulsion is a disperse system consisting of two immiscible liquids (oil and water) in which the disperse phase (liquid droplets) is dispersed in the continuous phase (liquid medium). The droplet size in the food system typically ranges from 0.1 to 100 μm (McClements, 2005). The emulsion can be divided into two main types

(Fig. 4): 1) water-in-oil (W/O) emulsion: the water is dispersed in oil and is normally a solid-like structure (like margarine and butter), and 2) oil-in-water (O/W) emulsion: the oil is dispersed in water and may be partially crystalline with respect to the oil phase (such as salad dressing, cream and milk) (Dalgleish, 1996). However, in food systems, emulsions have a broad meaning, covering all systems, and may include solids, gases and/or liquid crystals, such as cake batter, ice cream, and mayonnaise (Rousseau, 2000).

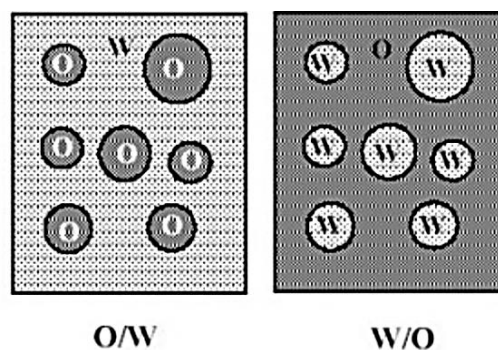


Figure 4 The structure of oil-in-water and water-in-oil emulsion

Source: Chiralt (2010)

An emulsion will occur after applying mechanical force by shaking, blending, or stirring, which increases the surface free energy and decreases the interfacial tension between the two phases. One liquid will change to small droplets and become dispersed in the other phase, but this result in an unstable emulsion. After the force is discontinued, the liquid will become agglomerated and separate into 2 parts due to the difference in the density of the liquids, with the upper part being the low-density liquid and the lower part being the high-density liquid. Generally, there are three main interactions among emulsion droplets and their combinations: dipole-dipole interactions, dipole-induced dipole interactions, London interactions, electrostatic repulsion, and steric repulsion. Several methods may be applied to achieve emulsification, for example, the use of static mixers or general

stirrers, high-speed mixers (such as the Ultra turrax homogenizer, colloid mills and high-pressure homogenizers), or ultrasound generators (Tadros, 2013).

2.2.1 Emulsion stability

Emulsions are potentially unstable if there are no kinetic factors to prevent phase separation. The liquid phases are not miscible, and the density difference between phases induces phase separation. Emulsions are unstable due to the action of different forces, such as flow forces, interparticle repulsive and attractive forces, gravitational forces, and molecular forces. To differing degrees, these forces are responsible for the action of the destabilization mechanisms (Fig. 5). The emulsion stability refers to the potential of an emulsion to resist changes in its physicochemical properties during storage (Hu et al., 2017). The mechanisms of instability are the following:

1. Phase inversion

This refers to a phenomenon that occurs when the emulsion is disturbed. The emulsion changes from an O/W emulsion to a W/O emulsion or vice versa. Phase inversion results from environmental or composition changes, such as changes in temperature, mechanical forces, emulsifier type or concentration.

2. Creaming or sedimentation

This separation is caused by the upward or downward (sometimes) motion of emulsion droplets due to gravity acting differently on the droplets and the continuous phase. Lower-density droplets tend to form cream and rise up to the surface, while the higher-density phase forms sediment on the bottom.

3. Coalescence

This occurs when an interfacial film between two droplets loses its integrity, and irregular aggregation forms a single larger droplet that results in free oil

at the top of the emulsion (oiling off). The coalescence phenomenon will reduce the number of droplets and cause a loss of identity.

4. Flocculation

The emulsion droplets are in continuous motion due to their kinetic energy, gravity or force during processing. The droplets will aggregate as they collide due to the prevailing attractive forces that exist at a predetermined distance. In flocculation, the droplet aggregates retain their integrity without a breakdown of the structural integrity of the film surrounding the droplets. Flocculation may be strong or weak depending on the magnitude of the attractive energy involved.

5. Ostwald ripening

This is a size increase of larger droplets at the expense of smaller ones. This is due to the substances being more soluble in smaller droplets than in large droplets. Therefore, solutes move by diffusion with the concentration gradient to larger globules.

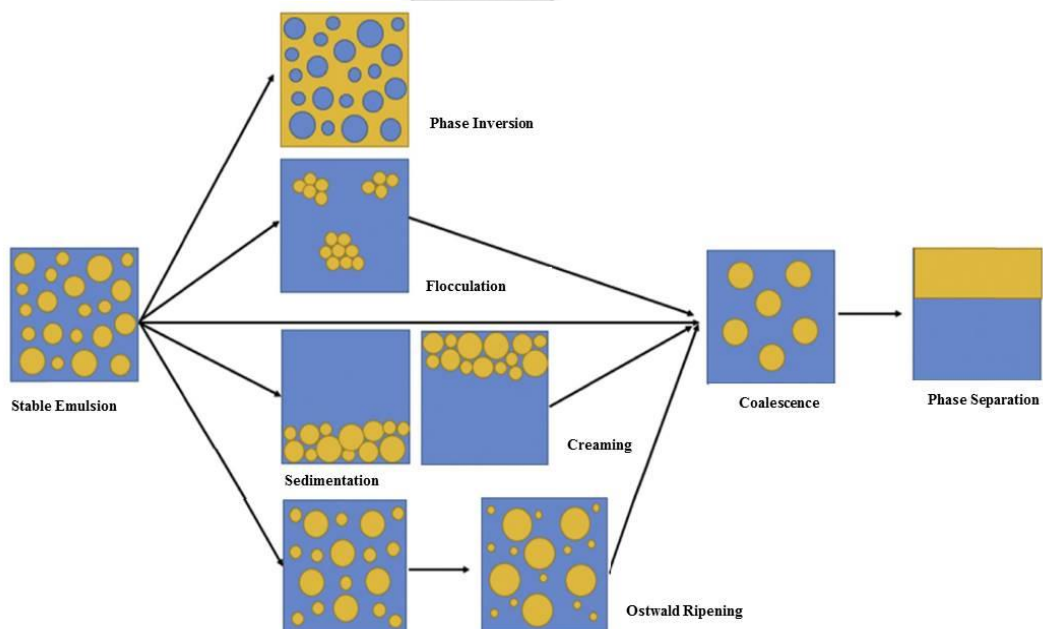


Figure 5 Schematic of the instability mechanisms responsible for emulsion breakdown

Source: Hu et al. (2017)

The role of solid fat particles (Pickering crystals) in the stability of emulsions has been studied. Organogels-based emulsions produced from monoglycerides, 12-hydroxystearic acid (12-HSA), and wax esters, such as sunflower wax, candelilla wax, shellac wax, beeswax, paraffin wax, and rice bran wax, can decrease droplet coalescence, increase the emulsion stability, and provide structure to solid-like W/O emulsions (Hodge & Rousseau, 2003; Hughes, Marangoni, Wright, Rogers, & Rush, 2009; Ögütçü, Arifoğlu, & Yılmaz, 2015; Pandolsook & Kupongsak, 2017; Toro-Vazquez et al., 2013) because gelator crystals are associated with either the immobilization of the water droplets throughout the crystal network or with the absorption of fat crystals at the water-oil interphase (Toro-Vazquez et al., 2013). In the emulsion, the hydrophobic section of the interfacial surfactant has a similar structure to the oil, which can increase the nucleation rate, and the solid droplets will induce nucleation within the liquid droplets that they are physically mixed through a collision mechanism (Coupland, 2002). Then, the solid particle network and the interfacial adsorption will provide kinetic stability to the dispersed phase (S. Ghosh, Tran, & Rousseau, 2011). Many types of foods, such as structured oils (margarine and butter), ice cream and whipped cream, are stabilized by surface-active fat crystals at the water and oil interface. In solid particles, surface-active fat crystals can create a steric barrier between adjacent water droplets to prevent droplet collision, film drainage and coalescence (Tambe & Sharma, 1994). If fat crystals at the surface are inactive, their effect at the interface will be greatly diminished. Such fats interact through van der Waals interactions and form a fat crystal network such that W/O emulsions are stabilized not by interfacial adsorption but by physically encasing the dispersed phase. The fat crystals may synergistically act as both Pickering and network stabilizers depending on the presence of a suitable surfactant that yields crystals with switchable polarity (S. Ghosh & Rousseau, 2011; Marangoni, 2004; Rousseau, Khan, Zilnik, & Hodge, 2003). The surface activity

of fat crystals will mainly dictate the role they play as an interface or stabilizer in the continuous phase. The interfacially active crystals accumulate at the interface of the droplet and anchor themselves at the droplet surface, providing a barrier to coalescence. For crystals that do not have any surface activity but are at a high concentration, the plastic network will be formed in the continuous phase, which thus enhances the water droplet dispersion and reduces droplet diffusion and sedimentation (Ghosh & Rousseau, 2011). Moreover, the emulsion crystal structure is an important factor in terms of the stability of semi-crystalline droplets against partial coalescence (Coupland, 2002).

2.3 Rice bran wax

Rice (*Oryza sativa* L.) is a major food consumed around the world. After harvest, rice is hulled and polished, and the by-products are the rice hull, rice germ, rice bran, and broken rice. The rice bran, which is the layer between the husk and endosperm of rice, is a highly nutritional edible oil resource. The rice bran contains approximately 12 to 25% crude oil. Rice bran oil is extracted from the rice bran layer. Rice bran oil is largely produced and consumed in East Asia, in such countries as India, Korea, Sri Lanka, China, Japan, Indonesia, Laos and Thailand. The primary fatty acid composition of rice bran oil is 12 to 28% palmitic (C16:0), 35 to 50% oleic (C18:1) and 29 to 45% linoleic acid (C18:2); minor compositions are 2 to 4% stearic acid (C18:0) and 0.5 to 1.8% linolenic acid (C18:3) (Gunstone, Harwood, & Dijkstra, 2007).

Rice bran wax (RBX) is a natural value-added by-product that is separated during the winterization or dewaxing step in the refining process of rice bran oil (Fig. 6). Crude rice bran oil is winterized by cooling to 20°C to 25°C and filtering the sludge. The crude wax sludge can be purified by washing with methyl alcohol, acetone, ether and finally chloroform. Mezouari et al. (2006) isolated rice bran wax

from crude rice bran oil using the solvent acetone at 4°C for 24 h to achieve dewaxing and separated the wax using filtration. The quantity of wax in crude rice oil can vary from 2 to 5% depending on the rice variety, rice bran source, history of the rice bran, milling technique, method of oil extraction, solvent used and extraction conditions (Dassanayake, Kodali, Ueno, & Sato, 2009). (Ito, Shzuki, & Fujino, 1983) reported that the wax content of rice bran oil is approximately 0.86%, while Saunders (1985) reported that there is 3–4% wax ester in rice bran oil base; Salunkhe, Chavan, Adsule, and Kadam (1992) reported that crude rice bran oil contains 4.8% wax and 5 – 8% unsaponifiable matter. Subsequently, (Arumughan, Skhariya, & Arora, 2004) showed that the crude oil had a wax composition of between 2 and 5%, and Gunawan, Vali, and Ju (2006) reported that the wax content in crude rice bran oil is 1.2 - 1.4%. Recent studies by Kim & Godber (2014) report that rice bran oil consists of 2–4% rice bran wax, which contains wax esters, hydrocarbons and other minor components.

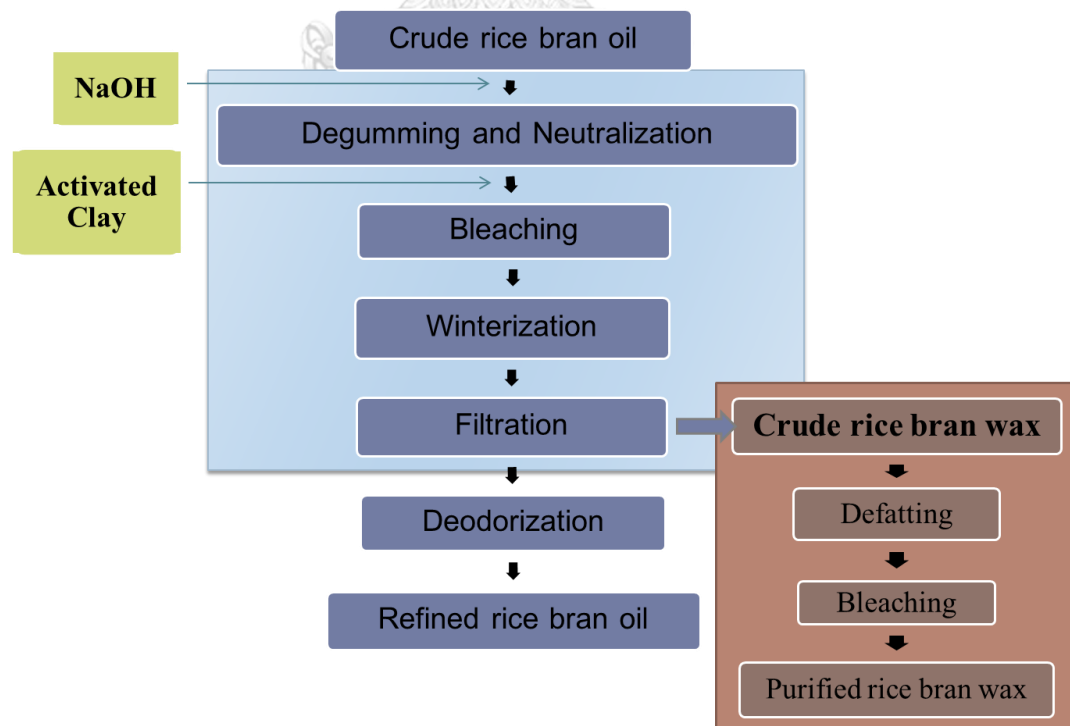


Figure 6 Crude rice bran oil refining process

Crude rice bran wax (CRX) is a brown material. Its contains is not only wax esters but also triacylglycerides (TAG), hydrocarbons, free fatty acids, free alcohols, other impurities and other substances, such as resinous matter (RM). Additionally, CRX is also high in iodine, acid, and phosphorus and has a high degree of saponification, which results in poor quality for applications. Vali, Ju, Kaimal, and Chern (2005) found that the major impurity in crude wax and defatted wax was RM, which is a mixture of aliphatic aldehydes, fatty alcohols, and fatty acids, and RM confers a dark reddish-brown colour and offensive odour to the crude wax when its contents are greater than 15 to 19%. CRX is a semi-solid and has no sharp melting point in a DSC thermatogram. In addition, CRX and bleached wax are different in terms of their wax ester composition and quantity. Removing RM from the wax is import to create high-quality food-grade wax. The purification of CRX occurs in two steps: defatting and bleaching. These steps can help reduce impurities and increase the quality. Vali et al. (2005) removed the oil trapped in crude wax using hexane and isopropanol to dissolve the oil followed by filtration. In the bleaching step NaBH_4 (sodium tetrahydridoborate) was used as the bleaching agent to remove the RM, which could not be removed by physical adsorption using charcoal or clay. Furthermore, the bleaching agents that have been used include sodium chlorite (NaClO_2), nitric acid (HNO_3), phosphoric acid (H_3PO_4), hydrogen peroxide (H_2O_2), chromium trioxide (CrO_3), sulphuric acid (H_2SO_4), and combinations of agents, such as the combination of H_2O_2 and CrO_3 , the combination of NaClO_2 or NaBH_4 with 30% H_2O_2 , the combination of CrO_3 and H_2SO_4 , the combination of NaClO_2 and H_2O_2 , and solar bleaching followed by H_2O_2 treatment (Bennett, 1963; Mezouari, Kochhar, Schwarz, & Eichner, 2006; Vali et al., 2005; Warth, 1956).

RBX contains saturated monoesters, long-chain fatty acids, long-chain fatty alcohols, wax esters, policosanols, phytosterols and other components. RBX

contains the esters of fatty acids varying from C16 to C32 and fatty alcohols varying from C24 to C38, of which the major fatty acids are C22, C24, C30, and C32 for the fatty alcohol. The majority of the wax esters contain C52, C54, and C56 (Dassanayake et al., 2009). Co and Marangoni (2012) reported that the major chemical composition of purified rice bran wax is aliphatic wax esters with carbon numbers between 44 and 64, with RBX being as much as 76% aliphatic wax esters. Approximately 88% of the waxy esters are even numbered and have 48–60 carbons. The hydrocarbon content of rice bran wax is typically as low as 2%. RBX substances have relatively high melting points of approximately 80°C to 83°C. At room temperature, they readily nucleate and crystalize, resulting in mixtures with oil with good dispersion (Global Agritech Inc, 2009).

RBX has many potential applications in many industries, such as in food, cosmetics, pharmaceuticals, polymers, polishes, crayons, candle making, shoe creams, paper coating, carbon paper, lubricants and leather. Most patents and research papers have focused on the use of RBX in cosmetic formulas, such as in creams, lipstick and hair conditioner. RBX is suitable for use as an ingredient and excipient in medicines in Australia with no restrictions (Australian Government, 2007). For food uses, RBX has been applied in various applications, including as an oil-structuring material, as a chocolate enrober, for coating fruits, vegetables, and cheese as a defoaming agent, as a microcapsule for flavours, and in the formulation of chewing gum (Dassanayake et al., 2009). There is a possible value-added role in oil structuring by replacing other expensive plant waxes, such as carnauba wax, candelilla wax, sunflower wax, and sugarcane wax (Blake, Co, & Marangoni, 2014; Rocha et al., 2013). Maru, Surawase, and Bodhe (2012) reported that RBX could potentially be a substitute for carnauba wax in pharmaceutical and cosmetic applications because the characterization and specification of RBX is in line with pharmacopoeia guidelines and are similar to the standard values of carnauba wax.

RBX is GRAS under its intended conditions of use under 21 CFR 170.35. RBX is listed in the Food Additive Status List by the U.S. FDA, section 172.890, U.S. Food and Drug Administration (2016). RBX specifications given by the US FDA indicate a melting point between 75°C and 80°C, a free fatty acid maximum of 10%, a maximum iodine number of 20, and saponification numbers of 75 to 120.

Plant waxes are of great interest due to their availability and low cost, and the gelation abilities of plant waxes, such as candelilla wax, rice bran wax, and sunflower wax, have been investigated in various edible oil systems. There is interest in RBX with respect to producing organogels due to its widespread applications, low cost, good gelation abilities and ability to form a gel at low concentrations. RBX can be used as a good organogelator. In recent years, many studies have been conducted using rice bran wax in organogels. Doan et al. (2015) studied the properties of rice bran wax in rice bran oil organogels. These researchers found that the minimum rice bran wax concentration was 5 wt%. The crystal morphology of the organogels demonstrated a large dendritic shape, weak gelling behaviour and a low elastic modulus. Dassanayake et al. (2009) studied the physical properties of rice bran wax organogels. They found that 1% rice bran wax was necessary for gelation to occur, whereas carnauba wax (CRX) and candelilla wax (CLX) required 4 and 2%, respectively. The thermal behaviour and the crystal morphology of rice bran wax organogels compared to CRX and CLX organogels exhibit a better structure ability, and RBX forms long, needle-shaped crystals. Dassanayake, Kodali, Ueno, and Sato (2012) studied the kinetics of rice bran wax organogels with different vegetable oils. These researchers concluded that the solvent type had no effect on the melting and crystallization temperatures but had an effect on the viscosity and textural properties of the organogels. Hwang, Kim, Singh, Winkler-Moser, & Liu (2012) produced organogels using soybean oil with natural waxes; the results showed that sunflower wax, candelilla wax, and rice bran wax were the best gelling agents for

soybean oil and could produce gels with concentrations as low as 0.5–1%. Subsequently, Hwang et al. (2013) produced margarine from plant wax organogels. They found that rice bran wax was rather effective at forming a gel with soybean oil but was not suitable for producing a firm margarine. Hwang et al. (2016) replaced the margarine in cookies with an organogel made of vegetable oil and rice bran wax, and the results showed a high potential application for margarine replacement in cookies. Daniele, Botega, Marangoni, Smith, & Goff (2013) investigated the potential application of 10% rice bran wax in making ice cream with high oleic sunflower oil organogels. These organogels induced the formation of a fat globule network and improved the properties of the ice cream. The researchers conclude that organogels could lead to an alternative to saturated fat sources in ice cream. Tavernier et al. (2017) combined two waxes, one high-melting wax (sunflower wax or rice bran wax) and a low-melting wax (berry wax), to enhance the deformation resistance of organogels. The results showed that the rice bran wax and sunflower wax crystallize and melt simultaneously. The berry wax crystals were able to support the network structure formed by the sunflower wax and rice bran wax by building bridges from the fat crystal.



2.4 Policosanol

Policosanol (PC) is a mixture of long-chain aliphatic primary C16-C36 alcohols (Fig. 7) of which docosanol (C22), tetracosanol (C24), hexacosanol (C26), octacosanol (C28) and triacontanol (C30) are the major components and heptacosanol (C27), nonacosanol (C29), dotriacontanol (C32) and tetratriacontanol (C34) are minor components (Greyling, Witt, Oosthuizen, & Jerling, 2006; Harrabi, Boukhchina, Mayer, & Kallel, 2009; Irmak, Dunford, & Milligan, 2006). The original sources of policosanol from plant or animal waxes were sugarcane (*Saccharum officinarum* L.) wax, beeswax, rice bran wax, carnauba wax and wheat germ wax (Cravotto, Binello,

Merizzi, & Avogadro, 2004; Irmak et al., 2006). Of these, sugarcane wax and rice bran wax are important sources of commercial policosanol.

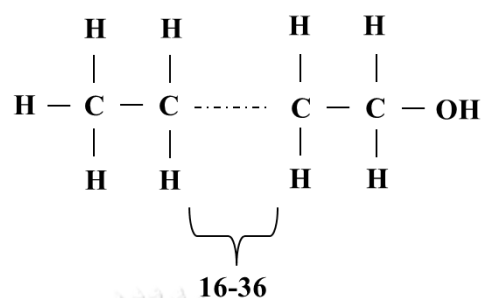


Figure 7 Policosanol structure

Many clinical studies have shown the benefits of policosanol to human health. Currently, policosanol is a popular food supplement for health enhancement. A daily intake of 5-20 mg of PC, especially of 24-34 carbon chain length, can reduce low-density lipoprotein cholesterol (LDL-C) in the blood by 21-29%, whereas high-density lipoprotein cholesterol (HDL-C) increases by 8-15%. Moreover, policosanol can prevent and cure cardiovascular disease, inhibit cholesterol biosynthesis, increase LDL decatabolism, reduce platelet aggregation, reduce endothelial damage, reduce foam cell formation, inhibit lipid peroxidation, prevent lipoprotein peroxidation in fat and protein, reduce LDL oxidation, which is the cause of atherosclerosis, and reduce triacylglycerol in the liver (Carbajal, Arruzazabala, Valdes, & Más, 1998; Hargrove, Greenspan, & Hartle, 2004; Menendez et al., 1994; Menendez et al., 2005; Varady, Wang, & Jones, 2003). Studies on the safety of policosanol have shown that it does not cause gene mutation, is non-carcinogenic, is non-toxic to genes and cell growth, and has been shown to be safe in long-term clinical use (Rendon et al., 1992).

Policosanol extraction from waxes is comprised of 2 main steps: extraction and purification. The purpose of extraction is the hydrolysis of the wax ester

into fatty acids using long chain fatty alcohol. Refluxing is a popular method to achieve hydrolysis of the wax ester. Normally, the hydrolysis of wax is achieved using saponification with an alkaline solvent, typically sodium hydroxide (NaOH) or potassium hydroxide (KOH), heated to 40-100°C for 1-8 h. Gamble et al. (2003) saponified beeswax using 10.7 M KOH by stirring at 40-100 rpm for 3 h. Vali et al. (2005) saponified rice bran wax using 30% KOH in isopropanol at 100°C for 4 h. Chen et al. (2005) used 0.2% KOH in butanol for 8 h. Wang et al. (2007) extracted PC from rice bran wax using a different solvent and saponification with alcohol or water (neutralized and non-neutralized), using dry saponification with 50% calcium hydroxide ($\text{Ca}(\text{OH})_2$) and using transesterification. The purification step separates the fatty alcohol (as policosanol) and the fatty acid. After hydrolysis, the saponified mixture is purified by recrystallization at low temperatures of less than 10°C and separated with fatty acids. Purification using a solvent, such as diethyl ether or ethyl acetate, and combined methods have been developed (Irmak et al., 2006; Vali et al., 2005). Gamble et al. (2003) purified the policosanol of beeswax using acetone with recrystallization in a temperature range of 2 to -10°C. The crystal is then purified again with heptane and acetone, resulting in 80-99% pure policosanol. Chen et al. (2005) used ethanol combined with molecular distillation to purify policosanol. Moreover, researchers have also studied other extraction and purification methods to reduce the use of chemicals solvents. Cravotto et al. (2004) developed an extraction method using high-intensity ultrasound as the catalyst for PC extraction from rice bran. Jackson and Eller (2006) reported a method for extracting PC using lipase-catalysed methanolysis in supercritical carbon dioxide (scCO_2). Lucas, Garcia, Alvarez, & Gracia (2007) studied the scCO_2 extraction of fatty alcohol from sugarcane wax at pressure ranges of 300-250 bar, temperature ranges of 50-100°C, and KOH concentrations of 1-20% w/w. Recently, Srisaipet, Yasamoot, and Somsri

(2016) studied the use of microwaves to activate the hydrolysis of PC. Beeswax was hydrolysed using 0.5 M KOH for 60 seconds at 300 watts of microwave, which was then purified by extraction with a mixture of organic solvents. The PC yield was 14.57%.

Many studies have demonstrated the potential application of long chain fatty alcohols or policosanol as an organogelator. Long chain fatty alcohols can self-assemble and form the three-dimensional structure of an oleogels. Gandolfo et al. (2004) investigated the ability of different fatty acids, fatty alcohols and their mixtures to form organogels. The organogelator in this study were palmityl alcohol, stearyl alcohol, arachidyl alcohol and behenyl alcohol. They found that the fatty alcohols produced harder organogels than the fatty acids at the same concentration. Schaink et al. (2007) studied the textural and structural properties of organogels produced by mixing stearic acid and stearyl alcohol (octadecanol). These researchers found that different mixture ratios resulted in different crystal morphologies, and a structuring synergistic effect was found at a ratio of 3 : 7 (stearic acid : stearyl alcohol). According to Co and Marangoni (2012), the organogels produced from fatty alcohol were arranged as stacks of platelets and formed large crystals. The mixture of fatty alcohols and fatty acids showed small needle-like crystals, which affected the rheology of the system. Lupi, Gabriele, Greco, et al. (2013) investigated organogels prepared from virgin olive oil and a mixture of fatty alcohols, as a policosanol, at different concentrations. Their results showed that the minimum concentrations of policosanol needed to form a network of crystal aggregates and gelation were 0.1 and 0.5% (w/w), respectively. If the policosanol content was greater than 0.5% (w/w), the oil phase demonstrated strong gel behaviour. A concentration of policosanol of between 2.5% and 3% (w/w) was sufficient to promote the formation of a large number of crystals that formed a three-dimensional network. (Lupi, Gabriele, Baldino, et al., 2013) produced a policosanol organogel to support

the oral administration of ferulic acid (5% w/w). Subsequently, Lupi et al. (2014) used the organogels produced from policosanol using an olive oil and sunflower oil blend in meat sauces. The policosanol was found to be more efficient in stabilizing the system even at low concentrations. Valoppi, Calligaris, & Marangoni (2017) examined the efficacy of fatty alcohols as an organogelator in peanut oil. They found that fatty alcohols can prevent oil separation and can be used as a stabilizer in peanut oil. The organogels crystallization, structure and physical properties depended on the fatty alcohol chain length. Tian & Acevedo (2018) suggested that policosanol can produce organogel that can protect retinyl palmitate from photodegradation and can improve retinyl palmitate photostability.



CHAPTER III

MATERIALS AND METHODS

3.1 Materials

3.1.1 Crude rice bran wax (CRX) containing 10% resin was used. The wax esters of acids and alcohols had even-numbered carbon chains (C44-63).

3.1.2 Bleached rice bran wax (BRX) that had 10% of the resin removed was supplied by Thai Edible Oil Co., Ltd., Thailand.

3.1.3 Rice bran oil (RO) (KING®) was purchased from a supermarket in Thailand.

3.2 Physical and chemical analysis of the raw material

Crude rice bran (CRX) and bleached rice bran waxes (BRX) were evaluated to obtain the following properties:

3.2.1 Oil content

The BRX was defatted. Then, 100 g of BRX was dissolved in 700 ml of hexane and refluxed at 80°C for 30 min. The mixture was then cooled to 30°C and filtered using an Ace Buchner funnel (25–50 µm) with a Whatman No.1 filter. The defatted wax was collected on the filter paper. Then, 350 ml of isopropanol was mixed with 50 g defatted wax and refluxed again at 85°C for 30 min. After that, the mixture was cooled to 75°C, and the wax crystals were filtered. The crystals were dried in a hot air oven at 90°C until the weight of the samples was stable to remove the solvent (modified from Vali et al., 2005). The oil content was calculated.

3.2.2 Colour

The colour of the CRX and BRX was measured using a Colourimeter (Minolta Chroma Meter, model CR-400, Japan), and the L^* , a^* , and b^* colour values were recorded.

3.2.3 Crystal morphology

The crystal morphology of all samples was determined using the method given by Toro-Vazquez, Charó-Alonso, Pérez-Martínez, and Morales-Rueda (2011). The CRX, BRX and RO were melted at 85°C and then dripped onto a microscopic slide and covered with a cover glass. Subsequently, the samples were held at room temperature for 1 h to achieve full gelation. Then, using a polarized light microscope (PLM) (Olympus, model BX51, Hamburg, Germany), the morphology was measured, and microphotographs were taken with a camera.

3.2.4 Crystal polymorphism

The crystal polymorphisms of CRX, BRX and RO were measured using an X-ray diffractometer (XRD) (Bruker, model AXS D8 Discover, Germany) at ambient temperature. The angular scans, $2\theta = 1$ to 50° at $2^\circ/\text{min}$, were performed using a copper X-ray source at 40 kV and 40 mA (Yılmaz & Öğütçü, 2014a).

3.2.5 Thermal behaviour

The thermal behaviour of the samples was determined according the method given by Dassanayake et al. (2009). To do this, 10 mg samples were accurately weighed in aluminium DSC sample pans, and the cover was sealed using a crimper press. The samples were heated from ambient temperature (30°C) to 90°C , cooled to 0°C and heated to 90°C at a heating and cooling rate of $2^\circ\text{C}/\text{min}$. The onset temperatures of crystallization (T_{OC}), onset temperatures of melting (T_{OM}), the crystallization temperatures (T_C), the melting temperatures (T_M), the melting enthalpy

(ΔH_M) and the crystallization enthalpy (ΔH_C) were analysed using a differential scanning calorimeter (DSC) (Perkin-Elmer, model PYRIS Diamond, USA).

3.2.6 Chemical analysis of the raw materials

3.2.6.1 Fatty acid composition

Fatty acid composition of waxes were analysed accordingly to the inhouse method based on the work of Lepage & Roy (1986) . The samples were blended using a blender, and 3 g samples were transferred into a screw cap tube. A 12 ml mixture of dicloromethane : methanol (2 : 1 v/v) was added and mixed using a vortex every 15 min for 1 h. The samples were filtrated using a Whatman No.1 filter. Then, approximately 20% of the total volume of 0.1 M KCl was added to the samples. The samples were then vortexed and centrifuged at 2,000 rpm for 10 min. The upper phase was discarded and collected to determine methylation.

The oil solutions were pipetted into a 200-L screw-cap tube, and then 1 ml of 0.5 mol/ml NaOH-methanol was added. The mixture was heated at 100°C for 15 min and cooled to room temperature. Then, 2 ml of BF₃-methanol (14%) was added to the mixture, and the mixture was heated again at 100°C for 1 min then cooled to room temperature. Then, 500 μ L of hexane and 5 ml of a saturated NaCl solution were added to the solution mixture, which was then mixed and centrifuged at 1,000 rpm at 25°C for 5 min. The upper phase was pipetted into a vial for injection into the GC.

FAME analysis by GC/MS/MS was conducted using a Thermo Trace Ultra GC with Polaris Q Ion Trap Mass Spectrometer GC/MS System (USA) equipped with a 60 m \times 0.25 mm 0.25 μ m i.d. MS TR-FAME capillary column (Thermo Scientific). The injector was set to 235°C and the detector to 220°C. Helium was used as the carrier gas at a flow rate of 1 ml/min. The split ratio was 20, and the split flow was 20 ml/min. The following temperature ramp was used: heated

initially in an oven at 50°C, held for 2 min, heated to 180°C (10°C/min, held for 15 min), and then heated to 230°C (4°C/min, held for 22.50 min).

3.2.6.2 Free fatty acids (FFA)

The FFA content of the CRX and BRX was determined using AOCS Official Method Ca5a-40 (2012).

3.2.6.3 Saponification number (SN)

The SN value of the CRX and BRX was determined using AOCS Official Method Cd 3-25 (2012).

3.2.6.4 Iodine value (IV)

The IV value of the CRX and BRX was determined using AOCS Official Method Cd1-25 (2012).

3.3 Bleached rice bran wax organogels and water-in-oil emulsions

3.3.1 Organogels from bleached rice bran wax preparation and physical properties analysis

3.3.1.1 Organogels preparation

The organogels were studied at 3, 5, 7 and 9% wax. The BRX was weighed and mixed with RO. The mixtures were heated to 85°C and held for 5 min to destroy all crystal nuclei; then, the samples were agitated using a magnetic stirrer at 200 rpm for 5 min resulting in a clear mixture of BRX and RO. The mixtures were cooled to room temperature (30°C). Bleached rice bran wax organogels (BRXO) were formed (Patel et al., 2013) and were stored at 4±2°C until analysis.

3.3.1.2 Physical properties analysis

1) Gelation time

The gelation time of the RO with BRX at different concentrations (3, 5, 7 and 9 wt%) was observed. After the mixtures were prepared as described in 3.3.1, the samples were cooled to room temperature, and gelation

was observed. The gelation time was measured as the time it took for the oil to stop flowing (Dassanayake et al., 2009).

2) Oil binding capacity (OBC)

The oil binding capacity was analysed following the method given by Yılmaz & Ögütçü (2014a). The weight of 1 ml of melted organogels was recorded (a) and placed in an Eppendorf tube. The tube was placed in a refrigerator for 1 h to allow organogel formation. Then, the tubes were weighed (b) and centrifuged at $9170 \times g$ for 15 min at 20°C . Any oil was drained from the tubes for 3 min, and they were weighed again (c). The oil binding capacity (% OBC) was calculated using the equations

$$\% \text{ Released Oil} = [(b - a) - (c - a)] / (b - a) \times 100$$

$$\% \text{ OBC} = 100 - \% \text{ Released Oil}$$

3) Texture analysis

The textural properties of the organogels, including the firmness, hardness and stickiness, were measured using a texture analyser (TA-XT2i, NY, USA) connected to a computer running the Stable Micro System (Texture Technologies Corp., Scarsdale, NY, USA). The organogels were analysed in their containers (4.2 cm diameter with an organogels depth of 3.5 cm) at room temperature ($30 \pm 2^{\circ}\text{C}$) with rounded-end probes with radial ends (diameter 12.5 mm). A 5-kg load cell was used to compress the samples at 1.0 mm/s to a depth of 10 mm from the surface. The load cell was then withdrawn at the same speed (modified from Hwang et al., 2013).

4) Solid fat content (SFC)

The SFC of the organogels was determined using nuclear magnetic resonance spectroscopy (NMR) (Bruker NMR Analyser 300 MHz Fourier 300, Bruker Optics, Inc., Billerica, Mass., USA). The organogels were melted and added to the NMR tubes to a height of approximately 5 cm. The samples were kept at 4

and 30°C for 24 h. Then, all samples were analysed at 4 and 30°C to determine the solid fat content (%SFC) values.

The colour, crystal morphology, crystal polymorphism and thermal behaviour of the organogels (BRXO) were measured using XRD following the procedures in 3.2.2, 3.2.3, 3.2.4 and 3.2.5, respectively.

The concentration at which the BRXO demonstrated the best qualities (shortest gelation time, highest OBC, a better texture, highest melting and crystallization temperatures, and highest SFC) was selected as the fat base to produce the water-in-oil emulsion and to study the storage stability.

3.3.2 Emulsion preparation and physical property analysis

3.3.2.1 Emulsion Preparation

A water-in-oil emulsion composed of 20 wt% water and 80 wt% bleached rice bran wax organogels (BRXO) was prepared. The organogels and water were heated to 90°C and held for 15 min. Then, the melted BRXO was slowly poured into the water and homogenized at 16,000 rpm for 10 min using IKA® Ultra-Turrax® T25 Homogenizer. The 30 g emulsion was placed into a glass container and cooled to room temperature, resulting in an emulsion prepared from the organogels (EO) (modified from Patel et al., 2013).

3.3.2.2 Physical property analysis

1) Emulsion stability index (ESI)

The ESI of all emulsion samples was determined following the method of Mirhosseini et al. (2008). The height of the emulsion (HE), cream (HC) and sediment (HS) phases were recorded. The emulsion stability index (% ESI) of the samples was calculated using the equation

$$\text{ESI (\%)} = 100 \times (\text{HE} - (\text{HC} + \text{HS}))/\text{HE}$$

2) Emulsion structure

The emulsion structure was studied according to the method given by Toro-Vazquez et al. (2011) using an Olympus BX51 (Hamburg, Germany). The sample was weighed, diluted with distilled water (ratio 1:50 w/v), placed on a microscopic slide, stained with methylene blue and covered with a cover glass. After that, photos were taken with a microscope and PLM equipped with a camera.

The colour, crystal morphology, and crystal polymorphism measured using an XRD and the thermal behaviour of the emulsion were measured following the procedures in 3.2.2, 3.2.3, 3.2.4 and 3.2.5, respectively.

3.3.3 Storage stability of bleached rice bran wax organogels and water-in-oil emulsions

After the BRXO, E and EO were produced, the samples were kept in clear glass containers with screw caps at 2 temperatures (4°C and 30°C) for 90 days. 1) Samples were stored at local room temperature (30±2°C), including rice bran oil stored at 30°C (RO30C), bleached rice bran wax organogels stored at 30°C (BRXO30C), an emulsion without BRXO stored at 30°C (E30C) and an emulsion prepared with BRXO stored at 30°C (EO30C). 2) Samples were stored in a refrigerator (4±2°C), including rice bran oil stored at 4°C (RO4C), bleached rice bran wax organogels stored at 4°C (BRXO4C), an emulsion without BRXO stored at 4°C (E4C) and an emulsion prepared with BRXO stored at 4°C (EO4C). The colour (L*, a*, b*), texture, crystal morphology, emulsion structure, emulsion stability index (%ESI), and oxidative stability of the samples were measured. During the storage period, measurements were performed at the end of each month, and for each measurement, the samples were used only once (Pandolsook & Kupongsak, 2018).

3.3.3.1 Physical properties analysis

The colour, texture, crystal morphology, and emulsion structure of the samples were measured following the procedures in 3.2.2, 3.3.1.2 (3), 3.2.3, and 3.3.2.2 (2), respectively.

3.3.3.2 Oxidative stability

Over the 90 days of storage at the two different temperatures (4°C and 30°C), the oxidative stability of the samples was monitored by measuring the peroxide value (PV) (Cd 8-53 method) and the thiobarbituric acid reactive substances (TBARS) value (Buege & Aust, 1978).

3.4 Policosanol organogels and water-in-oil emulsions

3.4.1 Extraction and purification of policosanol from bleached rice bran wax

3.4.1.1 Defatting

The bleached rice bran wax was defatted following the procedure in 3.2.1

3.4.1.2 Policosanol extraction and purification

The extraction method was modified from (Puengtham, Aryasuk, Kittiratanapiboon, Jeyashoke, & Krisnangkura, 2008). Five grams of the defatted bleached rice bran wax was mixed with 100 ml of 2 M of KOH in 80% ethanol and hydrolysed by refluxing for 3 h. The hydrolysed mixture was purified. The mixture was mixed with 140 ml toluene, 40 ml water and 20 ml ethanol and refluxed at 90°C with continuous stirring for 30 min. Subsequently, the temperature of the mixture was decreased to 70°C for 30 min without stirring. The mixture was placed into a separation funnel, and the toluene phase was separated. The toluene phase was purified by washing and overnight soaking with 140 ml isooctane, 40 ml water and 20 ml ethanol. The solvent was removed from the upper phase

using a rotary evaporator and was dried at 90°C in a hot air oven until the weight of the samples was stable, resulting in yellowish policosanols. The yield (%) of policosanols was calculated.

The policosanols were verified using thin layer chromatography on a 20 × 20 cm piece of aluminium and silica gel (60F254; Merck, Germany). The policosanols were dissolved in toluene, rice bran oil (as a triglyceride; TG), standard palmitic acid (as a free fatty acid; FFA) and stearyl alcohol (as a fatty alcohol) and were placed on a TLC plate. The developing solvent was a mixture of hexane, ethyl acetate and acetic acid (90:10:2, v/v/v), and the developed bands were resublimed using iodine.

3.4.1.3 Physical properties of policosanol

1) Compositional analysis of policosanol by GC-FID

Sample solutions were prepared by weighing the policosanols extracted from rice bran wax and mixing with isooctane. An Agilent 6890N series gas chromatograph (GC) with dual inlets and an FID detector was used to determine the policosanol composition. GC separations were performed using a HP-5 capillary column (5% phenyl methylpolysiloxane) (25 m × 0.32 mm × 0.17 m). The oven temperature was programmed as follows: the inlet temperature was set at 170°C. The temperature profile was 150°C for 3 min, increased to 280°C at 15°C/min and held at 280°C for 20 min. The carrier gas was nitrogen at a flow rate of 1 mL/min, and the detector temperature was 280°C. The hydrogen and air pressures were 40 and 450 mL/min, respectively. The injection volume was 1 L, and the split ratio was 1:30.

The colour and crystal polymorphism measured using an XRD and the crystal morphology and thermal behaviour of the policosanols (PC)

were measured following the procedures in 3.2.1, 3.2.2, 3.2.3 and 3.2.4, respectively.

3.4.2 Organogels from policosanol preparation and physical properties analysis

3.4.2.1 Organogel preparation

PC produced organogels at 12, 13.5 and 15 wt%. The PC was mixed with RO. The mixtures were heated to 90°C and held at that temperature for 5 min to destroy all crystal nuclei. Agitation using a magnetic stirrer at 200 rpm for 10 min resulted in a cleared mixture of PC and RO. The mixtures were cooled to room temperature (30°C). Policosanol organogels (PCO) were formed (Patel et al., 2013) and were stored at 4±2°C until analysis.

3.4.2.2 Physical properties analysis

The gelation time, oil binding capacity (OBC), texture analysis, and solid fat content (SFC) of the PCO were measured following the procedures in 3.3.1.2. The colour, crystal morphology, crystal polymorphism and thermal behaviour of the PCO were measured following the procedures in 3.2.2, 3.2.3, 3.2.4 and 3.2.5, respectively.

3.4.3 Emulsion preparation and physical property analysis

A policosanol emulsion was produced using 2 treatments: an emulsion prepared from policosanol organogels (PCE) and an emulsion prepared from 50% policosanol organogels mixed with 50% bleached rice wax organogels. This resulted in emulsions prepared from PCO mixed with BRXO (PCM).

3.4.3.1 Emulsion Preparation

Two water-in-oil emulsion samples were prepared following the method given in 3.3.2.1

3.3.2.2 Physical properties analysis

The emulsion structure and emulsion stability index (ESI (%)) were measured following the procedures in 3.3.2.2. The colour, crystal morphology, XRD crystal polymorphism and thermal behaviour of the emulsions were measured following the procedures in 3.2.2, 3.2.3, 3.2.4 and 3.2.5, respectively.

3.4.4 Storage stability of policosanol organogels and water-in-oil emulsions

The storage stability and physicochemical properties, such as the colour, texture, crystal morphology, emulsion structure, emulsion stability index and oxidative stability, of PCO, PCE and PCM were measured following the methods in 3.3.3.

3.5 Statistical analysis

All physical and chemical experiments were performed in triplicate, and the data were subjected to analysis using a completely randomized design (CRD) model. Analysis of variance (ANOVA) was performed at a 95% significance threshold. Significant differences among the means were determined via Duncan's new multiple range test (DNMRT).

CHAPTER IV

RESULT AND DISCUSSION

4.1 Physical and chemical properties analysis of raw materials

4.1.1 The physical and chemical properties

Table 2 showed the physicochemical properties of waxes. It was found that oils were trapped in both rice bran waxes, but more oil was found in CRX. For BRX, pigment substances and some oils are removed in the bleaching step. The oil content relates to the chemical quality of wax. Decreases in iodine and free fatty acids of the BRX indicated a substantial reduction of triacylglycerol, unsaturated oil, and free fatty acid, and improved the physicochemical properties of the wax (Pandolsook & Kupongsak, 2017).

The colour parameter including L* values (luminosity), a* values (redness/greenness), and b* values (yellowness/blueness) of the waxes were determined. The colour of CRX and BRX was significant different ($p < 0.05$). L* and b* values for CRX were lower than BRX, but the a* value was higher. CRX is dark brown. The material responsible for the colour and odour of wax is primarily resinous matter, a dark reddish-brown substance (Pandolsook & Kupongsak, 2017). It contributes the dark colour and off-odour of CRX (Fig. 8) (Vali et al., 2005).



Figure 8 The character of the CRX (a) and BRX (b)

Table 2 Physicochemical properties of crude and bleached rice bran wax

	CRX	BRX
Oil content (%w/w)	67.69 ^a ± 0.98	64.89 ^b ± 0.56
Colour		
L*	49.42 ^b ± 0.68	64.78 ^a ± 0.48
a*	7.66 ^a ± 0.99	5.04 ^b ± 0.48
b*	10.41 ^b ± 0.97	22.29 ^a ± 0.89
IV (mgI ₂ /g)	63.09 ^a ± 0.77	61.43 ^b ± 0.77
FFA (% as oleic)	0.27 ^a ± 0.00	0.16 ^b ± 0.00
SN (mgKOH/g)	141.13 ^b ± 0.94	153.72 ^a ± 0.87

Mean ± SD. Mean with different superscript letters along row are significantly different ($p < 0.05$)

Crystal morphology

The differences in fat crystal morphology were observed by microscopy. The morphology could be used to separate and identify the type of wax because each type of wax has different characteristics: the carnauba wax is dendritic crystals, the candelilla wax contains finely dispersed and grain-like particles, and the sunflower wax has fibrous crystals (Dassanayake et al., 2009). Fig. 9 demonstrates the crystal morphology of CRX and BRX in the bulk state at ambient temperature. The results indicate that the crystal morphology of both waxes was similar. The morphology of the wax crystals was long and needle-like, an appropriate characteristic for organogels formation (Terech & Weiss, 1997). The needle-like crystals are a good morphology for meshing well at intercrystalline interfaces to form the organogels network and assist in efficiently entrapping the liquid oils in the crystalline structure.

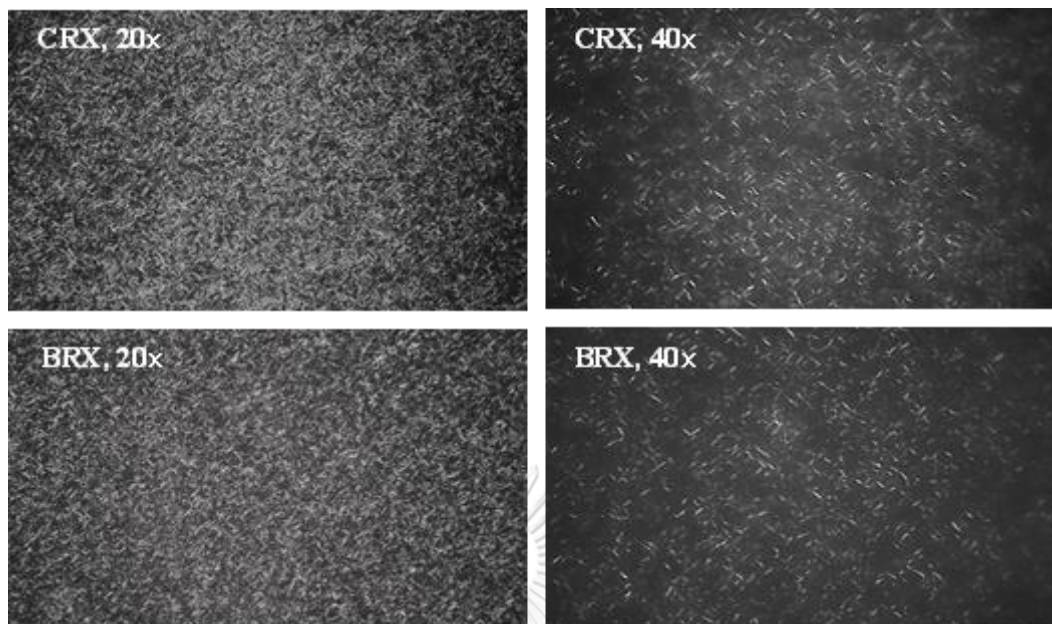


Figure 9 The polarized light microphotographs of CRX and BRX at magnification 20x and 40x

Crystal polymorphism

XRD was used to evaluate fat crystal polymorphisms of CRX and BRX. Fig.10 shows the XRD patterns of wax crystals in the bulk state at ambient temperature. The wide-angle analysis (WAXS) provides the characterized fat crystal polymorphism, the α , β' and β form was indicated. The strong intensity of two peaks was shown at 3.67-3.83 Å and 4.18-4.43 Å indicated the orthorhombic perpendicular or β' polymorphic form, which peaked near 4.6 or 4.71 Å, indicating to the triclinic parallel or β -polymorphic form. Two strong WAXS intensity peaks of CRX and BRX were located at 4.10, 3.70 Å and 4.12, 3.72 Å, respectively. The peak at 4.54 and 4.55 Å appeared in CRX and BRX, respectively. This result indicates that both waxes have a mixed β' - and β - polymorphic form. The BRX in this study had main peaks where similar results with purified rice bran wax are described by Blake et al. (2014). The small angle scattering analysis (SAXS; $2\theta = 1^\circ - 5^\circ$) provides the

information on lamellar longitudinal packing of the crystal. SAXS was related to chain length and chain tilt of the crystal structure (Campos, 2013; Schaink et al., 2007). The longitudinal organization of the fat crystal is formed in 2 configurations, a double (2L) and triple (3L) chain length lamellar structure, located in the range of d-space at approximately 14–50 Å and 55–75 Å for 2L and 3L, respectively (Kalnin, Schafer, Amenitsch, & Ollivon, 2004; Lopez, Bourgaux, Lesieur, & Ollivon, 2007). The BRX exhibited the SAXS peaks at 71.47, 42.5, 35.51 and 24 Å (Fig. 10 b), indicating that the chain length lamellar structure of BRX crystal was mixed with 2L and 3L.

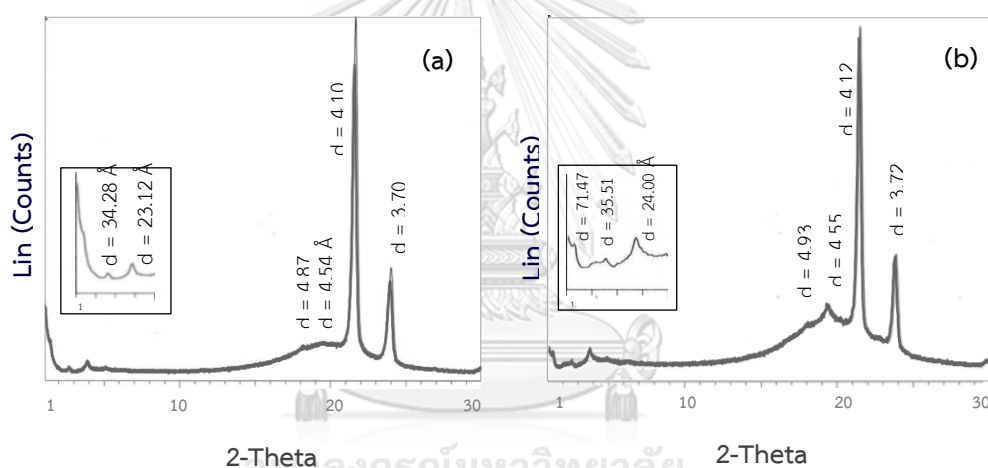


Figure 10 The X-ray diffraction patterns of the samples CRX (a) and BRX (b) in bulk states

Thermal behaviour

Fig. 11 shows DSC heating and cooling thermopeaks of CRX and BRX in bulk states. The samples melted at 90°C to destroy all seed crystals, then cooled to 0°C and reheated to 90°C again. The compositional differences affected the thermal behaviour of the waxes (Dassanayake et al., 2009). A DSC thermogram indicate the characteristics of the wax, which are different among the wax types. CRX is

composed of multi-components in the system (Table 3). These multicomponents still contain the impurities such as TAG, resinous matter (RM), and other substances that are mixed together in the wax with different ranges of crystallization and melting point. Therefore, the crystallization and melting peaks of CRX showed a broad and blunt character. When CRX was bleached, resulting in BRX, the other impurities including RM were removed. Thus, the BRX showed narrower and sharper melting and crystallization peaks than CRX.

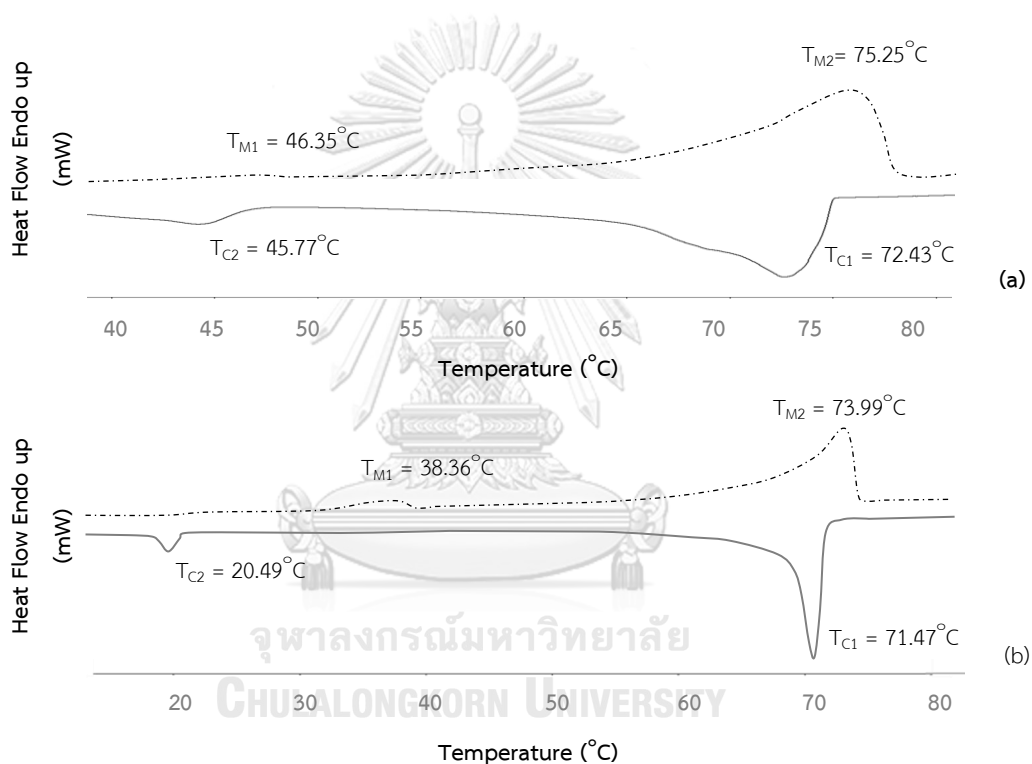


Figure 11 Cooling (solid line) and heating (dotted line) DSC thermograms of CRX (a) BRX (b) in bulk states

Moreover, the compositions of CRX and BRX both consisted of multiple chemical types. Therefore, multiple melting and crystallization peaks were shown. The melting and crystallization peaks of purified rice bran wax showed a single peak (Dassanayake et al., 2009). Melting is an endothermic process that the system requires energy to process. On the other hand, crystallization is exothermic,

as energy is released during the process. The thermal behaviour including onset temperatures of melting (T_{OM}), onset temperatures of crystallization (T_{OC}), melting temperatures (T_M), crystallization temperatures (T_C), melting enthalpy (ΔH_M) and crystallization enthalpy (ΔH_C) of CRX were higher than the corresponding parameters for BRX. The highest ΔH_M values of CRX and BRX were 68.76 and 51.38 J/g, respectively, whereas the highest values of ΔH_C for CRX and BRX were -61.19 and -49.81 J/g, respectively (data not shown). The enthalpies between melting and crystallization were different, with the enthalpy of melting higher than the enthalpy of crystallization. The higher ΔH_M and T_M were related to the thermal stability and thermal resistance of wax. Thermal stability refers to the good stability and resistance to decomposition at high temperatures, which is an important property of fat-based products, producing the high melting points of margarine and shortening. Although CRX includes melting and crystallization temperatures that are better than those for BRX, CRX is composed of many impurities such as residual oil, resinous matter, gum, phosphorus and other traces (Vali et al., 2005). These impurities affect gel formation and crystallization of rice bran wax (Jadhav et al., 2012). In addition, Ghosh & Bandyopadhyay (2005) found that the crystal growth was influenced by the cooling rate, temperature, gum, and triglyceride content. Therefore, BRX was chosen for study to produce the organogels.

Fatty acid composition

Table 3 presents the fatty acid compositions of the raw materials, CRX and BRX. The fatty acid composition of CRX contained 21 fatty acids varying from C12 to C24, while the BRX contained 15 fatty acids from C14 to C24. For both waxes, the main common fatty acid was C18:1, followed by C16, C24, C18, C18:2, C20, C14, C16:1, C:17 and C12. Tada et al. (2007) and Dessanayake et al. (2009) reported that the purified rice bran wax was composed of fatty acids with carbon numbers

varying from 16 to 32. The 10 unidentified fatty acids were found in CRX but after the wax was bleached, only 5 unidentified fatty acids were found, possibly caused by the bleaching step removing some oil related to composition and the amount of fatty acids changing. Moreover, the colourant substance from raw material pigment was removed in this step.

Table 3 Fatty acid composition of crude and bleached rice bran wax

Fatty acids	CRX	BRX	Fatty acids	CRX	BRX
C12	0.40 ± 0.00	nd	C20	1.01 ^b ± 0.01	1.25 ^a ± 0.11
C14	0.57 ^a ± 0.01	0.19 ^b ± 0.02	Un4	2.11 ^b ± 0.06	2.53 ^a ± 0.06
C16	18.29 ^b ± 0.13	25.75 ^a ± 2.23	Un5	0.32 ± 0.03	nd
C16:1 ^{Ns}	0.11 ± 0.02	0.11 ± 0.01	Un6	2.19 ^b ± 0.10	2.78 ^a ± 0.16
C17	0.04 ^b ± 0.00	0.07 ^a ± 0.01	Un7	6.74 ^b ± 0.18	8.26 ^a ± 0.15
C18	4.91 ^a ± 0.05	4.38 ^b ± 0.19	Un8 ^{Ns}	1.35 ^b ± 0.06	2.01 ^a ± 0.59
Un1	0.82 ± 0.04	nd	C22	9.31 ^a ± 0.01	7.39 ^b ± 0.02
Un2	0.19 ± 0.04	nd	Un9	0.37 ± 0.00	nd
C18:1 cis	29.07 ^b ± 0.09	32.74 ^a ± 1.91	C24	20.04 ^a ± 0.31	11.05 ^b ± 0.09
Un3	0.38 ^b ± 0.01	0.43 ^a ± 0.01	Un10	0.63 ± 0.00	nd
C18:2cis ^{Ns}	1.59 ± 0.05	1.61 ± 0.12			

Mean ± SD Mean with different superscript letters along row are significantly different ($p < 0.05$)

Un mean unidentified, nd mean not detect, Ns mean not significantly different ($p \geq 0.05$)

4.2 Bleached rice bran wax organogels and water-in-oil emulsions

4.2.1 Physical properties of organogels from bleached rice bran wax

Gelation time

The BRX contained 64.89% oil so that the organogels at 3, 5, 7 and 9% wax concentration used BRX at 8.55, 14.25, 19.95 and 25.64 wt%, respectively. The physicochemical properties of the BRX organogels (BRXOs) are presented in

Table 4. The gelation time is the duration time for the organogelator to form the gel. At 3% wax concentration, the gel did not form. From the results, the minimum concentration of BRX required for gel formation was 5%. At 5, 7 and 9% wax concentration, the gelation times were approximately 8, 16 and 25 min, respectively. The gelation time was faster by approximately 2-3 times when the wax concentration increases; similar results with different rice bran wax concentrations were found by Dassanayake et al. (2009).

Oil binding capacity

The oil binding capacity (OBC) is an important property of organogels that indicates the potential of the organogelator to form the gel (Yılmaz and Öğütçü, 2014a). The OBC value represents the efficacy of the 3D gel network for the organogelator to entrap the liquid droplets. The highest OBC shows the strongest network structure. As shown in Table 4, the results indicate that the volume of additional wax affected the OBC values. The OBC values of organogels at a wax amount of 7 and 9% were higher than 98%, showing that these levels were enough to stabilize network gel formation. In this study, there was no application of the shearing force during crystal formation. Therefore, the high OBC was observed. The factor influencing the OBC value was the high temperature and shear force application during crystal formation. Da Pieve, Calligaris, Co, Nicoli, & Marangoni (2010) determined the OBC of organogels from monoglyceride with cod liver oil. They found that the shearing condition during crystal formation resulted in a weaker gel and increased the oil release.

Colour

At low wax concentrations, the gel was translucent and at higher wax concentrations the gels were opaque. The optical clarity of organogels was related to the cross-sectional shape and thickness of the fibre bundles. At the high

concentrations, the opaque property was illustrated (Terech, Pasquier, Bordas, & Rossat, 2000). The cross-sections and fat crystals had scattering properties that cause the organogels to be highly luminous (L^*) (Table 4). The wax amount in the organogels increased the effect as the L^* values increased, and similar results were obtained for a^* and b^* values ($p < 0.05$). Moreover, the colour of the organogels was dependent on the original colour of the raw material and the organogelator (Öğütçü & Yılmaz, 2015a).

Texture analysis

The textural parameters, including firmness, hardness and stickiness of the organogels, were determined (Table 4). All parameters of the samples were significantly varied with the increase in the wax concentration ($p < 0.05$). The organogels with 9% wax concentration were harder and more adhesive than the organogels at a lower wax level. The needle-like crystal shape of BRX produced the stronger crystal network, and the amount of solid fat content (SFC) and the strongly dense fat crystal network of the organogels resulted in increased hardness (Dassanayake, Kodali, & Ueno, 2011; Liang, Li, Xu, & Li, 2014).

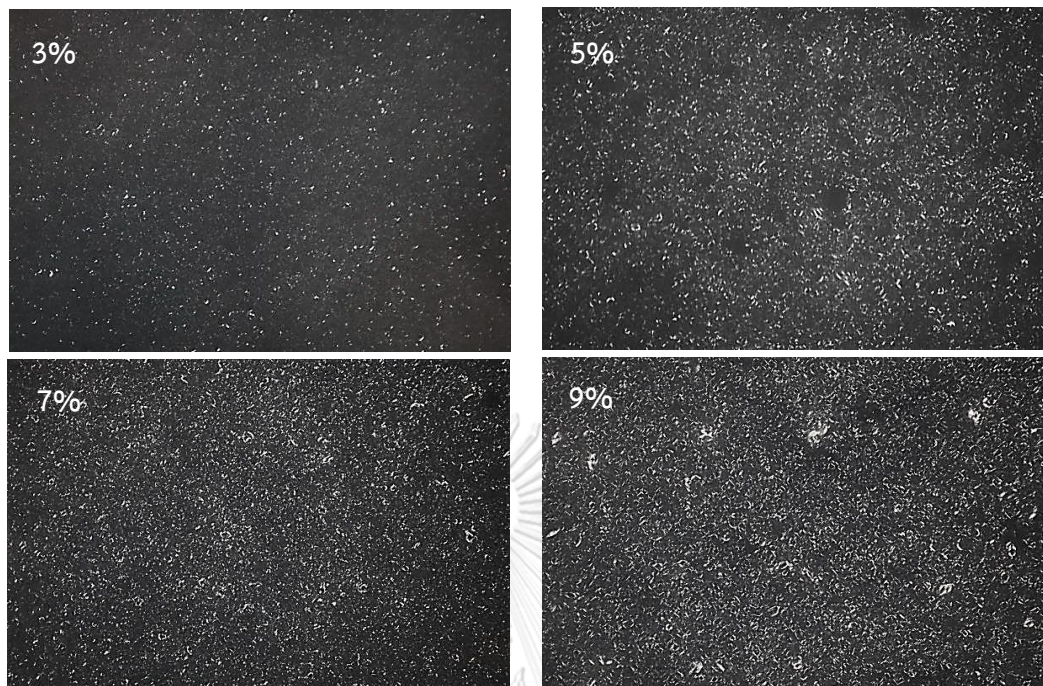
Table 4 Physical properties of organogels at different concentration of bleached rice bran wax

Wax concentration (%)	Gelation time (min:sec)	Oil binding capacity (%)	Colour			Texture		
			L*	a*	b*	Firmness (g)	Hardness (g.sec)	Stickiness (g.sec)
3	No gelation	57.49 ^c ± 0.79	28.71 ^d ± 0.53	-1.21 ^d ± 0.06	6.39 ^d ± 0.36	5.39 ^d ± 0.48	37.61 ^d ± 3.16	-3.37 ^a ± 0.35
5	25 : 11	86.80 ^b ± 1.66	32.79 ^c ± 0.78	-0.82 ^c ± 0.08	9.67 ^c ± 0.58	21.37 ^c ± 1.46	154.47 ^c ± 4.65	-11.88 ^b ± 0.67
7	16 : 29	98.81 ^a ± 1.72	35.87 ^b ± 0.84	-0.39 ^b ± 0.20	12.18 ^b ± 1.05	68.17 ^b ± 2.79	520.61 ^b ± 5.54	-32.05 ^c ± 2.54
9	8 : 16	99.75 ^a ± 0.42	39.68 ^a ± 0.78	-0.18 ^a ± 0.15	14.55 ^a ± 0.82	170.82 ^a ± 3.80	1430.29 ^a ± 12.37	-88.14 ^d ± 5.72

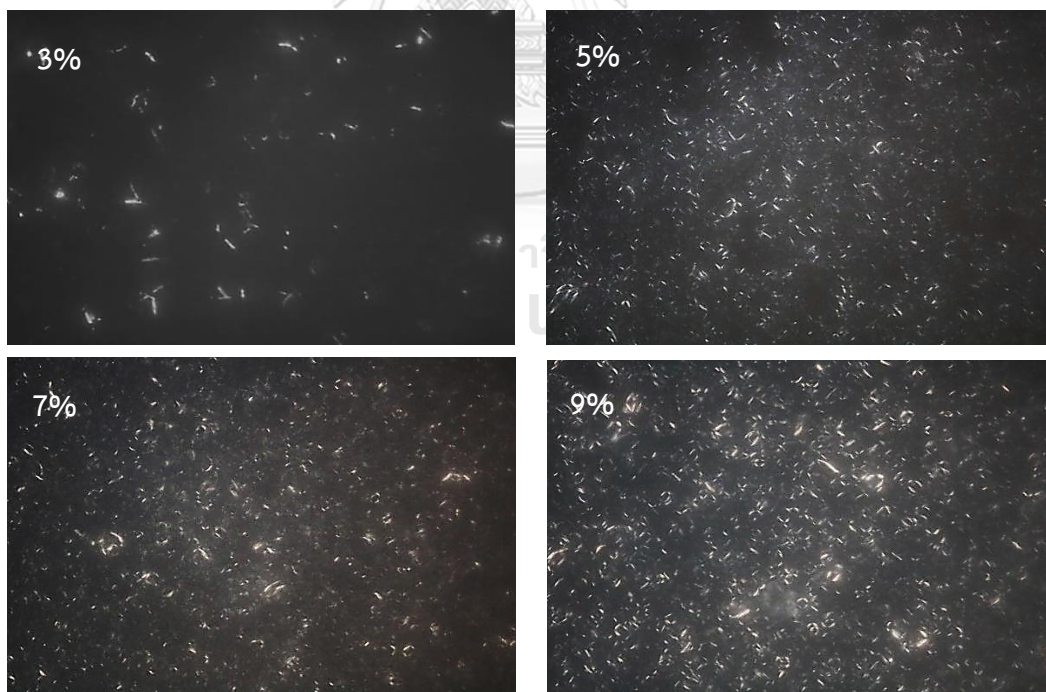
Mean ± SD. Mean with different superscript letters along a column are significantly different (p < 0.05)

Crystal morphology

The polarized light microscopy (PLM) measurement of BRXO at different wax concentrations are shown in Fig. 12. The PLM microphotographs provide the information of the fat crystal structures in organogels. The crystal morphology of all organogels samples showed long needle-like fibrous. The amount and sizes of the crystals in the organogel network increased with the wax addition level. The microphotograph of organogel showed results similar to the results of Dassanayake et al. (2009), who reported that the rice bran wax organogels have a needle-like and/or fibre-like crystal structure with the crystal lengths varying between 10 to 20 μm and the size of the crystal increased with increased rice bran wax concentration, which induced a strong network and harder gels. Blake et al. (2014) stated that the fibre-like conformation of the gelator is ideal for gelation forming because the surface area for high-aspect-ratio morphology of the fibre structure was much better than the surface area for lower-aspect-ratio morphology of sphere or platelet structures, for an equal volume of organogelator mass. The high surface area of morphology allowed the formation of microstructural elements that was responsible for the elastic or solid-like character of organogels, while also fostering greater interaction between molecules of gelator and the organic solvent. This helped in the entrapment of the oils in the crystal network, which related to higher OBC, higher melting and crystallization temperatures of the organogels (Pandolsook & Kupongsak, 2017; Dassanayake et al., 2011).



(a)



(b)

Figure 12 The polarized light microphotographs of the BRXO at different wax concentration at magnification 20x (a) and 40x (b)

Crystal polymorphism

The polymorphisms of RO and BRXO at different wax concentrations (3, 5, 7 and 9 wt%) were indicated by XRD. The RO showed only one main peak in WAXS at 4.57 Å, indicating the β -form crystal form, while all BRXOs showed multiple peaks at 3.72, 4.11 or 4.12 and 4.56 to 4.59 Å, specifying that the fat crystals of the organogels were composed mainly of β' -form crystals and next β -form crystals. The β -form occurred, and it may have been caused by fat crystals transformed from β' - change to the β -form, due to change towards the most thermodynamically stable form (Sato, 2001). Among of the three types of fat crystal polymorphs, α -, β' -, and β - form, the β' -form type in lipid-based products presented good functional properties such as the higher melting properties, texture smoothness, and good mouthfeel (Dassanayake et al., 2009; Parish, Boos, & Li, 2002; Sato, 2001). In addition, the β' -form polymorph type had the proper form to incorporate the air into structure of lipid-based products such as margarine and shortening, which promoted the good quality of baked goods (Ako & Min, 2002). The peaks of BRXO located in WAXS and SAXS region were like the candelilla wax, similar in composition. The SAXS peaks of all samples appeared at approximately 21 Å which can identify the 2L longitudinal packing forms (Fig. 13).

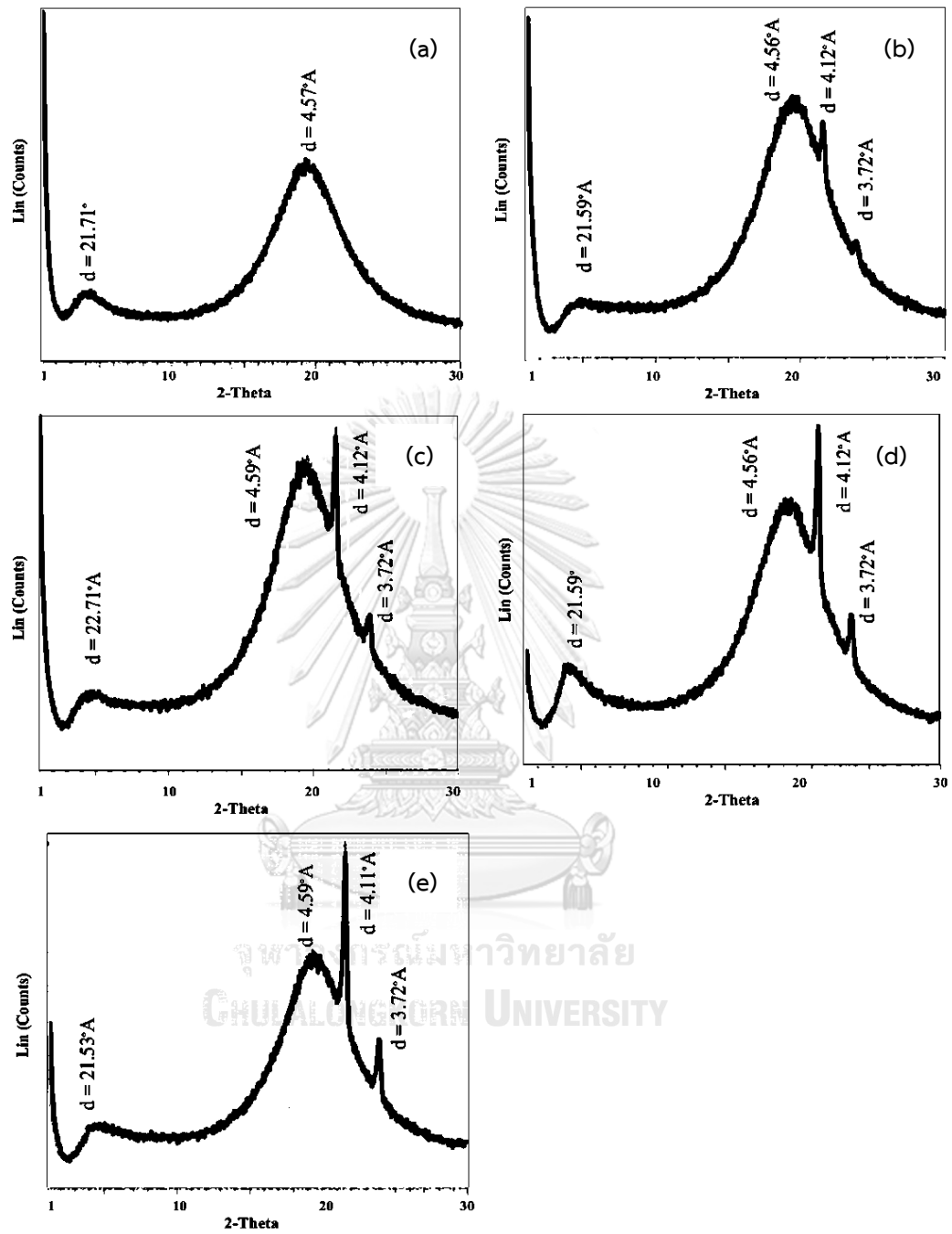


Figure 13 The X-ray diffraction patterns of 0% wax (RO) (a) and the BRXO at 3% (b), 5% (c), 7% (e), and 9% (f) wax concentration

Thermal behaviour

The results of thermal behaviour analysis are shown in Table 5. The crystallization behaviour (T_{oc} , T_c and ΔH_c) and melting behaviour (T_{om} , T_m , and ΔH_m) increased with increasing wax concentrations ($p < 0.05$). Moreover, the degree of supercooling ($\Delta T = T_m - T_c$) of samples decreased with increasing wax levels from 8.05 to 4.76°C of 3 to 9% wax concentration, respectively. These results related to the rate of crystallization, which showed that, at high wax concentrations, the crystallization rate was relatively high.

The solid fat content (SFC) can be measured by nuclear magnetic resonance (NMR), which presents the changes in consistency and plasticity at different temperatures in lipid food products (Augusto, Soares, Chiu, & Gonçalves, 2012). Table 5 shows the SFC of organogels at 2 temperatures, refrigerator temperature (4°C) and room temperature (30°C). The SFC increased with increasing wax concentration increases ($p < 0.05$). All samples with SFC at higher temperatures (30°C) were lower. However, the SFC of the samples was lower or similar to the additional levels of the wax, possibly because at those temperatures, some of wax was in a liquid state (Co & Marangoni, 2012).

At 9% wax concentration, the organogels had a shorter gelation time and higher OBC. Moreover, the physical properties of organogels such as the firmness and hardness values were statistically significant ($p < 0.05$). Therefore, the 9% wax as the fat base was selected to produce the water-in-oil emulsion (EO).

Table 5 Thermal properties and solid fat content (%) of bleached rice bran wax organogels (BRXO)

Wax concentration (%)	Crystallization				Melting				SFC (%)	
	T _{oc} (°C)	T _c (°C)	ΔH _c (J/g)	T _{om} (°C)	T _M (°C)	ΔH _M (J/g)	4°C	30°C		
3	55.30 ^d ± 0.04	54.09 ^d ± 0.35	-3.21 ^d ± 0.01	50.85 ^d ± 0.33	62.14 ^d ± 0.28	3.10 ^d ± 0.69	3.26 ^d ± 0.14	3.01 ^d ± 0.03		
5	58.98 ^c ± 0.00	58.03 ^c ± 0.07	-6.11 ^c ± 0.61	54.45 ^c ± 0.75	64.53 ^c ± 0.16	5.14 ^c ± 0.64	4.36 ^c ± 0.27	3.58 ^c ± 0.06		
7	61.79 ^b ± 0.21	60.76 ^b ± 0.31	-9.98 ^b ± 0.10	56.47 ^b ± 0.73	66.38 ^b ± 0.24	7.09 ^b ± 0.81	5.42 ^b ± 0.45	4.21 ^b ± 0.02		
9	64.31 ^a ± 0.16	62.25 ^a ± 0.23	-13.76 ^a ± 1.05	61.54 ^a ± 0.02	67.01 ^a ± 0.05	11.11 ^a ± 0.17	6.22 ^a ± 0.69	4.96 ^a ± 0.03		

Mean ± SD. Mean with different superscript letters along a column are significantly different (p < 0.05)

4.3 Water-in-Oil emulsion from organogels

4.3.1 Physical properties

The emulsion was composed of 80% fat base (or organogels) and 20% aqueous phase, without the addition of a stabilizer or an emulsifier. The physical properties of those emulsions are shown in Table 6. EO showed no separated oil or sediment, but this was found in emulsions without BRXO (E). The ESI results showed that the BRX had good functional properties to stabilize the water-in-oil emulsion. The colour values (L^* , a^* , and b^*) were significantly different between E and EO, with the EO higher than the E. The crystal fat had refraction properties resulting in significant lightness (L^*) in EO. The firmness, hardness and adhesiveness of EO were 103.78 g, 736.70 g.sec, and -60.86 g.sec, respectively, but were not detected in the E. All the textural parameters of EO were lowered approximately 1.4- to 1.9- fold compared with the BRXO at 9% wax concentration (Table 4) due to the 20% water in the emulsion.

Table 6 Physical properties of emulsion (E) and emulsion prepared from 9% wax concentration organogels (EO)

Emulsion	Stability (%)	Colour			Texture		
		L^*	a^*	b^*	Firmness (g)	Hardness (g.sec)	Stickiness (g.sec)
E	14.54 ^b ±0.49	54.52 ^b ±1.89	-2.78 ^b ± 0.07	8.35 ^b ± 0.33	nd	nd	nd
EO	100.0 ^a ±0.00	59.59 ^a ±0.53	-0.32 ^a ± 0.09	20.17 ^a ± 0.07	103.78±5.63	736.70±19.47	-60.86±5.63

Mean ± SD. Mean with different superscript letters in column are significantly different ($p < 0.05$)

nd: Non-detect

The thermal behaviour analysis is shown in Table 7. The thermal behaviour of EO shows higher values than that of E. The EO can form crystals at the

high temperature ranges of 62.43 to 63.13°C. The temperature at which the fat started to melt was 49.61°C, and the melting temperature was 66.99°C. The enthalpy of melting (ΔH_M) and crystallization (ΔH_C) of emulsion were 8.68 and -9.25 J/g, respectively. The fat crystal polymorph of EO was composed of β' - and β - form crystals with the 2L longitudinal packing forms similar to BRXO (Fig. 14).

Table 7 Thermal properties of emulsion (E) and emulsion prepared from 9% wax organogels (EO)

	Crystallization			Melting		
	T_{oc} (°C)	T_c (°C)	ΔH_C (J/g)	T_{om} (°C)	T_M (°C)	ΔH_M (J/g)
E	$22.45^b \pm 0.06$	$22.59^b \pm 0.12$	$-0.02^b \pm 0.00$	$22.78^b \pm 0.02$	$22.54^b \pm 0.09$	$0.02^b \pm 0.00$
EO	$63.13^a \pm 0.61$	$62.43^a \pm 0.80$	$-9.25^a \pm 0.08$	$49.61^a \pm 0.78$	$66.99^a \pm 0.23$	$8.68^a \pm 0.51$

Mean \pm SD. Mean with different superscript letters in column are significantly different ($p < 0.05$)

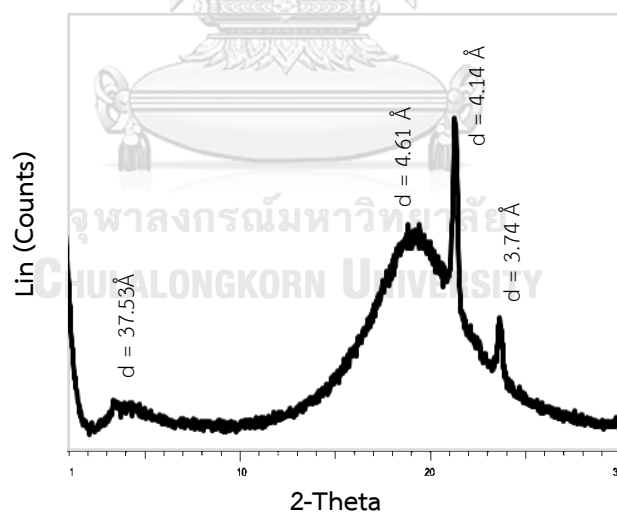


Figure 14 The X-ray diffraction patterns of EO

The EO microstructure is shown in Fig. 15. The water droplets were dispersed in the continuous fat phase as a crystal network. They were strongly trapped by the crystal network and by interfacially adsorbed particles or Pickering crystal

particles. This structure occurred due to the unique character of organogels, which can provide emulsion kinetic stability by hindering droplet-droplet contact. Moreover, the Pickering particle built a steric barrier between the adjoining water droplets, thereby preventing droplet clashing, film drainage, coalescence, and phase separation (Ghosh & Rousseau, 2011) related to the high emulsion stability index of EO.

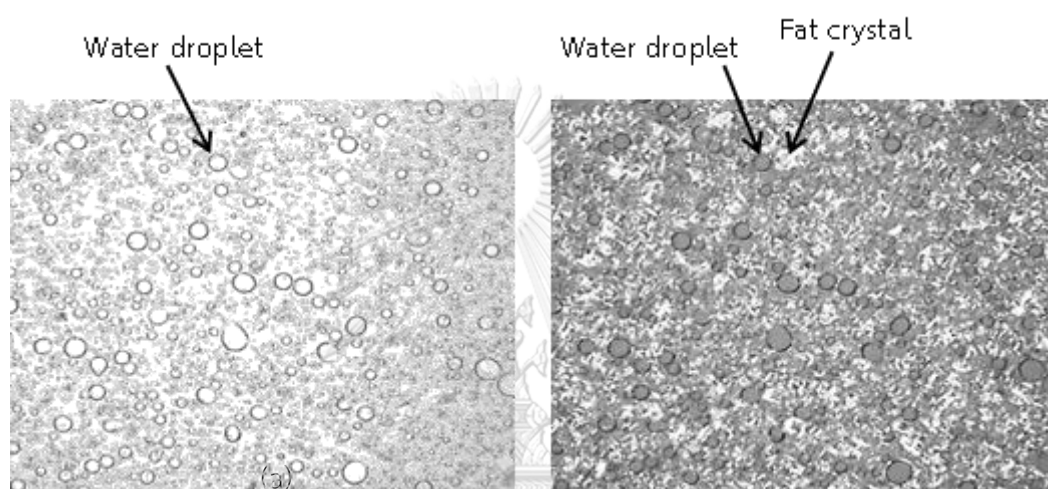


Figure 15 Microstructure of the EO using optical microscopy under normal (a) and polarized light (b) at magnification 40x

4.4 Storage stability of bleached rice bran wax organogels and water-in-oil emulsions

Colour

The colour of the samples was analysed and is shown in Fig. 16. The sample lightness (L^*), especially for the sample stored at 30°C, showed a significantly decreased ($P < 0.05$). L^* value with storage time increase except for the lightness value of EO4C, which did not change. This change may be caused by the lipid oxidation induction that showed loss and change of colour, the nutrient value, and accumulation of altered compounds, including the production of off-flavours characteristic in food products (Wąsowicz et al., 2004). Moreover, the droplet

aggregate size in the structure increased due to the oil droplet flocculation aggregates produced, which led to the increased light transmission through the emulsion (Kupongsak & Sathitvorapojjana, 2017). These results affected the lightness (L^*) values as the E4C and E30C decreased. Additionally, the storage temperatures affected the colour. At low temperature (4°C) dense fat crystals and increased crystal branching were induced, resulting in more light diffraction that increased the L^* values. Therefore, the BRXO4C showed more lightness value than BRXO30C. For the red ($+a^*$) and yellow colour ($+b^*$) of the sample during storage at 90 days, a slight increase occurred in the a^* value, but the b^* values were significantly decreased ($p < 0.05$) as the storage time increased. The lipid oxidation may affect the change in a^* and b^* values, and the colour of foods can be changed by the oxidation of labile pigments such as carotenoids and chlorophyll (Finley & Given, 1986).

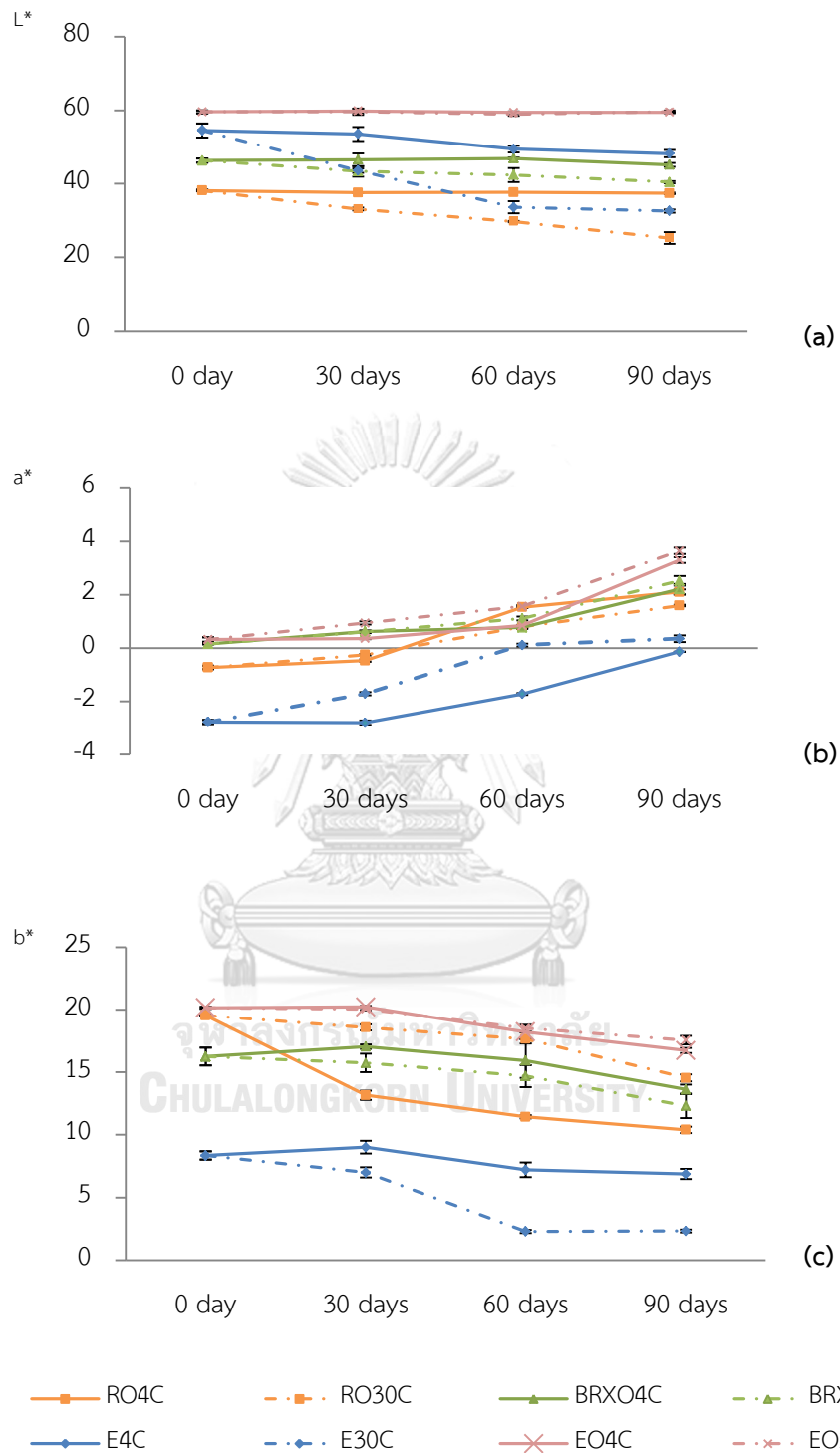


Figure 16 The colour L* (a), a* (b) and c* (c) value of RO, BRXO, E and EO storage at 4°C and 30°C for 90 days

Texture

The texture parameters, including the firmness, hardness and stickiness, changed during storage and are presented in Fig. 17. The BRXO4C had highest values of all textural parameters, while EO30C showed the lowest value. The firmness value of BRXO4C and BRXO30C ranged from 175.77 to 250.15 g and from 54.75 to 66.42 g, respectively. The EO4C and EO30C showed firmness values ranging from 74.87 to 181.47 g and 10.02 to 17.57, respectively (Fig. 17 a). The firmness of both EOs was lower than BRXO at both storage temperatures ($p < 0.05$) because the EO is composed of 20 wt% water. The samples stored at 4°C had higher firmness than the samples stored at 30°C. In addition, the firmness of the samples stored at 30°C did not change during the storage. The hardness value (Fig. 17 b) had similar trends with firmness during storage for both the temperature and time of storage. The lowest hardness value of BRXO30C was 368.80 g.sec and BRXO4C was highest at 1926.71 g.sec, while the ranges for EO30C and EO4C were from 63.44 g.sec to 1244.58 g.sec, respectively. The strong consistency of solid bridges between fat crystals were associated with an increase in the hardness of the fat systems (Ribeiro et al., 2015). Moreover, the differences in the crystalline structure, including crystal size, size distribution, crystal shape, crystal polymorphism, and surface characteristics affected textural properties in fat-based products (Ciftci et al., 2009). The stickiness of BRXO4C and BRXO30C ranged from -163.06 to -18.6 g.sec, and the stickiness value of EO4C and EO30C ranged from -66.22 g.sec to -6.07 g.sec. Fig. 17 c showed that, when the storage time increased, the stickiness of BRXO4C and EO4C obviously changed, possibly because the fat crystal network was formed and dense, due to strong mutual adhesion. Thus, an increased amount of force was required to overcome the attractive and adhesion forces between the probe and sample resulting in an increase in the stickiness value. Moreover, increasing the strength of the structured network affected the values of hardness and firmness, which were increased. From

the textural properties, the BRX fat crystals and BRXO efficiently formed and developed the crystal network in the emulsion structure, which inhibited the coalescence of water droplets and resulted in a highly stabilized emulsion, which could also improve the stability of the emulsion system without addition of the emulsifier or stabilizer. This result agreed with the research of Dassanayake et al. (2009), which reported that the rice bran wax led to the greater texture properties and stronger network organogels than the carnauba and candelilla. Furthermore, they found that the wax type influences the texture of organogels due to the thermal behaviour, crystal behaviour, shape and size of each wax. The needle-like fibrous crystal shape enhanced the stronger network, higher viscosity and harder gel followed by high melting temperatures and crystallization temperatures. Öğütçü & Yilmaza (2014) found that wax-based organogels (such as the carnauba wax) had higher textural properties than organogels from monoglycerides, the hardness and firmness of monoglyceride organogels at 4 and 20°C obviously decreased, whereas the carnauba wax organogel was slightly changed, during the 90 day storage period.

This study showed that the texture properties of the EO samples changed slightly, and the EO samples were quite stable in texture during the storage period, indicating that BRXO and EO could be stored at ambient temperature without the need for refrigeration during storage or transportation. Moreover, this result demonstrated that, BRXO and EO had a good potential application for use to produce the commercial oil- structured product and W/O emulsion products.

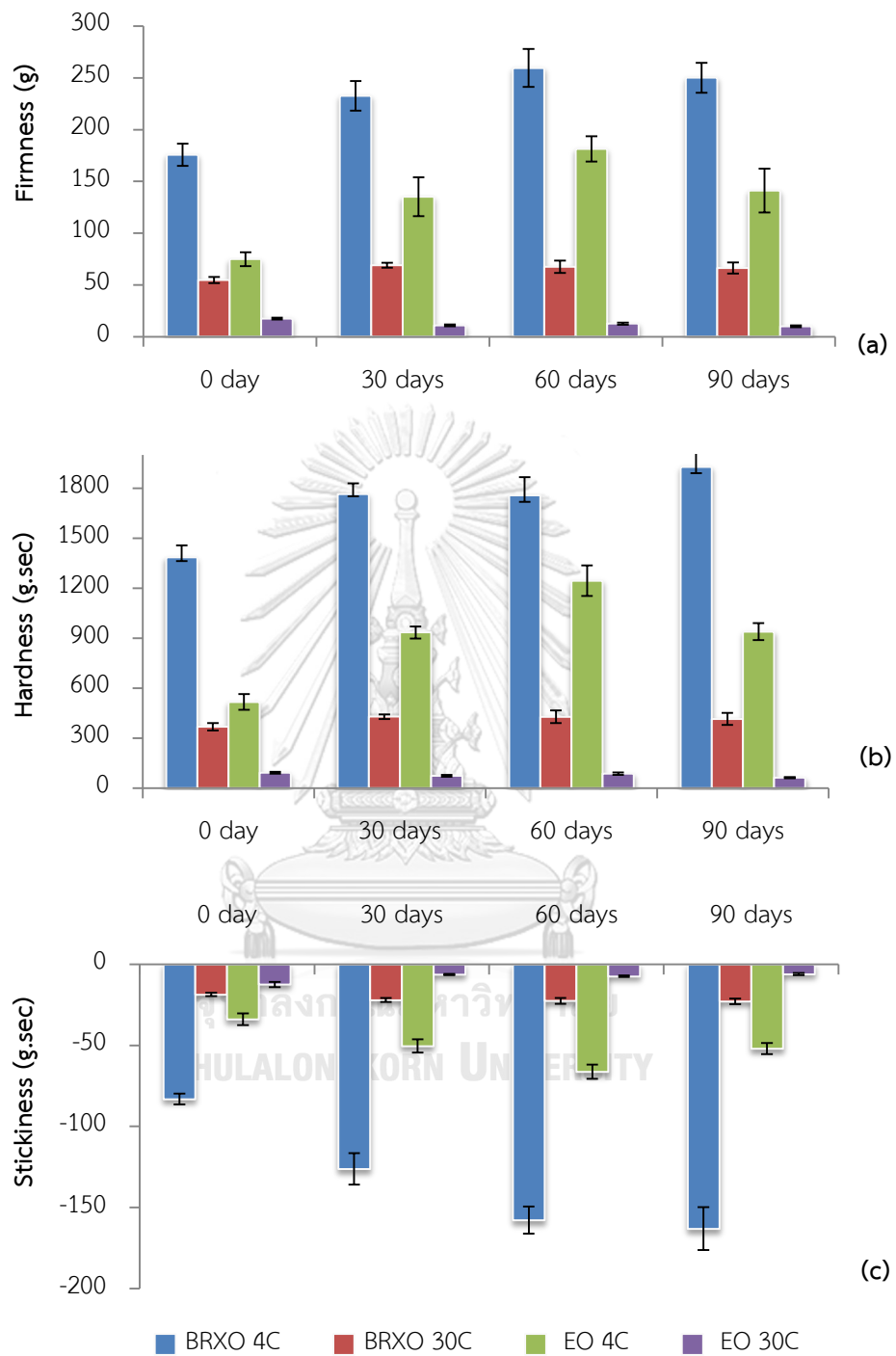


Figure 17 Textural changes in firmness (a), hardness (b) and stickiness (c) during storage in BRXO and EO at 4°C and 30°C for 90 days

Crystal morphology

The crystal morphology of the samples was observed by PLM. The morphology of a fat crystal can give some information to explain the changes in the textural properties. The PLM images are shown in Fig. 18 and 19. Most of the fat crystals were small, overlapping and clustered, making it difficult to count the number and size of the crystals by PLM. When observed, all the samples from PLM images showed that the amount and size of the crystals were increased with increased storage time, whereas the RO30C appeared unchanged. The storage conditions such as temperature and time are major factors influencing the crystallization process. The nucleus is the smallest crystal contained in the liquid oil at the appropriate temperature. During storage at constant temperature, the nucleation process may occur, with new nuclei forming in the presence of the existing crystal. This nucleation process also acts as the nuclei for a further crystallization under constant conditions or certain conditions, and the nuclei also develop via integration of triacylglycerol (TAG) molecules of liquid oil (Walstra, 1987). Then, the crystals grew, and the molecule of liquid oil migrated and moved to the crystal surface. Then, they rearranged and orientation occurred (Metin & Hartel, 2005). Furthermore, during storage, the different complex spectacles occurred and changed to the crystalline network. The post-crystallization, including the polymorphic transitions, changed the low stability polymorphs to more stable polymorphs, the new crystalline particles appeared, and the formation of a solid bridge between the molecule and Ostwald ripening occurred (Ojijo et al., 2004). The crystalline particles at the juncture area and within the network have rearranged their molecular packing, which developed the structural organization. In Fig. 18, the RO30C crystal shape was dispersed and small plate-like crystals formed. However, the crystals of RO4C were densely packed and appeared as a crystal group within the system. Moreover, these crystals appeared larger in size than those of RO30C for all

the storage periods. The morphology of all BRXO samples (shown as Fig. 19) exhibited the needle-like and fibrous shape. When the temperature and storage period differed, the crystal volume, crystal size and available crystalline agglomerate were increased varying by lower storage temperature and longer storage time. The result from this research was the same as the results of Dassanayake et al. (2009); they reported that the crystal morphology of the three wax types (rice bran wax, candelilla wax, and carnauba wax) differed, especially the rice bran wax crystal. The morphology of the rice bran wax crystal had a needle-like shape, which was related to good gel formation, whereas the crystal morphology of carnauba and candelilla wax showed spherulitic structures, which was not good for inducing the formation of organogels. Blake et al. (2014) reported that organogelator of fibre-like shape had an ideal structure because this structure forms good gelation because the organogelator mass is equal and the surface area for a high-aspect-ratio morphology, such as a fibre shape, is much better than the surface area for a low-aspect-ratio morphology, such as sphere or platelet shape.

Post-crystallization processes occur in the organogels system during storage and forming the solid bridges between crystals that increase the gel hardness (deMan & deMan, 2001; Himawan, Starov, & Stapley, 2006; Walstra, Klok, & van Vliet, 2001). The transformation stage, in addition to transforming the polymorphism to a more stable form, also changes the size distribution of the crystals via the Ostwald ripening in which nucleation growth and agglomeration occurred, resulting in an increase in the critical size for a stable crystal and nucleus (Aquilano & Sgualdino, 2001; Sonwai, Kaphueakngam, & Flood, 2012).

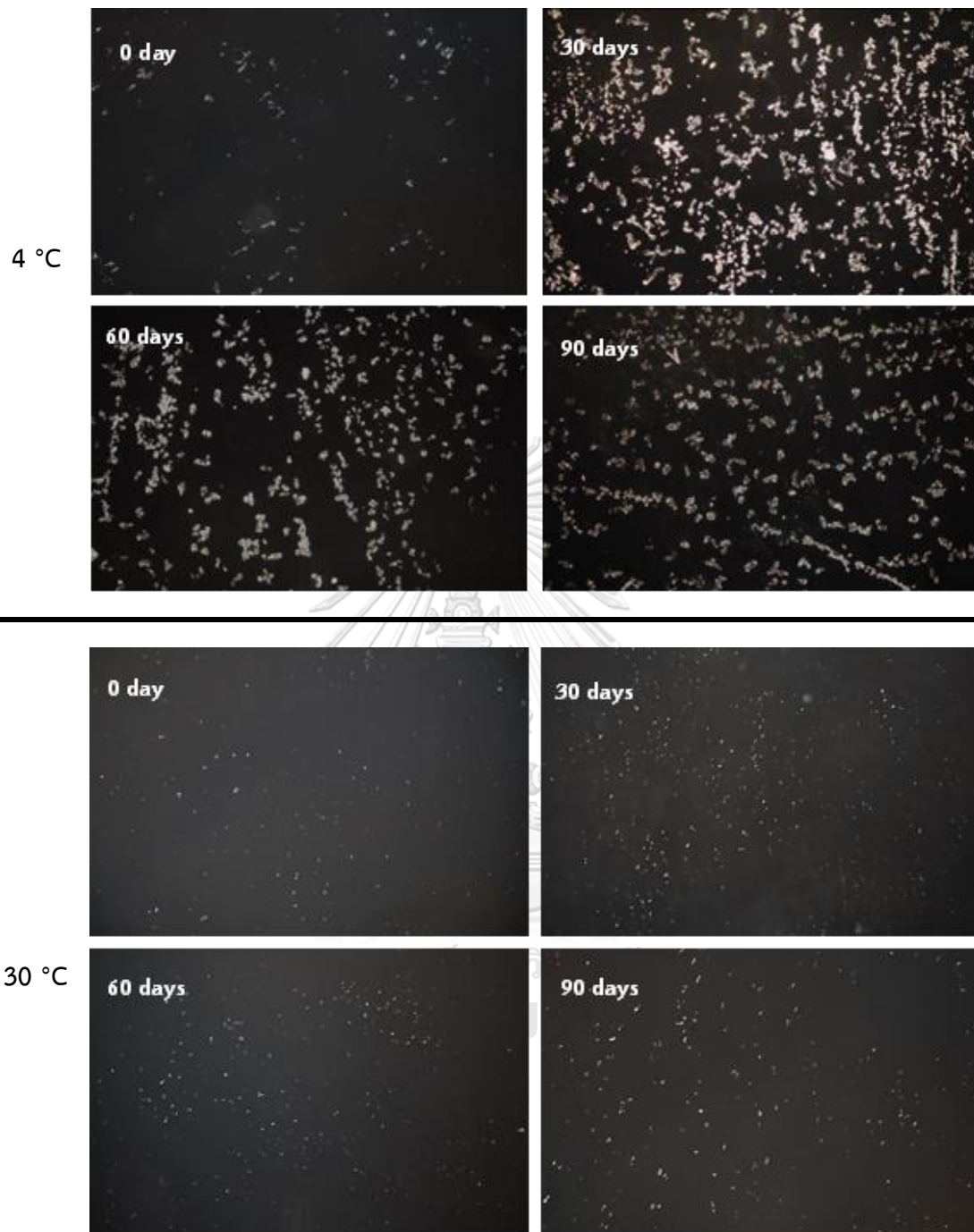


Figure 18 The polarized light microphotographs of the RO stored at 4°C and 30°C for 0 day, 30 days, 60 days and 90 days at magnification 40x

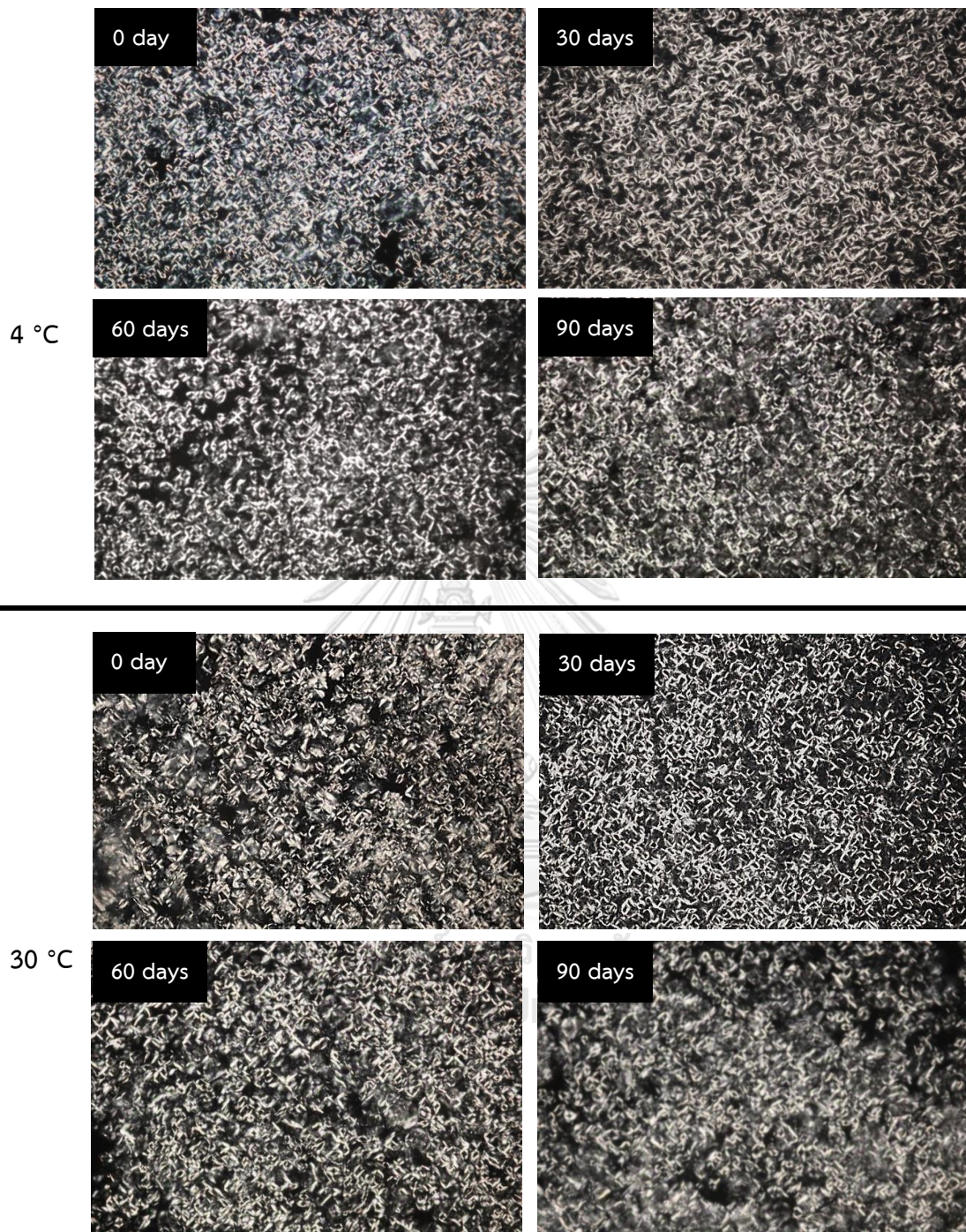


Figure 19 The polarized light microphotographs of the BRXO stored at 4°C and 30°C for 0 day, 30 days, 60 days and 90 days at magnification 40x

Emulsion stability index

The EO stored at 4 and 30°C for 90 days of storage did not appear to show phase separation. The ESI value shows that the BRX had good stabilization properties for W/O emulsion (Table 8). However, the E sample without the organogels addition showed lower ESI values than EO. The E30C showed 14.54% after producing sudden (0 day) and complete phase separation after 1 day of storage (data not shown). The ESI of E4C was 79.84 and 17.33% at 0 and 30 days, respectively, which showed higher stability than E30C.

Table 8 ESI (%) of E and EO during storage for 90days at 4°C and 30°C

	0 day	30 days	60 days	90 days
E4C	79.84 ^{bA} ± 2.35	17.33 ^{bB} ± 1.63	0.00 ^{bC} ± 0.00	0.00 ^{bC} ± 0.00
E30C	14.54 ^{cA} ± 0.49	0.00 ^{cB} ± 0.00	0.00 ^{bB} ± 0.00	0.00 ^{bB} ± 0.00
EO4C	100.00 ^{aA} ± 0.00			
EO30C	100.00 ^{aA} ± 0.00			

Mean ± SD.

^{a,b,c} Different letters show significant differences within each column ($p < 0.05$).

^{A,B,C} Different letters show significant differences within each row ($p < 0.05$).

Normally, the W/O emulsions type could stabilize due to the steric forces because the continuous phase had low electrical conductivity (Ushikubo & Cunha, 2014). W/O emulsions with wax addition stabilized because of fat crystallization. These particles can form a gel network that can absorb the liquid oil in the structure, therefore immobilizing the water droplets to prevent the sedimentation and phase separation of the emulsion. The crystals of the saturated triglyceride in the oil phase can be crystallized, interact and aggregate to form the gel network and provide the stability of the water droplets. Furthermore, these wax particles that are either bare

or coated can adsorb to the oil and water interface, which provides a steric barrier to drop fusion (Binks & Rocher, 2009; Dickinson, 2010; Hodge & Rousseau, 2005).

Emulsion structure

The microstructures of E and EO were shown as Figs. 20 and 21, respectively. The emulsion structure was composed of dispersed small water droplets in the oil phase. The emulsion without organogels addition was stored at 4°C for 30 days. The partial coalescence and the Ostwald ripening occurred, which transformed the water droplets from small droplets into larger ones (Fig. 20 b). The E4C and E30C showed creaming separated at 60 and 30 days of storage time, respectively.

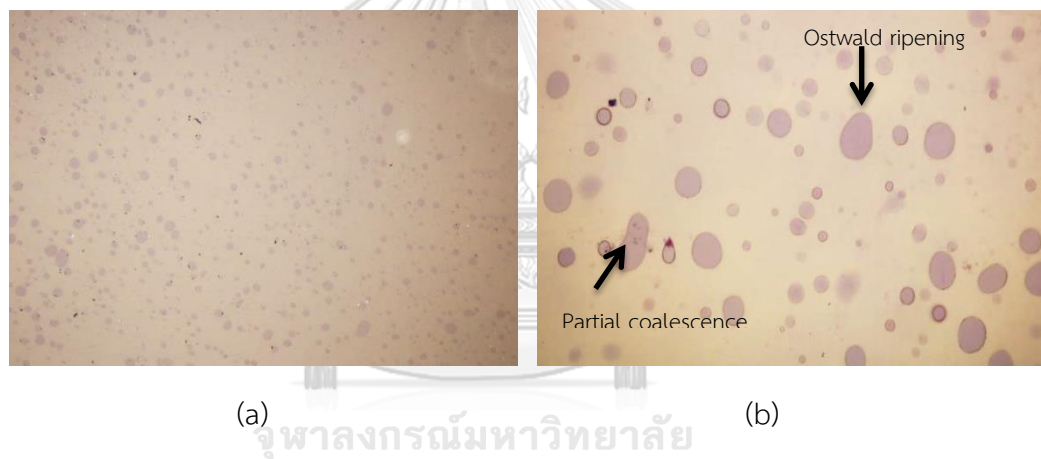


Figure 20 The microphotographs of the E4C during stored for 0 day (a) and 30 days (b) at magnification 40x

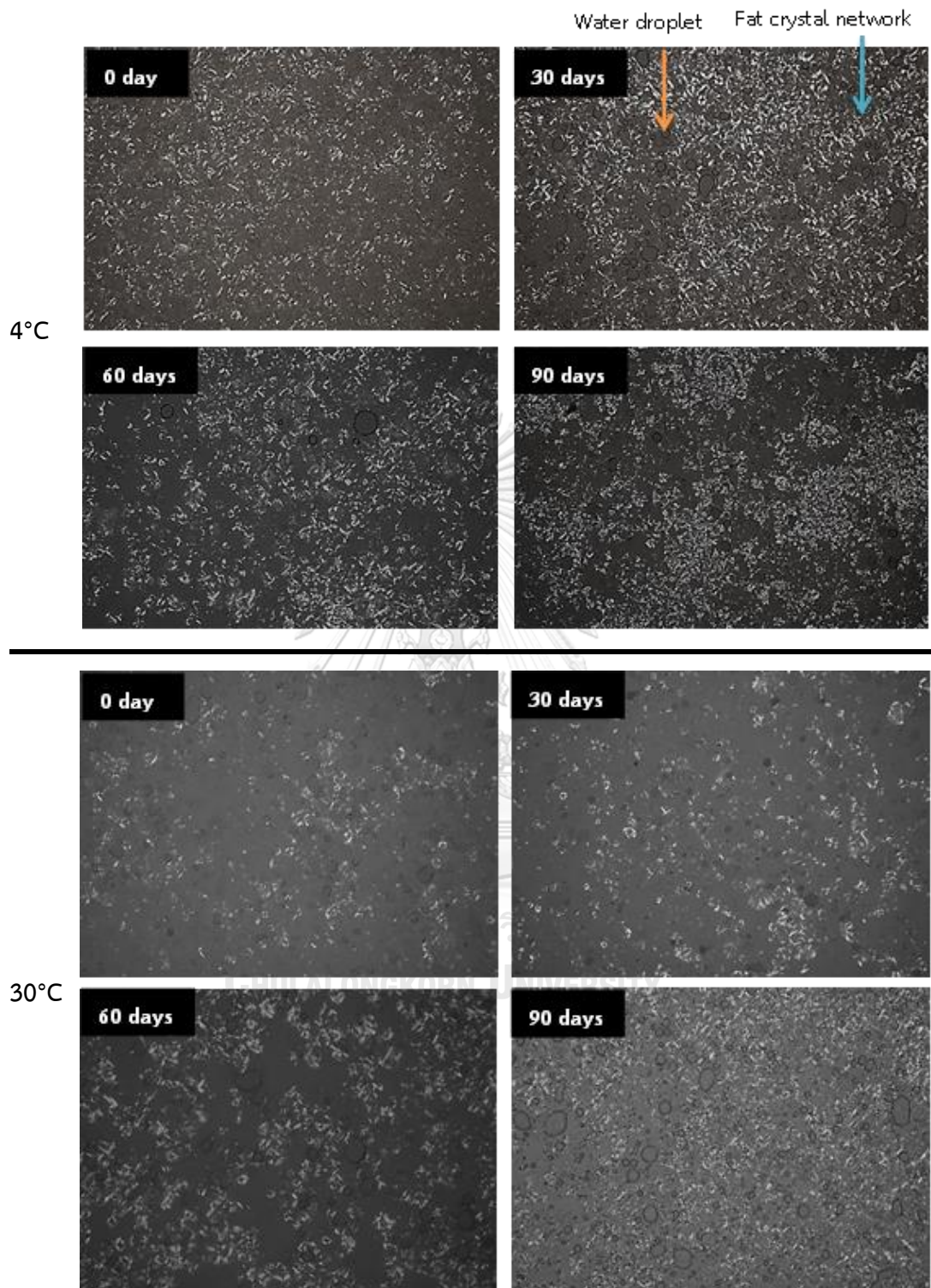


Figure 21 Polarized light microphotographs of EO stored at 4°C and at 30°C for 0 day, 30 days, 60 days and 90 days at magnification 40x

As shown in Fig. 21, the dispersed water droplets in the EO structure were trapped in the crystal network and were interfacially adsorbed (Pickering) particles. The fat crystal network in the emulsion structure was very important to the emulsion stability, affecting to the stability of semi-crystalline droplets for partial coalescence (Coupland, 2002). The structure of organogels occurs because of the special characteristics of the organogelator, which can provide stabilization of the kinetics of the emulsion by inhibiting the contact between droplets. Moreover, the Pickering crystal establishes the barrier between close water droplets, which can prevent the droplet collisions, film drainage, coalescence, and phase separation in the system (Ghosh & Rousseau, 2011) This is related to the higher ESI of EO than that of E. Hodge & Rousseau (2003) reported that wax crystals can enhance W/O emulsion stability. The results of this study showed results similar to the results of Ögütçü et al. (2015). These authors demonstrated that the fat crystal with a needle-like shape had the efficacy to trap the water droplets within the fat crystal network. Although the emulsions were stored at room temperature for 90 days, they did not show droplet coalescence or phase separation; however, the structure showed that the water droplet size was increased.

Oxidative stability

The effect of storage time and temperature on the oxidative stability of the organogels and W/O emulsion was studied. The measurements of PV and TBARS of the samples stored at 4 and 30°C were monitored for 90 days of storage time. The peroxide value (PV) is a parameter used for measuring the quality of the oil. The products from the induction period are hydroperoxides. PV can estimate the quantity of peroxide and hydroperoxide, especially in the induction period of the oxidation mechanism of lipid or lipid products. However, during lipid oxidation, PV reaches a peak and then lessens because the hydroperoxides decompose (Ciftci, Fadiloglu, &

Gogus, 2009; Ushikubo & Cunha, 2014). Thus, it is improper to use only PV for measuring the oil quality so that the TBARS are often measured together with PV.

The PV of RO, BRXO, E and EO are presented in Fig. 22 a). In early storage, the BRXO has PV (3.82 mEq/kg sample) higher than that of RO (1.99 mEq/kg sample) because of the BRX purity. The BRX used in this study is not sufficiently purified and contains approximately 0.16% free fatty acids, which may induce lipid oxidation. Although at the start, the PV of BRXO was higher than the PV of RO, the PV of BRXO then increased slightly and was lowest throughout the storage period whereas that of RO was obviously changed, possibly because the RO is composed of unsaturated fatty acids at approximately 81.4%, when fatty acid oxidation can easily occur. Among all samples, the RO30C stored at 60 days showed the highest PV (7.88 mEq/kg sample), and the lowest value (0.44 mEq/kg sample) was shown by BRXO4 stored for 90 days. When the PV of E and EO was compared, both EO samples showed the lowest value and changed slightly whereas the E showed a higher value, especially EO30C. Obviously, the PV of all samples exhibited an increase until 60 days of storage and then decreased as shown in 90 days. This effect may be the hydroperoxides from the early oxidation stage decomposing (Abramovic & Abram, 2005). At 90 days of storage, the BRXO had lower PV than RO, and the EO was lower than the E for both temperatures. The results of this study were same as the results from other studies. Ögütçü & Yılmaz (2014) found that the virgin olive oil organogels produced from carnauba wax and monoglyceride showed good oxidative stability. Ögütçü & Yılmaz (2015b) reported that hazelnut oil wax-based organogels with sunflower wax and carnauba wax were highly stable to oxidation.

The storage temperature and time storage affected the PV of all samples. At a low temperature (such as 4°C), lipid oxidation could be inhibited, with more oxidation at higher temperatures (such as 30°C), causing the sample stored at 4°C to show lower PV than the samples stored at 30°C. Codex Alimentarius (2001) specified

that the PV of edible vegetable oil should be below 15 mEq/kg sample, whereas vegetable oil in the range of 30 to 40 mEq/kg sample shows a rancid taste in the product. Popa, Glevitzky, Dumitrele, Glevitzky, & Popa (2017) recommended that the PV limits when the oil leaves the factory should be below 3 mEq/kg sample and less than 5 and 10 mEq/kg sample after the bottle is opened and in use, respectively.

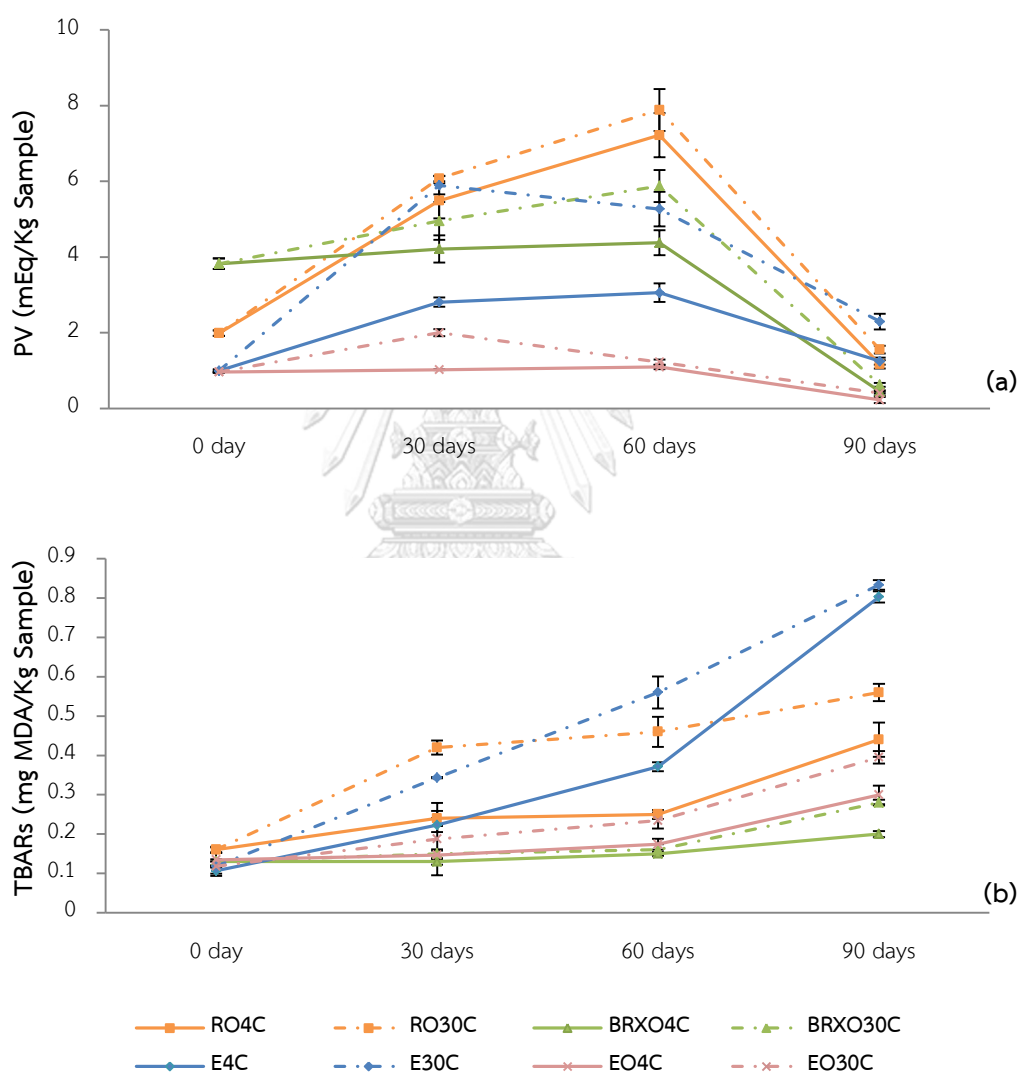


Figure 22 PV (a) and TBARS (b) change of RO and BRXO, E and EO stored at 4°C and 30°C for 90 days during storage time

Fig. 22 b) shows TBARS values from secondary oxidation monitoring aldehyde compounds such as malondialdehyde (MDA) that was produced. The MDA associated with off-flavour, rancid odour and an undesirable taste in food (Azman et al., 2016; Pangloli, Melton, Collins, Penfield, & Saxton, 2002). Fig. 22 b) shows the highest increase in TBARS values for the RO30C (0.16 to 0.56 mg MDA/kg sample) when compared with the BRXO samples approximately 1.6 to 2.8 times at 90 days of storage time. Additionally, E samples show higher TBARS values than EO for both temperatures (Fig. 22 b). The TBARS value of BRXO was close to the TBARS value of EO and below 0.4 mg MDA/kg sample over the storage period. The TBARS values of RO and E are nearly 1 mg MDA/ kg sample. However, it did not exceed the acceptable limit of TBARS as less than 1 mg MDA/kg sample for fat products (Nollet & Toldra, 2011), ascribable to the natural antioxidants in rice bran oil such as phytosterols, gamma-oryzanol, and other phytosterol conjugates, so that the lipid oxidation at no more than this level (Wang, 2002). Gunstone (2004) showed that the refined rice bran oil consists of a high level of tocopherols and tocotrienols at approximately 860 ppm, which is excellent to resist the oxidative stability in salad and frying oil. The results of the lipid oxidation measurements showed that the BRXO and EO were stable to lipid oxidation.

4.5 Policosanol organogels and water-in-oil emulsions

In this part of the study, the policosanol was extracted from BRX and then was used as the organogelator to produce the organogels. The policosanol extraction consists of 3 main steps, namely, defatting, extraction and purification. Since the BRX used in this study is composed of triglycerides and other impurities, it is necessary to remove these impurities using reflux with hexane. Then, defatted BRX is extracted by hydrolysis with KOH and is purified by using toluene and isooctane. The

confirmation of policosanol extraction was determined by TLC. In the last steps of the extraction process, the mixture separated into 2 phases, isooctane phase (upper) and water phase (lower phase). The salts of fatty acids and fatty acids (FAs) are dissolved in water, whereas the fatty alcohols (FALs) are dissolved in isooctane. From the results shown as Fig. 23, the TLC plate had been present to complete hydrolysis of the BRX. Therefore, samples 6 and 7, which are the hydrolysed mixture upper and lower phase, respectively, did not appear as the wax ester composition on the TLC plate because the wax was hydrolysed, yielding the long chain fatty acids and long chain fatty alcohols as products. The lower phase contained FAs while the upper phase mainly contained FALs, FAs and other components that cannot be removed from the extract, indicating that the policosanol extracted from this study is not purified.

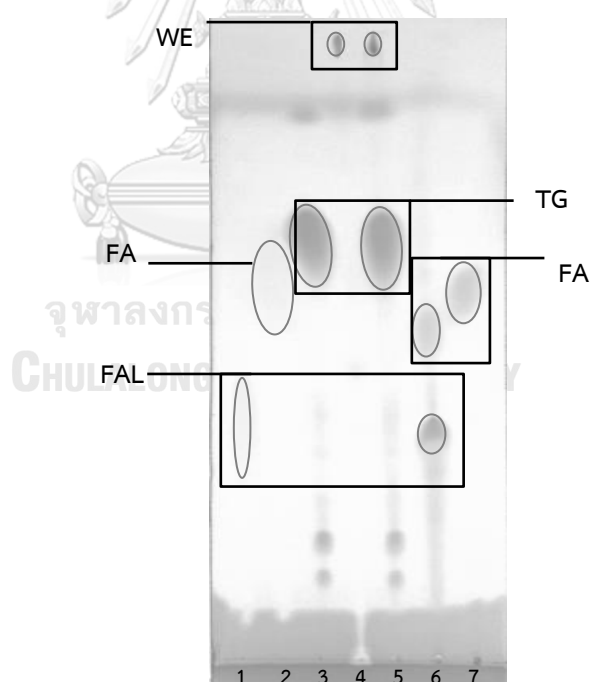


Figure 23 Thin layer chromatography of stearyl alcohol (fatty alcohol; FAL) (1), palmitic acid (fatty acid; FA) (2), rice bran oil (triglyceride; TG) (3), purified rice bran wax (wax ester; WE) (4), bleached rice bran wax (5), upper phase (6), and lower phase (7) extracted from policosanol extraction

The yield of policosanol (PC) obtained from Thai bleached rice bran wax was approximately 37.21 wt %, whereas Puengtham et al. (2008) reported that the yield of policosanol from rice bran wax was 26.56 wt% and (Ishaka, Imam, Mahamud, Zuki, & Maznah, 2014) reported the yield of policosanol from rice bran wax was 10.82 wt %. The PC extracted had a yellowish-brown colour (Fig. 24), and the L*, a* and b* values were 59.02, 8.03, and 31.96, respectively (Table 9). In general, the composition of the PC mixtures mainly includes tetracosanol (C24), hexacosanol (C26), octacosanol (C28), and triacosanol (C30) (Ishaka et al., 2014). The quantity of fatty alcohols was analysed by GC-FID. The PC extract of 1 g contained 58.63 mg of C24, 75.93 mg of C26, 125.50 mg of C28 and 143.24 mg of C30. The yield, composition and quantity of policosanol varied due to the kind of wax, the wax source, the extraction method, the chemical used and the purification method (Irmak et al., 2006).

Table 9 The physical properties and fatty alcohol composition of policosanol

		Composition (mg/g of sample)	
Yield (wt%)	37.21 ± 2.97	Fatty alcohol	
Colour		C24	58.63 ± 0.72
L*	59.02 ± 0.81	C26	75.93 ± 2.56
a*	8.03 ± 0.84	C28	125.50 ± 3.64
b*	31.96 ± 0.92	C30	143.24 ± 4.18



Figure 24 The policosanol extracted from Thai bleached rice bran wax

The polymorphism of the PC extract was shown in Fig. 25. The longitudinal packing of PC was indicated by SAXS. The PC showed an organized structure within a range of 16.95 to 42.44 Å, indicating a double chain length structure (2L). Lamellar packing was indicated by WAXS. In this WAXS area, the PC showed peaks at 3.71, 4.13, and 4.66 Å. The strong WAXS intensity showed at 4.13 and 3.71 Å was indicated to an β' -type polymorph. The peak presented at 4.66 Å corresponded to a β -type of polymorph.

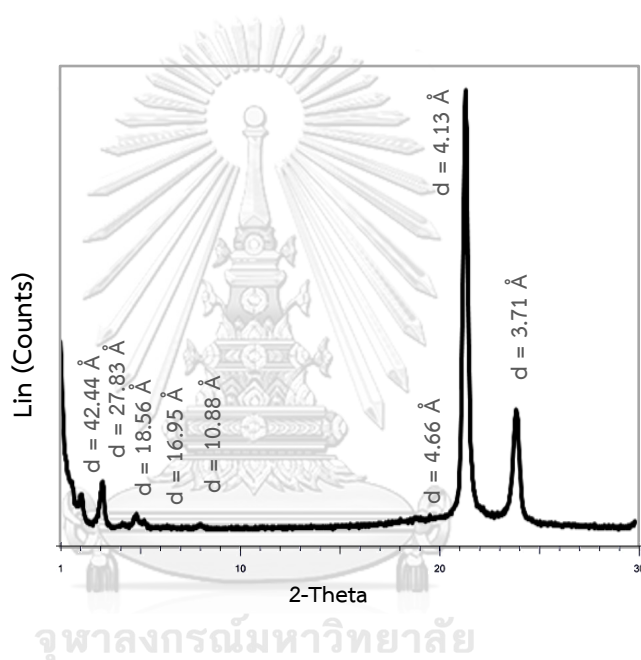


Figure 25 The X-ray diffraction patterns of the PC

The thermal behaviour of PC was shown in DSC patterns (Fig. 26). From the results, the melting (T_M) and crystallization (T_C) temperature of PC exhibited two wide and blunt peaks similar to the CRX because it consisted of many components. The major T_M and T_C of PC are 79.53 and 78.15°C, respectively. The value is close to the report of Madhavi & Kagan (2013), who reported that the major melting temperature of PC is 81.9°C. However, Kim et al. (2015) reported the major melting endotherm of policosanol started at approximately 80°C with a melting temperature at

approximately 88°C, which caused the melting temperature of fatty alcohols octacosanol, hexacosanol, and triacontanol to be 81.3, 83.0, and 85.7°C, respectively. The T_C and T_M of PC were higher than the BRX approximately 6.68°C and 5.54°C, respectively. The high temperature melting point and crystallization point of PC exhibit the heat resistance property, and the crystallization occurs easily although at high temperature. The high onset of crystal (T_{oC}) results in strong crystal interactions and supramolecular formation, with a good liquid entrapment property in the 3D network.

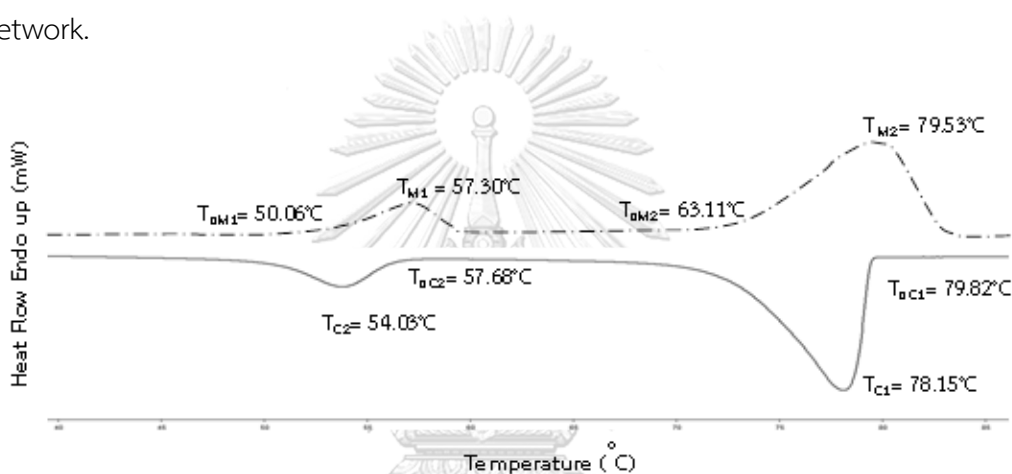


Figure 26 DSC patterns taken during cooling (solid line) and heating (dotted line) processes of policosanol

The gelation time of PCO decreased while PC concentration increased, whereas the OBC increased as the PC concentration increased. These results had a similar trend to BRXO. When the potential of the oil binding capacity between PC and BRX is compared, the BRX is found to have more potential than PC. Observed at the highest concentration of BRX (Table 4) and PC (Table 10), BRXO at 9% wax had OBC higher than PCO at 15% PC at approximately 6.45%, possibly from the needle-like and fibrous crystalline structure in BRXO, which has a good potential to create a strong network adsorbing the oil. However, the crystal form of PCO was dendrite-like crystal aggregates (Fig. 27), which have the potential to form the network for the

trapped oil lower than the BRX. The PC concentration affected the colour of the organogels (Table 10), the terms L^* , a^* and b^* of colour increased with increasing PC concentration ($p < 0.05$). The colour of PCO is lighter and more yellow than the colour of BRXO, an effect from the colour of the raw material. The PC showed a higher L^* and b^* than BRX by approximately 1.2- and 3.1- fold, respectively. Moreover, the PC concentration affected the texture of PCO, and the values of all textural parameters were increased along with concentration. The results showed that the firmness, hardness and stickiness values of PCO were lower than those values for BRXO (Table 4) by approximately 2.8-, 3.4- and 2.4-fold, respectively, at the highest concentration of the gelator type. This reason is likely to be the same as the reason for low OBC of PCO, due to the low efficiency of the dendrite-like shape for the gel formation. Moreover, the fatty alcohols also influence the oil gelling, which depends on the chain length (Doan et al., 2017).

The thermal behaviour of PCO is presented in Table 11. The crystallization and melting behaviour varied with PC concentration ($p < 0.05$), which was similar to the trend with BRXO. The crystallization (T_C) and melting temperature (T_M) of PCO was highest at 15% PC levels. The T_C of PCO at 15% of PC (62.42°C) was nearly at temperature with BRXO at 9% wax (62.25°C). The enthalpy of crystallization (ΔH_C) of PCO (31.45 J/g) was higher than that of BRXO (13.76 J/g), indicating that the BRXO used the energy less than PCO for the crystallization that was occurring. The melting temperature of PCO was lower than the melting temperature of BRXO at approximately 3.53°C, whereas the enthalpy of melting (ΔH_M) was higher than the enthalpy of melting for BRXO at approximately 14.93°C, demonstrating that the PCO is high in thermal stability, with the SFC at 4°C nearly the same as at 30°C.

Table 10 Physical properties of organogels at different concentration of policosanol

Policosanol concentration (%)	Gelation time (min:sec)	Oil binding Capacity (%)	Colour			Texture		
			L*	a*	b*	Firmness (g)	Hardness (g.sec)	Stickiness (g.sec)
12	7:24	82.49 ^b ± 1.31	51.52 ^c ± 0.48	-2.60 ^c ± 0.10	18.37 ^c ± 0.28	38.22 ^b ± 0.61	267.02 ^c ± 0.56	-64.92 ^a ± 0.51
13.5	5:49	91.79 ^a ± 2.03	53.20 ^b ± 1.42	-2.24 ^b ± 0.12	18.68 ^b ± 0.26	55.67 ^a ± 0.39	395.24 ^b ± 2.48	-46.45 ^b ± 0.13
15	4:16	93.30 ^a ± 0.52	55.61 ^a ± 1.14	-1.91 ^a ± 0.13	19.90 ^a ± 0.09	61.32 ^a ± 0.68	422.89 ^a ± 1.66	-37.30 ^c ± 0.27

Mean ± SD. Mean with different superscript letters along a column are significantly different ($p < 0.05$).

Table 11 Thermal properties and solid fat content (%) of policosanol

Policosanol concentration (%)	Crystallization			Melting			SFC (%)	
	T _{oc} (°C)	T _c (°C)	ΔH _c (J/g)	T _{om} (°C)	T _m (°C)	ΔH _m (J/g)	4 °C	30 °C
12	63.28 ^c ± 0.01	60.45 ^b ± 0.03	-25.05 ^b ± 1.01	52.72 ^c ± 0.43	61.46 ^b ± 0.01	21.71 ^b ± 0.09	6.86 ^b ± 0.30	6.27 ^c ± 0.08
13.5	64.02 ^b ± 0.02	61.42 ^{ab} ± 0.72	-30.20 ^a ± 0.29	58.64 ^b ± 0.78	62.46 ^b ± 0.01	22.33 ^b 0.51	7.35 ^{ab} ± 0.01	6.78 ^b ± 0.05
15	65.67 ^a ± 0.06	62.42 ^a ± 0.17	-31.45 ^a ± 0.54	60.83 ^a ± 0.47	63.49 ^a ± 0.01	26.04 ^a ± 0.25	7.90 ^a ± 0.07	7.54 ^a ± 0.11

Mean ± SD. Mean with different superscript letters along a column are significantly different

The PC and PCO microstructure images are shown in Fig. 27. The crystal morphology of PC shows a large needle-like morphology (Fig. 27 a) similar to the BRX, but the crystal size and volume are smaller than PC, possibly due to the policosanol at higher concentrations than the BRX (containing approximately 65% rice bran oil), when compared at equal weight. It was surprising when the PC came to produce the organogels, the crystal morphology is changed. These results are similar to the results from the studies of Tian & Acevedo (2018). They reported that at low concentration (approximately 7% PC), the crystal showed a needle-like shape because the crystals were formed and diffused far from each other in the system without much interaction and found that the crystal morphology of PCO was changed after adding the PC of more than 10%. When the concentration increased, the higher supersaturation occurred in the system which promoted the growth, the expansion, and branching of the crystal structures (Tian & Acevedo, 2018). Therefore, the PCO microstructure showed a dendrite-like crystal aggregate with a multi-branching form and a dense crystal formation with large crystalline aggregates when the PC concentration increased (Fig. 27 c). This crystal shape morphology did not support the strong gelling network because the gelling network had many spaces from the interconnected dendritic crystals to form a branched network, which affected the weak gelling ability and low value in texture properties (Doan et al., 2015).

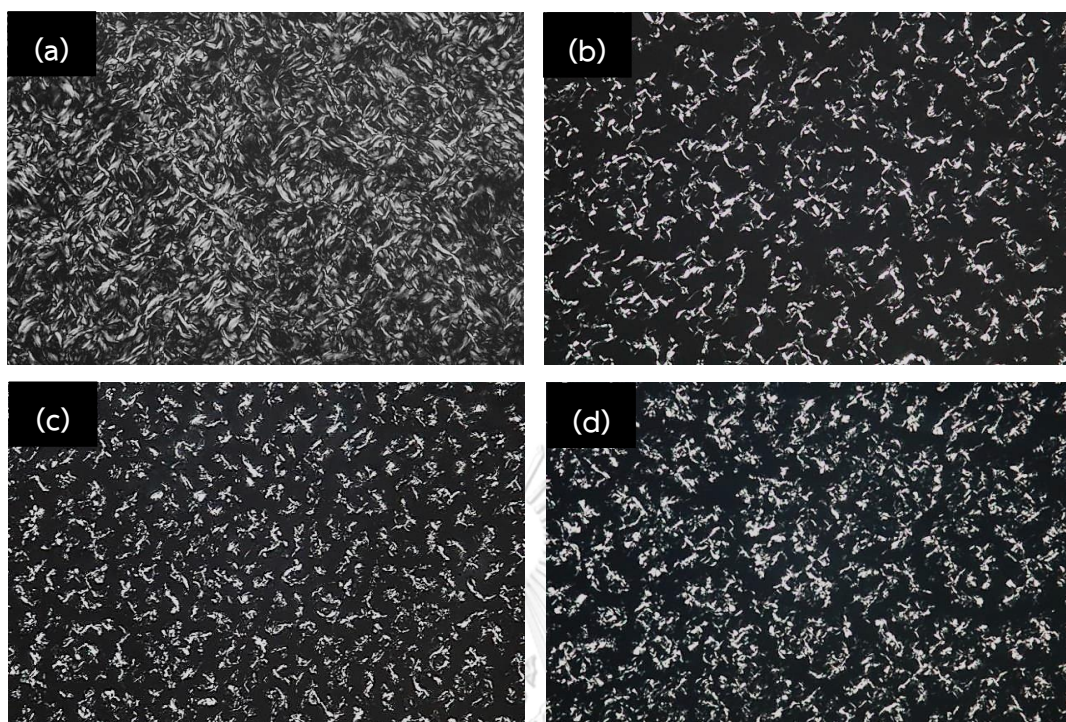


Figure 27 Polarized light microphotographs of policosanol extracted (PC) (a) and policosanol organogels (PCO) at different policosanol level at 12% (b) 13.5% (c) and 15% (d) at magnification 40x

Fig. 28 shows the XRD pattern of PCO at different PC concentrations. These results are similar to the results with the XRD of BRXO (Fig. 13). The peak in SAXS was in the range of 28.01-29.32 Å and WAXS showed 3 main peaks at 4.6, 4.1 and 3.7Å, indicating that the longitudinal organization of the fat crystal is 2L packing. The crystal form of PCO was mixed with the β - and β' - crystals that β' - form are observed in higher amounts compared to the β - form.

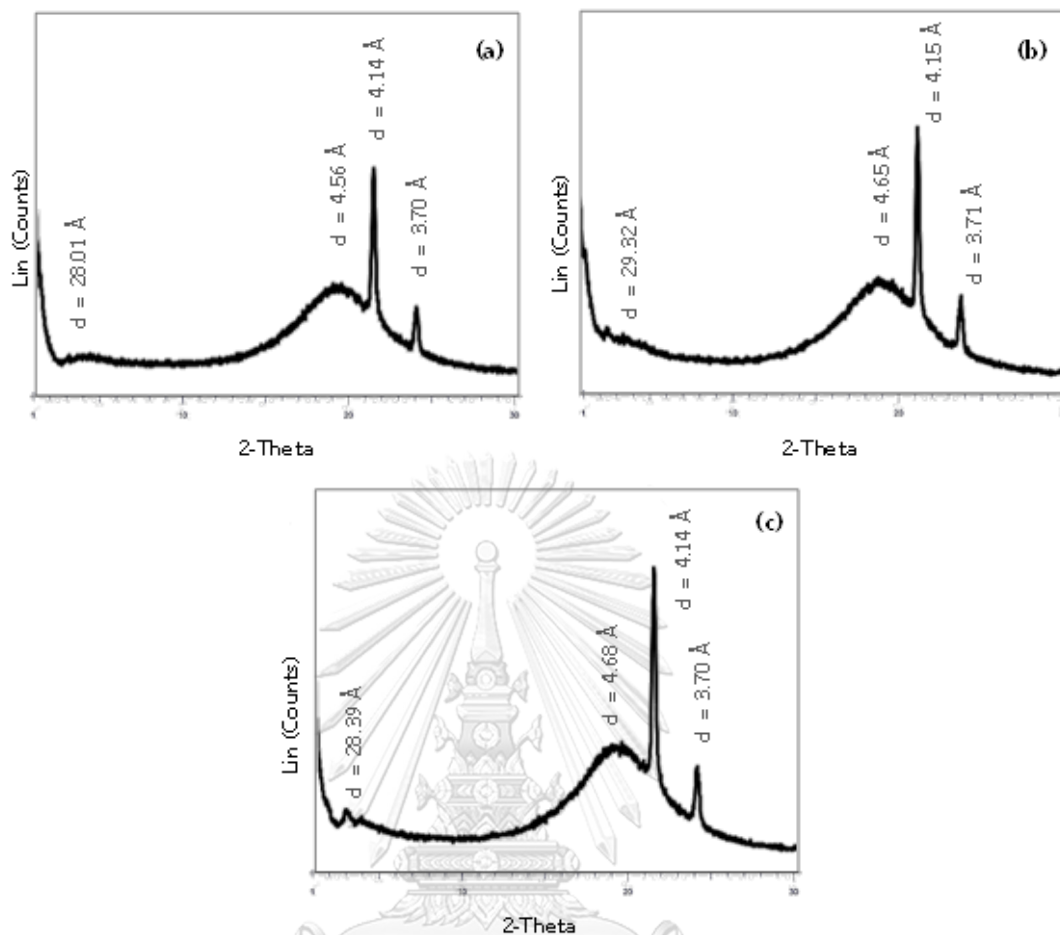


Figure 28 The X-ray diffraction patterns of the PCO sample at 12% (a), 13.5% (b) and 15% (c) of PC concentration

4.5.1 Physical property of water-in-oil emulsion prepared from policosanol organogels and policosanol and bleached rice bran wax organogels mixture

This section includes the studies on the physical properties of the water-in-oil emulsion prepared from PCO and PCO mixed with BRXO. The PCO at 15% PC concentration was selected to prepare the PCE and BRXO at 9% wax concentration to mix with PCO in the Ratio of 50:50 (wt/wt) to prepare the PCM.

Table 12 presents the physical properties of PCE and PCM. Both emulsions did not show phase separation, indicating the high emulsion stability index of 100%. For the colour, the L^* was not significantly different ($p \geq 0.05$) between PCE and PCM, whereas the a^* and b^* were different ($p < 0.05$). Both emulsion samples showed the lightness of an emulsion tending to increase when compared before emulsification by homogenization, as the small fat and water droplets increased due to greater light scattering (McClements, 2002). The PCE showed more greenness and yellowness than PCM. The textural values of the emulsification samples (PCE and PCM) showed a higher value than PCO, contrasting with BRXO that decreased in value after the emulsification production (EO), possibly because of the synergistic interaction between fatty alcohol (as PC) and fatty acid, which are still contained in the PC extract to enhance the gel strength. Schaink et al. (2007) found synergistic interaction effects in a fatty acid and fatty alcohol mixture at the ratio of 3:7, which showed the highest hardness value. At a reasonable ratio, the hardness value was more than 2.5 times higher than any other ratio. Gandolfo et al. (2004) also reported the synergistic effect of fatty acid and fatty alcohol. The firmness of both samples did not differ ($p \geq 0.05$) while there was a significant difference ($p < 0.05$) in hardness and stickiness values. The PCE showed higher values than PCM, which may be the effect of BRX. The evaluation of firmness and stickiness together can estimate the spreadability of plastic-fat products. The stickiness increase was related to more force required to pull the probe back from the sample, which indicated the possible difficulty of spreading (Öğütçü & Yılmaz, 2015b)

The crystallization of PCE occurred at high temperatures of approximately 56.92 to 64.65°C when compared to the PCM (55.66 to 60.99°C), as indicated from T_{oc} and T_c (Table 13). T_M values of PCE and PCM were not significantly different ($p \geq 0.05$). The enthalpy of crystallization (ΔH_c) and melting

(ΔH_M) of PCM was lower than those values for PCE. These results reflect the stronger structure of PCE, thus crystallization and melting required high energy to form or melt those crystals. The SFC of both samples did not significantly differ at 4°C, but PCE showed higher values than PCM at 30°C. Those samples showed that SFC at 4°C was higher than 30°C. The PCE showed high SFC (9.81%) at 30°C which indicated the PCE is stable to high temperature more than PCM.

The XRD pattern of PCE and PCM is shown as Fig. 29. The peaks in SAXS of PCE and PCM are in the range of 27.82 Å and 21.36 Å. The WAXS still showed 3 main peaks like all of the samples in this study, at 4.6, 4.1 and 3.7 Å, indicating that the crystals of PCE and PCM formed were mixed with the β - and β' - crystals with 2L longitudinal packing.

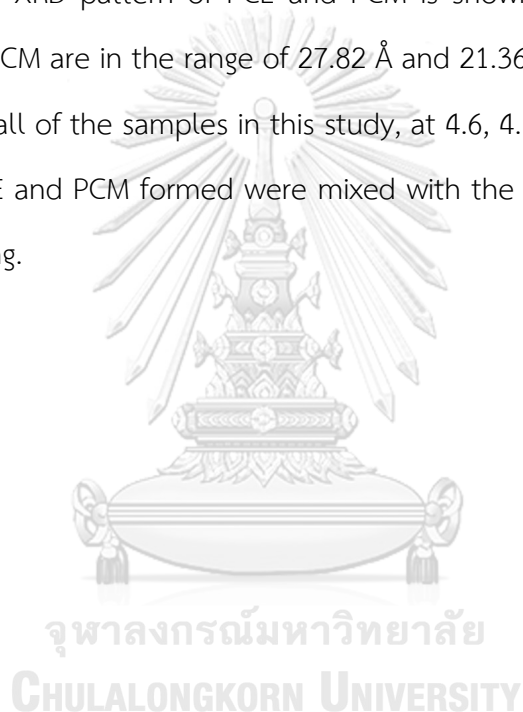


Table 12 Physical properties of PCE and PCM

Emulsion	Colour			Texture			
	Stability (%) ^{Ns}	L* ^{Ns}	a* ^{Ns}	Firmness (g) ^{Ns}	Hardness (g.sec)	Stickiness (g.sec)	
PCE	100.00 ± 0.00	74.94 ± 0.20	-0.87 ^a ± 0.04	15.85 ^a ± 0.20	327.25 ± 17.71	2065.79 ^a ± 85.72	-146.83 ^b ± 5.14
PCM	100.00 ± 0.00	74.96 ± 0.27	-0.68 ^b ± 0.05	14.10 ^b ± 0.38	340.94 ± 25.55	1659.38 ^b ± 104.14	-107.01 ^a ± 7.95

Mean ± SD. Mean with different superscript letters along a column are significantly different (p < 0.05)

Ns: not significantly (p ≥ 0.05)

Table 13 Thermal properties of PCE and PCM

Emulsion	Crystallization			Melting			SFC (%)
	T _{oc} (°C)	T _c (°C)	ΔH _c (J/g)	T _{om} (°C)	T _m (°C) ^{Ns}	ΔH _m (J/g)	
PCE	64.65 ^a ± 0.80	56.92 ^a ± 0.12	-24.60 ^a ± 0.58	41.13 ^b ± 0.08	59.32 ± 0.13	14.39 ^a ± 0.97	12.42 ± 0.15
PCM	60.99 ^b ± 0.62	55.66 ^b ± 0.33	-14.77 ^b ± 0.73	46.57 ^a ± 0.63	59.41 ± 0.01	9.65 ^b ± 0.14	12.76 ± 0.06

Mean ± SD. Mean with different superscript letters along a column are significantly different (p < 0.05)

Ns: not significantly (p ≥ 0.05)

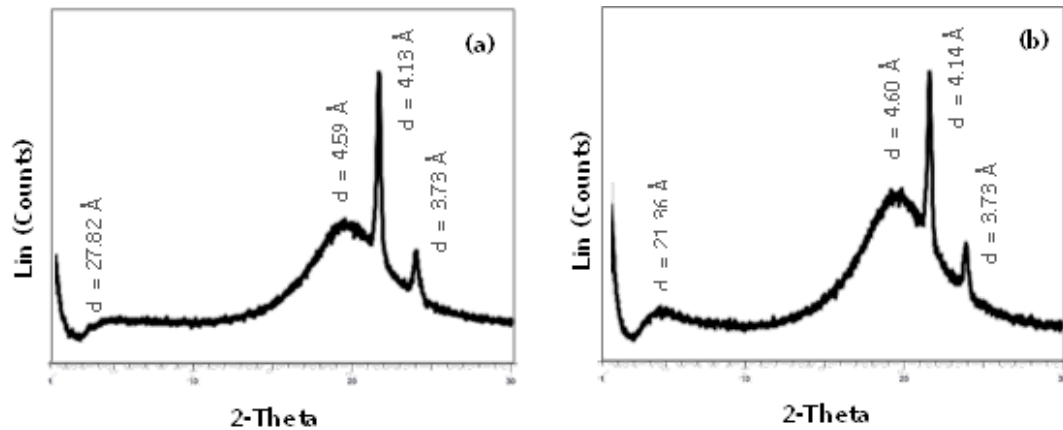


Figure 29 The X-ray diffraction patterns of the PCE (a) and PCM (b)

4.5.2 Storage stability of policosanol organogels and water-in-oil emulsions

Colour

The colour change during 90 days of storage is shown in Fig. 30. The results showed that the shade of lightness (L^*) of all samples is divided into two groups. The PCO samples showed the lowest values (49.79-56.87) and PCE and PCM groups were nearly the same value (70.4-77.58). The L^* value of all samples decreased followed storage time. The samples stored at low temperature (4°C) showed little change compared to those at high temperature (30°C). The a^* value showed a slightly green shade. The PCM showed a lower a^* value than PCO and PCE. During storage time, the PCE and PCM decreased, whereas PCO increased with increased storage time.

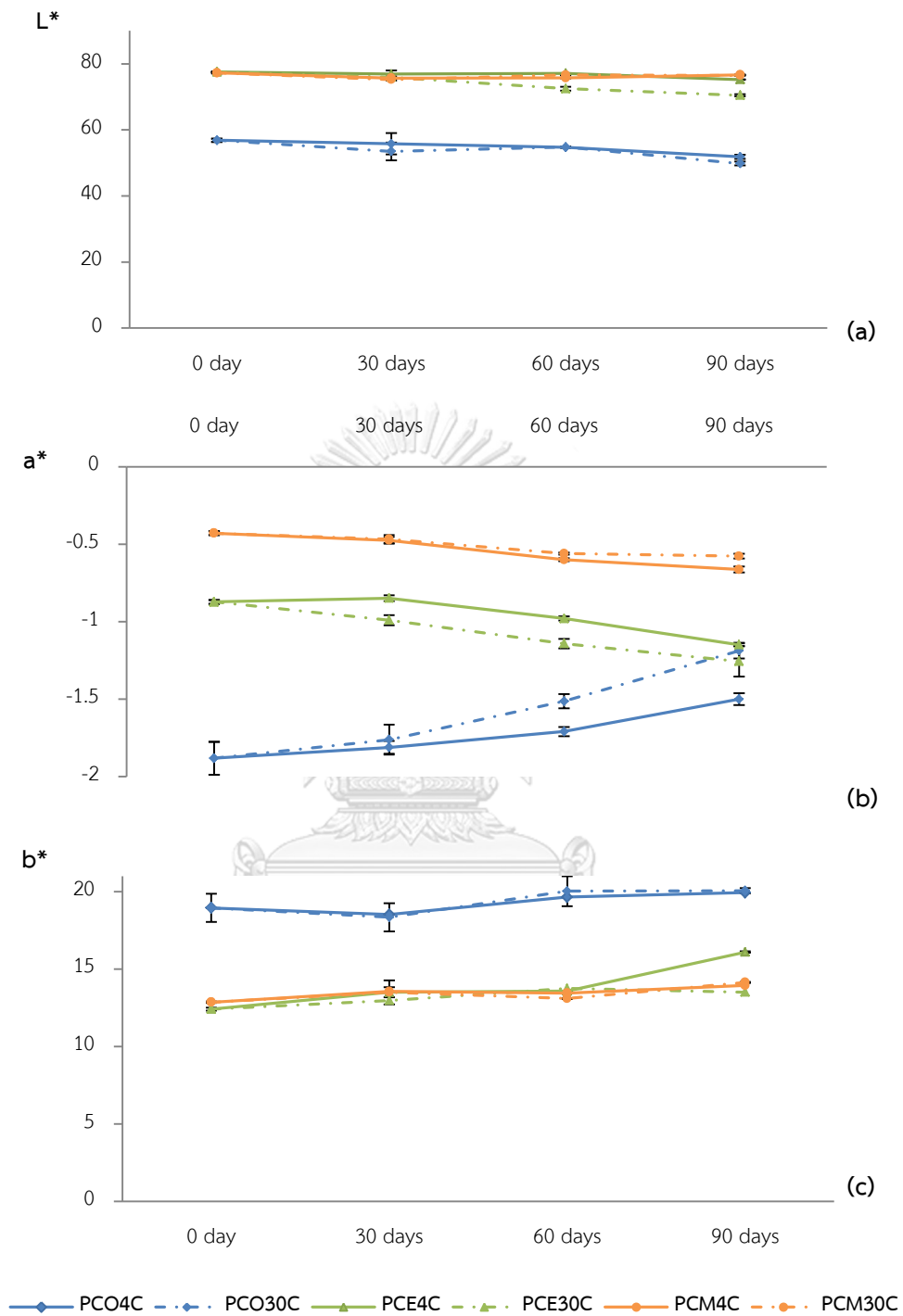


Figure 30 Colour change in L* (a), a* (b) and b* (c) of PCO, PCE and PCM during storage at 4°C and 30°C for 90 day

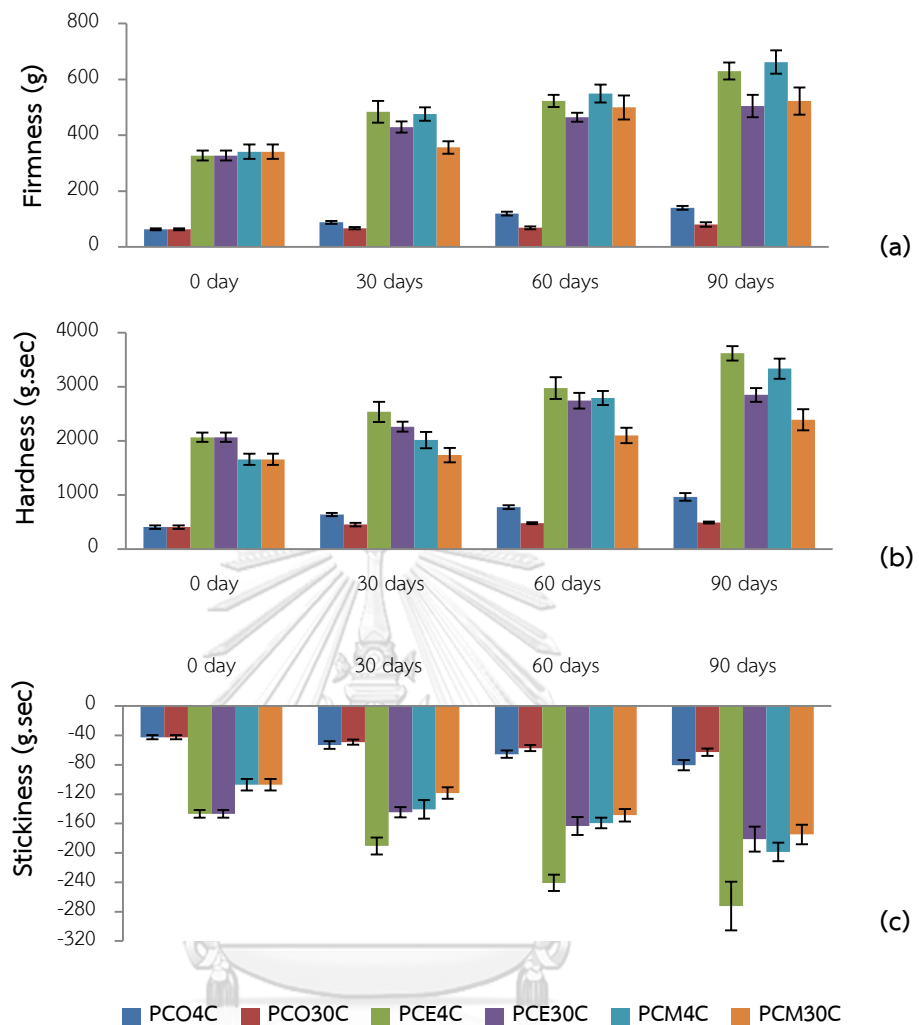


Figure 31 Textural changes in firmness (a), hardness (b) and stickiness (c) of PCO, PCE and PCM during storage at 4°C and 30°C for 90 days

Texture

The textural properties changed during storage, as presented in Fig. 31. The texture of all samples increased as the storage time increased. The samples were kept at 4°C, showing more changes than the samples kept at 30°C, as the samples kept at 30°C showed a little change. This reason is similar with the properties of

BRXO and EO changing during storage. The texture value of PCO showed less change when compared with PCE and PCM, which showed more change.

Crystal morphology

Fig. 32 presented the crystal morphology of PCO at 15% PC concentration. The crystal morphology changed again when the storage time increased, changing from needle-like (bulk PC state) to dendrite-like (organogel state) and finally formed spherulite-like crystals. The spherulitic crystalline aggregates first appeared after 30 days and remained through the 90 days of storage time. The spherulite formation is divided into 2 categories. First, a central multidirectional growth formed and second, a unidirectional growth with low angle branching formed, which formed from folded-chain single crystal to complete development as spherulite (Gránásy, Jack & Douglas, 2013). From the observation, the character of the crystals formed in this study was category 2 formation. The stabilization of PCO and from BRXO occurred differently, the stability of BRXO occurred from Pickering stabilization whereas the PCO occurred from network stabilization. The network stabilization presented the continuous fat crystal network which fixed droplets and separated from other droplets due to the presence of interstitial crystals, thus flocculation and/or coalescence were decreased (Ghosh et al., 2011; Ghosh & Rousseau, 2011). The PCO stored at 4°C shows crystal amount, crystal size and crystal density more than that the PCO stored at 30°C. Their crystals were rearranged in the network and formed a denser structure during storage, while the shape of the crystals remained unchanged.

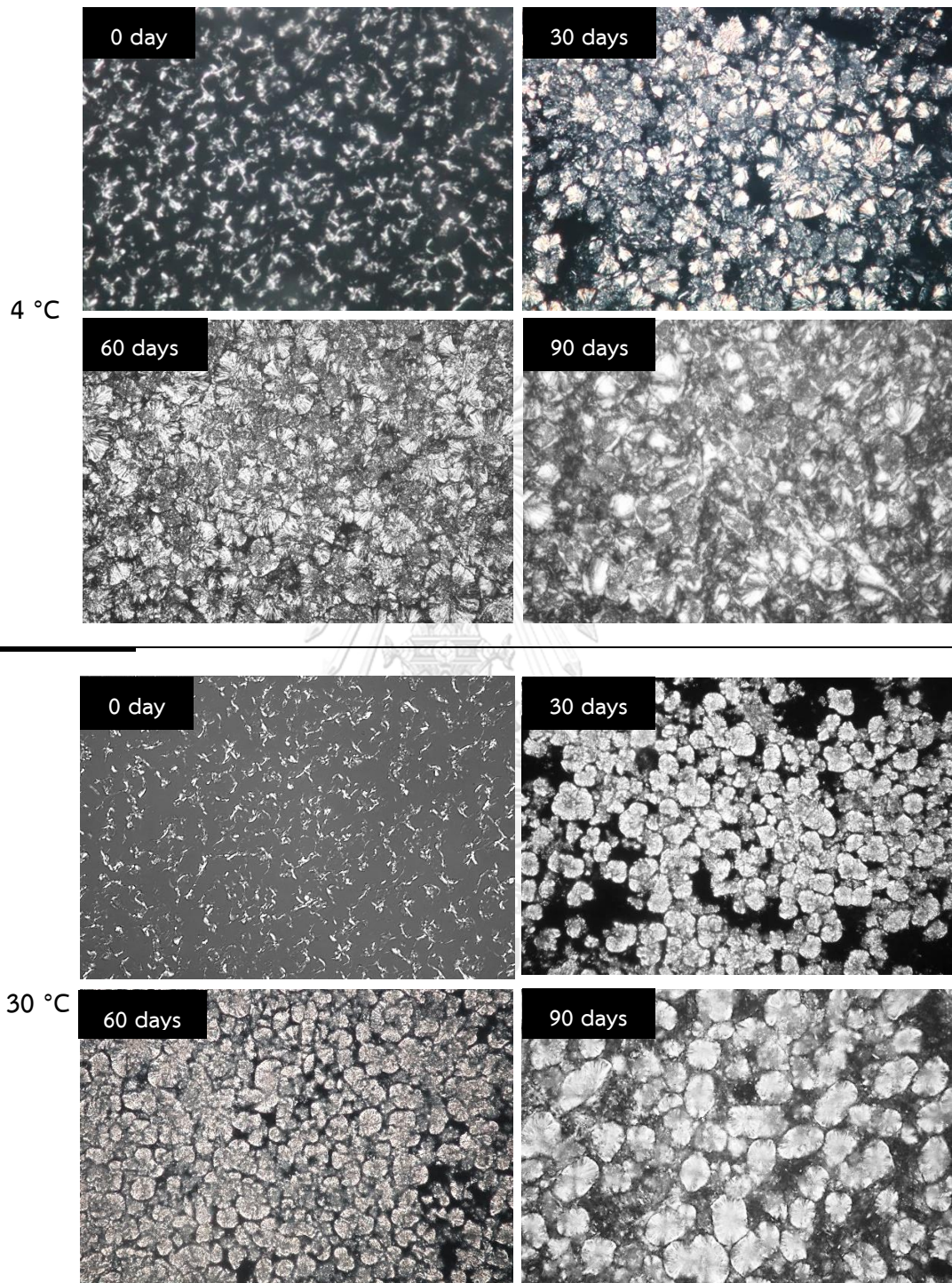


Figure 32 Polarized light microphotographs of PCO stored at 4°C and at 30°C for 0 day, 30 days, 60 days and 90 days at magnification 40x

Emulsion structure

The tracking the morphology changes of PCE and PCM is presented in Fig. 33 and Fig. 34, respectively. The emulsion structures of both samples were similar, the fat phases showed small water droplets were trapped in the crystal. The emulsion structure of PCE and PCM showed the combination Pickering and network crystals. Both Pickering and network crystals can synergistically contribute to emulsion stability (Ghosh & Rousseau, 2011) which may be due to high textural value when compared with EO. This stabilization is the most obvious in the PCE stored at 4°C for 90 days of storage (Fig. 33), during which time the coalescence and sedimentation of the droplets were retarded resulting in emulsion stabilization. When the PCM microphotograph (Fig. 34) is compared with the PCE microphotograph, the continuous fat phase of the PCM presents a fine particle network. Ghosh & Rousseau (2011) reported that the tablespreads such as butter and margarine showed emulsion stabilization by both Pickering and network crystals. The PCE and PCM microphotographs from this section showed a result similar to the work of Rousseau, Ghosh, & Park (2009), who showed the Pickering and network stabilization in table spreads. Time and temperature of storage also induced Ostwald ripening producing results in the larger crystal cluster formation, shown at long time storage (60 and 90 days). Moreover, new crystals appeared.

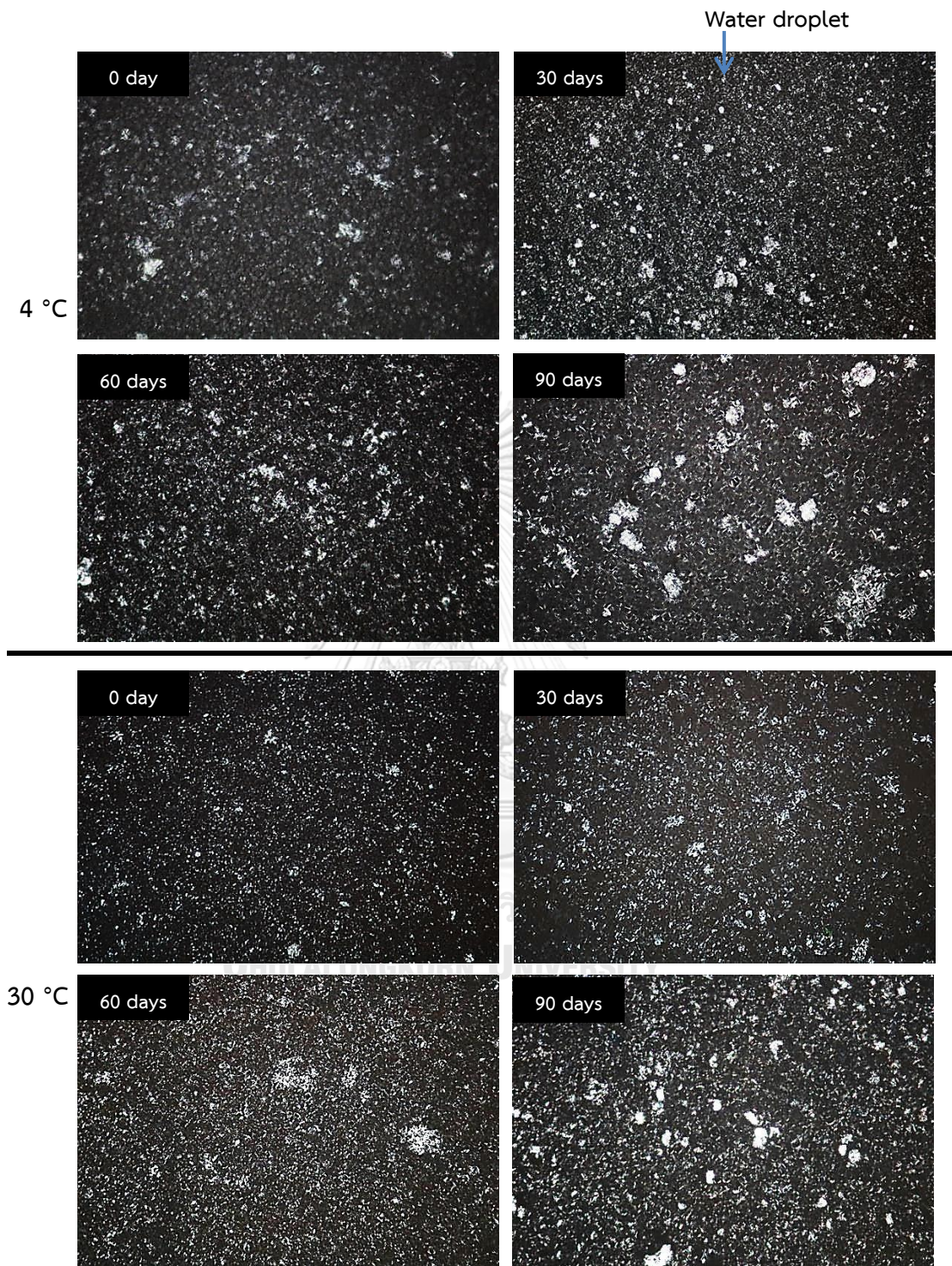


Figure 33 Polarized light microphotographs of PCE stored at 4°C and at 30°C for 0 day, 30 days, 60 days and 90 days at magnification 40x

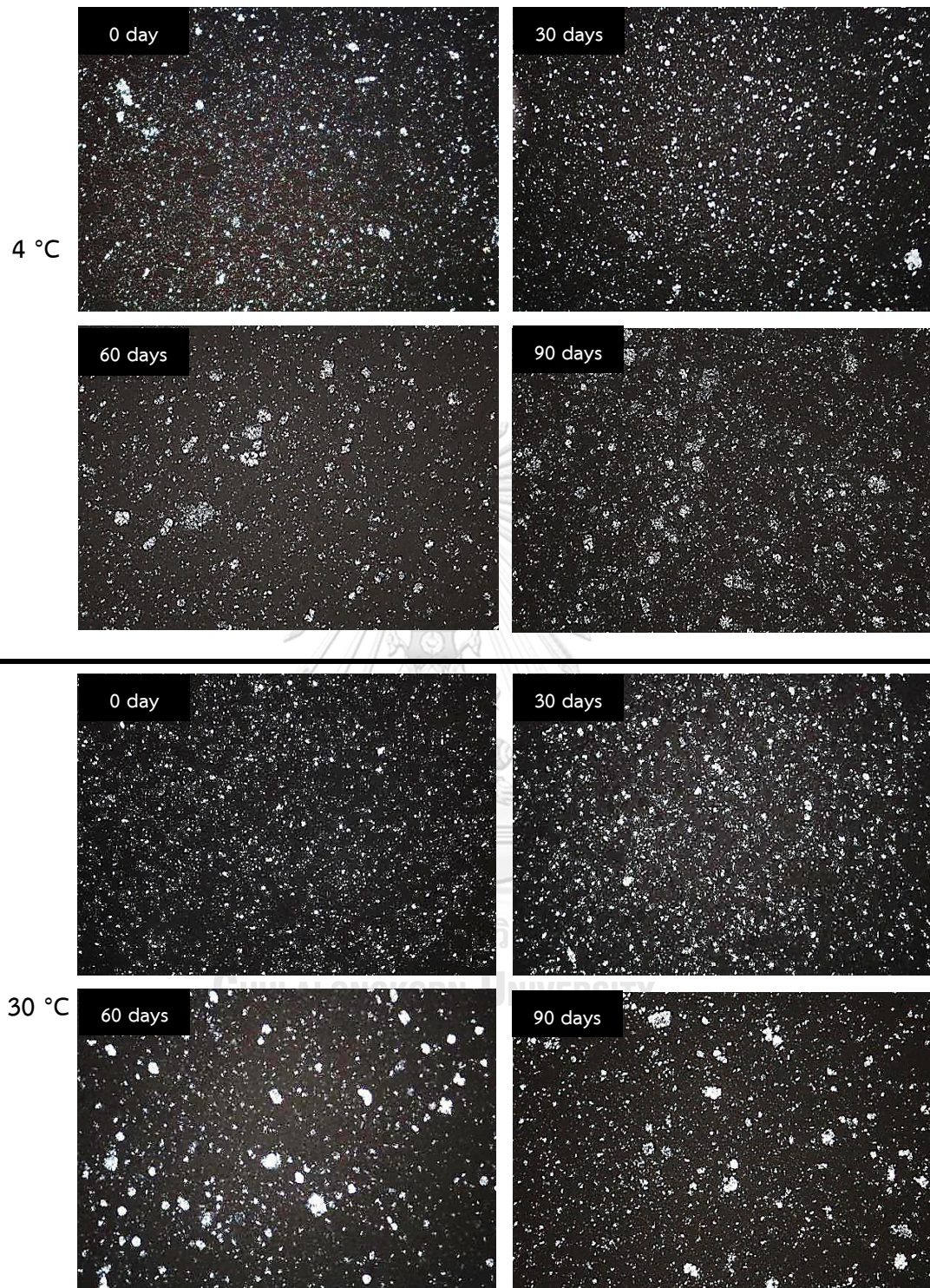


Figure 34 Polarized light microphotographs of PCM stored at 4°C and at 30°C for 0 day, 30 days, 60 days and 90 days at magnification 40x

Oxidative stability

The oxidative stability of the PCO, PCE and PCM samples stored at 4 and 30°C during 90 days of storage were monitored by PV and TBARS measurement. The results are shown in Fig. 35. Both storage temperatures of all samples showed the PV and TBARS increasing through the storage time. Among all samples, the highest PV (7.75 mEq/kg) was detected in PCO30C at 90 days of storage, and lowest PV (2.83 mEq/kg) was detected at PCM4C. The difference in composition like the organogels is an anhydrous system, but the emulsion contains water, and this situation causes differences in oxidative stability during storage (Yılmaz & Öğütçü, 2014a). The PV and TBARS of BRXO (Fig 22) showed higher values than PCO at both storage temperatures. For the emulsion, PCE and PCM showed higher values than EO. These results indicate that PCO stored at 4°C is stable in terms of oxidation, more than BRXO but less stable when stored at 30°C. However, the PCE and PCM show less oxidation stability than EO.

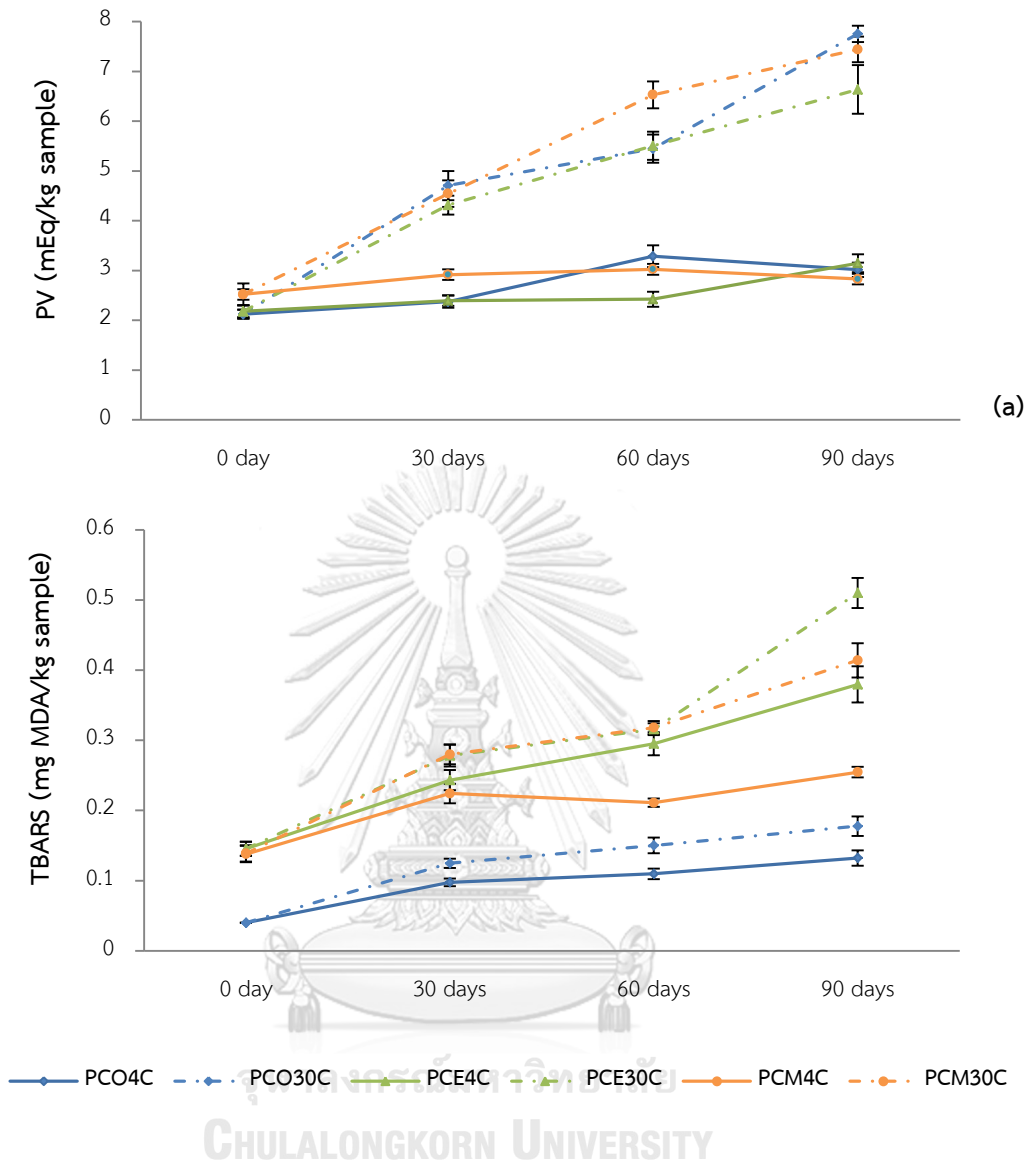


Figure 35 PV (a) and TBARS (b) reactive substances change of PCO, PCE and PCM stored at 4°C and 30°C for 90 days during storage time

CHAPTER V

CONCLUSIONS

The physicochemical properties of BRXOs and PCOs differed. The critical concentrations of BRX to form a gel were a minimum of 5 wt% wax concentration and 12 wt% PC. Regarding crystal morphology, BRX, PC, BRXO and EO had needle-like crystals, whereas PCO had dendrite-like crystals. The concentrations of the organogelator were correlated with the organogels' properties. At the highest organogelator concentration, organogels formed gels quickly and showed high oil-binding capacity and SFC as well as good textural properties and thermal behaviour, including with respect to crystallization temperature, melting temperature and enthalpy. BRX with a 9 wt% wax concentration and PC extracted at 15 wt% have potential as organogelators. BRXOs, PCOs and a mix of BRXOs and PCOs at a 50:50 ratio can be used in W/O emulsions produced without the addition of an emulsifier or a stabilizer. Emulsions prepared with organogels can be stabilized, and phase separation did not occur. PCE and PCM have greater firmness, hardness and stickiness than EO. All emulsions showed high crystallization and melting temperatures.

Storage time and storage temperature affected the quality of all organogels and emulsions, especially for storage at a high temperature (30°C) or for a long period. Greater changes in quality were observed for samples stored at 30°C than for those stored at 4°C for all properties except texture value, which was higher for samples stored at 4°C. Minimal changes in sample quality were observed for samples stored at 4°C for a short time. During storage, colour, texture, ESI, and oxidative stability changed less for organogels and emulsions prepared with organogels than for RO and E. BRXOs and EO had needle-like and fibrous morphology for all storage times, whereas the morphology of PCOs changed from dendrite-like to spherulite-like

formations when storage time increased. With respect to crystals, PCE and PCM showed a combination of Pickering and network crystals. Moreover, the effects of longer storage time included increased crystal volume, crystal sizes and crystal agglomerates of available crystalline materials, as was clearly observed when samples were stored at low temperatures.

The results of this study demonstrated that bleached rice bran wax and policosanol can be organogelators for organogels and emulsions. Moreover, these substances can increase the stability of oil-structured products and emulsion products.



REFERENCES

- Abdallah, D. J., & Weiss, R. G. (2000). Organogels and low molecular mass organic gelators. *Advance Materials*, 12(17), 1237-1247.
- Abramovic, H., & Abram, V. (2005). Physico-Chemical properties, composition and oxidative stability of camelina sativa oil. *Food Technology and Biotechnology*, 43(1), 63-70.
- Akoh, C. C., & Min, B. D. (2002). *Food lipids chemistry, nutrition & biotechnology*. New York: Marcel Dekker.
- American Oil Chemistry Society. (2012). Official methods and recommended practices.
- Aquilano, D., & Sgualdino, G. (2001). In K. Sato, & Garti, N. (Ed.), *Crystallization processes in fats and lipid systems*. New York: Marcel Dekker.
- Arumughan, C., Skhariya, R., & Arora, R. (2004). Rice bran oil: an untapped health food. *Inform*, 15, 706-707.
- Augusto, P. E. D., Soares, B. M. C., Chiu, M. C., & Gonçalves, L. A. G. (2012). Modelling the effect of temperature on the lipid solid fat content (SFC). *Food Research International Journal*, 45(1), 132-135.
- Australian Government. (2007). *Substances that may be used in listed medicines in Australia*.
- Azman, N. A. M., Gallego, M. G., Segovia, F., Abdullah, S., Shaarani, S. M., & Pablos, M. P. A. (2016). Study of the properties of bearberry leaf extract as a natural antioxidant in model foods. *Antioxidants*, 5-11.
- Bennett, H. (1963). *Industrial Waxes* (Vol. 1). New York: Chemical Publishing Company, Inc.
- Binks, B. P., & Rocher, A. (2009). Effects of temperature on water-in-oil emulsions stabilised solely by wax microparticles. *J Colloid Interface Sci*, 335(1), 94-104. doi:10.1016/j.jcis.2009.03.089
- Blake, A. I., Co, E. D., & Marangoni, A. G. (2014). Structure and physical properties of plant wax crystal networks and their relationship to oil binding capacity. *Journal of the American Oil Chemists' Society*, 91, 885-903.

- Bot, A., & Agterof, W. G. M. (2006). Structuring of edible oils by mixtures of γ -oryzanol with β -sitosterol or related phytosterols. *Journal of the American Oil Chemists' Society*, 83(6), 513-521. doi:10.1007/s11746-006-1234-7
- Botega, D. C. Z., Marangoni, A. G., Smith, A. K., & Goff, H. D. (2013). The potential application of rice bran wax oleogel to replace solid fat and enhance unsaturated fat content in ice cream. *Journal of Food Science*, 78, C1334-C1339.
- Buege, J., & Aust, S. (1978). Microsomal Lipid Peroxidation. *Methods Enzymology*, 52, 302-310.
- Campos, R. (2013). Experimental methodology In A. G. Marangoni, & Wesdorp, L. H., (Ed.), *Structure and properties of fat crystal networks second edition* (pp. 419-489): Academic Press and AOCS Press.
- Carbajal, D., Arruzazabala, M. L., Valdes, S., & Más, R. (1998). Effect of policosanol on platelet aggregation and serum levels of arachidonic acid metabolites in healthy volunteers. *Prostaglandins Leukotrienes and Essential Fatty Acids*, 58, 61-64.
- Carretti, E., Dei, L., & Weiss, R. G. (2005). Soft matter and art conservation. rheoreversible gels and beyond. *Soft Matter*, 1, 17-22.
- Chen, F., Cai, T., Zhao, G., Liao, X., Guo, L., & Hu, X. (2005). Optimizing conditions for the purification of crude octacosanol extract from rice bran wax by molecular distillation analyzed using response surface methodology. *Journal of Food Engineering*, 70, 47-53.
- Chiralt, A. (2010). Food emulsion. In G. V. Barbosa-Cánovas (Ed.), *Food Engineering - Volume II: Eolss*.
- Choudhary, P., Agrawal, S., Choukse, R., & Chaturvedi, P. (2013). A review of novel drug delivery system of pluronic lecithin organogel. *International Journal of Pharmaceutical Erudition*, 3(2), 65-80.
- Ciftci, O. N., Fadiloglu, S., & Gogus, F. (2009). Conversion of olive pomace oil to cocoabutter-like fat in a packedbed enzyme reactor. *Bioresource Technology*, 100, 324-329.
- Co, E. D., & Marangoni, A. G. (2012). Organogels: An alternative edible oil-structuring method. *Journal of the American Oil Chemists' Society*, 89, 749-780.

- Codex Alimentarius. (2001). *Codex standard for named vegetable oils CX-STAN 210-1999*. Rome: Secretariat of the Joint FAO/WHO Food Standards Programme, FAO.
- Coupland, J. N. (2002). Crystallization in emulsions. *Current Opinion in Colloid and Interface Science*, 7, 445-450.
- Cravotto, G., Binello, A., Merizzi, G., & Avogadro, M. (2004). Improving solvent-free extraction of policosanol from rice bran by high-intensity ultrasound treatment. *European Journal Lipid Science Technology*, 106, 147– 151.
- Da Pieve, S., Calligaris, S., Co, E., Nicoli, M. C., & Marangoni, A. G. (2010). Shear nanostructuring of monoglyceride organogels. *Food Biophysics*, 5, 211–217.
- Dalgleish, D. G. (1996). Food emulsions. In J. Sjöblom (Ed.), *Emulsions and emulsion stability*. New York: Marcel Dekker.
- Daniele, C., Botega, Z., Marangoni, A. G., Smith, A. K., & Goff, H. D. (2013). Oleogel to replace solid fat and enhance unsaturated fat content in ice cream. *Journal of Food Science*, 78, C1334- C1339.
- Das, R. K., Kandaneli, R., Linnanto, J., Bose, K., & Maitra, U. (2010). Supramolecular chirality in organogels: a detailed spectroscopic, morphological, and rheological investigation of gels (and xerogels) derived from alkyl pyrenyl urethanes. *Langmuir*, 26, 16141 –16149.
- Dassanayake, L. S. K., Kodali, D. R., & Ueno, S. (2011). Formation of oleogels based on edible lipid materials. *Current Opinion in Colloid & Interface Science*, 16(5), 432-439.
- Dassanayake, L. S. K., Kodali, D. R., Ueno, S., & Sato, K. (2009). Physical properties of rice bran wax in bulk and organogels. *Journal of the American Oil Chemists' Society*, 86, 1163-1173.
- Dassanayake, L. S. K., Kodali, D. R., Ueno, S., & Sato, K. (2012). Crystallization kinetics of organogels prepared by rice bran wax and vegetable oils. *Journal of Oleo Science*, 61(1), 1-9.
- deMan, J. M., & deMan, L. (2001). Polymorphism and Texture of Fats In R. H. N. Widlak, & S.S. Narine, (Ed.), *Crystallization and solidification properties of lipids*. (Vol.

225). Illinois: AOCS Press.

- Dickinson, E. (2010). Food emulsions and foams: Stabilization by particles. *Current Opinion in Colloid and Interface Science*, 15, 40-49.
- Doan, C. D., To, C. M., De Vrieze, M., Lynen, F., Danthine, S., Brown, A., . . . Patel, A. R. (2017). Chemical profiling of the major components in natural waxes to elucidate their role in liquid oil structuring. *Food Chemistry*, 214, 717 –725.
- Doan, C. D., Van de Walle, D., Dewettinck, K., & Patel, A. R. (2015). Evaluating the oilgelling properties of natural waxes in rice bran oil: Rheological, thermal, and microstructural study. *Journal of the American Oil Chemists' Society*, 92(6), 801 –811.
- Espositoa, C. L., Kirilovb, P., & Gaëlle Roullina, V. (2018). Organogels, promising drug delivery systems: an update of state-of-the-art and recent applications. *Journal of Controlled Release*, 271, 1–20.
- Finley, J. W., & Given, P. (1986). Technological necessity of antioxidants in the food industry. *Food and Chemical Toxicology*, 24, 999–1006.
- Gamble, W. R., Liu, Z., Bailey, D. T., Perez, P. P., Stull, D. P., Richheimer, S. L., . . . Lenoble, R. (2003).
- Gandolfo, F. G., Bot, A., & Flöter, E. (2004). Structuring edible oils by long-chain FA, fatty alcohols, and their mixtures. *Journal of the American Oil Chemists' Society*, 81, 1-6.
- Garg, T., Bilandi, A., Kapoor, B., Kumar, S., & Joshi, R. (2011). Organogels: advanced and novel drug delivery system. *International Research Journal of Pharmacy*, 2(12), 15-21.
- Ghosh, M., & Bandyopadhyay, S. (2005). Studies on the crystal growth of rice bran wax in a hexane medium. *Journal of the American Oil Chemists' Society*, 82, 229-231.
- Ghosh, S., & Rousseau, D. (2011). Fat crystals and water-in-oil emulsion stability. *Current Opinion in Colloid & Interface Science*, 16, 6589–6597.
- Ghosh, S., Tran, T., & Rousseau, D. (2011). Comparison of Pickering and network stabilization in water-in-oil emulsions. *Langmuir*, 27, 6589–6597.

- Global Agritech Inc. (2009). *Stabilization of long chain polyunsaturated oils*: U.S. Patent (PTC/US2008/071178).
- Gránásya, L., Jack, T. P., & Douglas, F. (2013). Insights into polymer crystallization from phase-field theory. *Encyclopedia of Polymers and Composites*, 1-35.
- Greyling, A., Witt, C. D., Oosthuizen, W., & Jerling, J. C. (2006). Effects of a policosanol supplement on serum lipid concentrations in hypercholesterolaemic and heterozygous familial hypercholesterolaemic subjects. *British Journal of Nutrition*, 95, 968–975.
- Gunawan, S., Vali, S. R., & Ju, Y. H. (2006). Purification and identification of rice bran oil fatty acid steryl and wax esters. *Journal of the American Oil Chemists' Society*, 83(5), 449-456.
- Gunstone, F. D. (2004). *The chemistry of oils and fats: sources, composition, properties and uses*. United Kingdom: Blackwell Publishing.
- Gunstone, F. D., Harwood, J. L., & Dijkstra, A. J. (2007). *The Lipid Handbook*. New York: Taylor & Francis Group.
- Hargrove, J. L., Greenspan, P., & Hartle, D. K. (2004). Nutritional significance and metabolism of very long chain fatty alcohols and acids from dietary waxes. *Experimental biology and medicine*, 229(215-226).
- Harrabi, S., Boukhchina, S., Mayer, P. M., & Kallel, H. (2009). Policosanol distribution and accumulation in developing corn kernels. *Food Chemistry*, 115(918–923).
- Himawan, C., Starov, V. M., & Stapley, A. G. F. (2006). Thermodynamic and kinetic aspects of fat crystallization. *Advances in Colloid and Interface Science*, 122, 3-33.
- Hodge, S. M., & Rousseau, D. (2003). Flocculation and coalescence in water-in-oil emulsions stabilized by paraffin wax crystals. *Food Research International*, 36, 695–702.
- Hodge, S. M., & Rousseau, D. (2005). Continuous-phase fat crystals strongly influence water-in-oil emulsion stability. *Journal of the American Oil Chemists' Society*, 82(3), 159-164.
- Hu, L., Zhang, Y., & Ramström, O. (2015). Gelation-driven dynamic systemic resolution:

- in situ generation and self-selection of an organogelator. *Scientific reports*, 5, 11065.
- Hu, Y. T., Ting, Y., Hu, J. Y., & Hsieh, S. C. (2017). Techniques and methods to study functional characteristics of emulsion systems. *Journal of Food and Drug Analysis*, 25(1), 16-26.
- Hughes, N. E., Marangoni, A. G., Wright, A. J., Rogers, M. A., & Rush, J. W. E. (2009). Potential food applications of edible oil oleogels. *Trends in Food Science & Technology*, 20, 470-480.
- Hwang, H. S., Kim, S., Singh, M., Winkler-Moser, J. K., & Liu, S. X. (2012). Organogel formation of soybean oil with waxes. *Journal of the American Oil Chemists' Society*, 89, 639-647.
- Hwang, H. S., Singh, M., Bakota, E. L., Moser, J. K. W., Kim, S., & Liu, S. X. (2013). Margarine from organogels of plant wax and soybean oil. *Journal of the American Oil Chemists' Society*, 90, 1705-1712.
- Hwang, H. S., Singh, M., & Lee, S. (2016). Properties of cookies made with natural wax-vegetable oil organogels. *Journal of Food Science*, 81(5), C1045-C1054.
- Hwang, H. S., Singh, M., Winkler-Moser, J. K., Bakota, E. L., & Liu, S. X. (2014). Preparation of margarines from organogels of sunflower wax and vegetable oils. *Journal of Food Science*, 79, C1926-C1932.
- Irmak, S., Dunford, N. T., & Milligan, J. (2006). Policosanol contents of beeswax, sugar cane and wheat extract. *Food Chemistry*, 95, 312-318.
- Ishaka, A., Imam, M. U., Mahamud, R., Zuki, A. B. Z., & Maznah, I. (2014). Characterization of rice bran wax policosanol and its nanoemulsion formulation. *International Journal of Nanomedicine*, 9, 2261-2269.
- Ito, S., Shzuki, T., & Fujino, Y. (1983). Wax lipid in rice bran. *Cereal Chemistry*, 60, 252-253.
- Jackson, M. A., & Eller, F. J. (2006). Isolation of long-chain aliphatic alcohols from beeswax using lipase-catalyzed methanolysis in supercritical carbon dioxide. *The Journal of Supercritical Fluids*, 37, 173-177.
- Jadhav, N. K., Patil, K. A., Patil, J. K., Patil, P. A., & Pawar, S. P. (2012). A review on organogels: Lipid based carrier systems. *Pharma science Monitor*, 3(4), 3132-

3143.

- Jang, A., Bae, W., Hwang, H. S., Lee, H. G., & Lee, S. (2015). Evaluation of canola oil oleogels with candelilla wax as an alternative to shortening in baked goods. *Food Chemistry*, 187, 525–529.
- Kalnin, D., Schafer, O., Amenitsch, H., & Ollivon, M. (2004). Fat crystallization in emulsion: influence of emulsifier concentration on triacylglycerol crystal growth and polymorphism. *Crystal Growth & Design*, 4(6), 1283 -1293.
- Kaushik, I., Jain, A., Grewal, R. B., Siddiqui, S., Gahlot, R., Rekha, & Anju. (2017). Organogelation: It's Food Application. *MOJ Food Processing & Technology*, 4(2), 66-72.
- Kim, J., & Godber, J. S. (2014). Comparison of rice bran oil and wax yields; a systematic approach to wax ester analysis. *International Journal of Food Science and Technology*, 49(2), 410-415.
- Kim, J. Y., Lee, J. H., Jeong, D. Y., Jang, D. K., Seo, T. R., & Lim, S. T. (2015). Preparation and characterization of aqueous dispersions of dextrin and policosanol composites. *Carbohydrate Polymers*, 121, 140–146.
- Kupongsak, S., & Sathitvorapojjana, S. (2017). Properties and Storage Stability of O/W Emulsion Replaced with Medium-Chain Fatty Acid Oil. *Polish Journal of Food and Nutrition Sciences*, 67(2), 107–115.
- Lepage, G., & Roy, C. C. (1986). Direct transesterification of all classes of lipids in a one-step reaction. *Journal of Lipid Research*, 27, 114–120.
- Liang, Z., Li, L., Xu, Z., & Li, B. (2014). *Influence of lipid composition, solid fat content and temperature on hardness of margarines*. Paper presented at the 3rd International Conference on Nutrition and Food Sciences.
- Lopez, C., Bourgaux, C., Lesieur, P., & Ollivon, M. (2007). Coupling of time-resolved synchrotron X-ray diffraction and DSC to elucidate the crystallisation properties and polymorphism of triglycerides in milk fat globules. *Dairy Science and Technology*, 87(4), 459-480.
- Lucas, A. d., Garcia, A., Alvarez, A., & Gracia, I. (2007). Supercritical extraction of long chain n-alcohols from sugar cane crude wax. *Journal of Supercritical Fluids*, 41(2), 267-271.

- Lupi, F. R., Gabriele, D., Baldino, N., Mijovic, P., Parisic, O. I., & Puocic, F. (2013). Olive oil/policosanol organogels for nutraceutical and drug delivery purposes. *Food and Function*, 4, 1512–1520.
- Lupi, F. R., Gabriele, D., & Cindio, B. (2011). Effect of shear rate on crystallization phenomena in olive oil-based organogels (Publication no. DOI : 10.1007/s11947-011-0619-2).
- Lupi, F. R., Gabriele, D., Greco, V., Baldino, N., Seta, L., & de Cindio, B. (2013). A rheological characterisation of an olive oil/fatty alcohols organogel. *Food Research International*, 51, 1512–1520.
- Lupi, F. R., Gabriele, D., Seta, L., Baldino, N., & Cindio, B. (2014). Rheological design of stabilized meat sauces for industrial uses. *European Journal of Lipid Science and Technology*, 116, 1734-1744.
- Madhavi, D. L., & Kagan, D. I. (2013). Water dispersible policosanol cyclodextrin complex and method of its production. *US8435967B2*.
- Marangoni, A. G. (2004). Crystallography. In A. G. Marangoni (Ed.), *Fat crystal networks* (pp. 1-13): Marcel Dekker.
- Marangoni, A. G., & Garti, N. (2011). An Overview of the Past, Present and Future of organogels. In A. G. Marangoni, & Garti, N., (Ed.), *Edible Oleogels: Structure and Health Implications* (pp. 1-18).
- Maru, A. D., Surawase, R. K., & Bodhe, P. V. (2012). Studies on physico-chemical properties of rice bran wax and its comparison with carnauba wax. *International Journal of Pharmaceutical and Phytopharmacological Research*, 4, 203-207.
- McClements, D. J. (2002). Theoretical prediction of emulsion colour. *Advances in Colloid and Interface Science*, 97, 63–89.
- McClements, D. J. (2005). *Food emulsion: principles, practices and techniques*. Boca Rata: CRC Press.
- Menendez, R., Fernandez, S. I., Del, R., A., Gonzalez, R. M., Fraga, V., Amor, A. M., & Mas, R. M. (1994). Policosanol inhibits cholesterol biosynthesis and enhances LDL processing in cultured human fibroblasts. *Biological Research*, 27, 199-203.
- Menendez, R., Mas, R., Amor, M. A., González, R. M., Fernández, J. C., Rodeiro, I., . . . Jiménez, S. (2005). Effects of policosanol treatment on the susceptibility of low

- density lipoprotein (LDL) isolated from healthy volunteers to oxidative modification in vitro. *British Journal of Clinical Pharmacology*, 50, 255-262.
- Mert, B., & Demirkesen, I. (2016). Evaluation of highly unsaturated oleogels as shortening replacer in a short dough product. *LWT - Food Science and Technology*, 68, 477-484.
- Metin, S., & Hartel, R. W. (2005). Crystallization of Fats and Oils. In F. S. A. E. Bailey (Ed.), *Bailey's industrial oil & fat products* (pp. 45-76): John Wiley & Sons.
- Mezouari, S., Kochhar, S. P., Schwarz, K., & Eichner, K. (2006). Effect of dewaxing pretreatment on composition and stability of rice bran oil: Potential antioxidant activity of wax fraction. *European Journal of Lipid Science and Technology*, 108, 679-686.
- Mirhosseini, H., Tan, C., Aghlara, A., Hamid, N., Yusof, S., & Chern, B. (2008). Influence of pectin and CMC on physical stability, turbidity loss rate, cloudiness and flavor release of orange beverage emulsion during storage. *Carbohydrate Polymers*, 73(1), 83-91.
- Mitre, F. M. A., Rueda, J. A. M., Alvarado, E. D., Alonso, M. A. C., & Vazquez, J. F. T. (2012). Shearing as a variable to engineer the rheology of candelilla wax organogels. *Food Research International*, 49, 580 – 587.
- Mujawar, N. K., Ghatage, S. L., & Yeligar, V. C. (2014). Organogel: factors and its importance. *International Journal of Pharmaceutical, Chemical and Biological Sciences*, 4(3), 758-773.
- Murdan, S. (2005). Organogels in drug delivery. *Expert Opinion Drug Delivery*, 2(3), 1-4.
- Nollet, L. M. L., & Toldra, F. (2011). *Handbook of Analysis of Edible Animal By-Products*. Gent, Belgium: CRC Pres.
- Öğütcü, M., Arifoğlu, N., & Yılmaz, E. (2015). Preparation and characterization of virgin olive oil-beeswax oleogel emulsion products. *Journal of the American Oil Chemists' Society*, 92(4), 459-471.
- Öğütcü, M., & Yılmaz, E. (2015a). Comparison of the pomegranate seed oil organogels of carnauba wax and monoglyceride. *Journal of Applied Polymer Science*. doi:10.1002/APP.41343.
- Öğütcü, M., & Yılmaz, E. (2015b). Characterization of hazelnut oil oleogels prepared with

- sunflower and carnauba waxes. *International Journal of Food Properties*, 18, 1741-1755.
- Ögütcü, M., & Yilmaza, E. (2014). Oleogels of virgin olive oil with carnauba wax and monoglyceride as spreadable products. *Grasas Y Aceites*, 65(3), 1-11.
- Ojijo, N. K., Kesselman, E., Shuster, V., Eichler, S., Eger, S., Neeman, I., & Shimoni, E. (2004). Changes in microstructural, thermal, and rheological properties of olive oil/ monoglyceride networks during storage. *Food Research International*, 37(4), 385 –393.
- Pandolsook, S., & Kupongsak, S. (2017). Influence of bleached rice bran wax on the physicochemical properties of organogels and water-in-oil emulsions. *Journal of Food Engineering*, 214, 182-192.
- Pandolsook, S., & Kupongsak, S. (2018). Storage stability of bleached rice bran wax organogels and water-in-oil. *Journal of Food Measurement and Characterization*. doi:10.1007/s11694-018-9957-3
- Pangloli, P., Melton, S. L., Collins, J. L., Penfield, M. P., & Saxton, A. M. (2002). Flavor and storage stability of potato chips fried in cottonseed and sunflower oils and palm olein/sunflower oil blends. *Journal of Food Science*, 67, 97-103.
- Parish, E. J., Boos, T. L., & Li, S. (2002). The chemistry of waxes and sterols. In C. C. Akoh, & Min, D.B. (Ed.), *Food lipids-Chemistry, nutrition, and biotechnology* (pp. 103-106): CRC Press.
- Patel, A. R., Rajarethinam, P. S., Grędowska, A., Turhan, O., Lesaffer, A., Vos, W. H. D., . . . Dewettinck, K. (2014). Edible applications of shellac oleogels: spreads, chocolate paste and cakes. *Food and Function*, 5, 645-652.
- Patel, A. R., Schattema, D., Vos, W. H. D., Lesaffer, A., & Dewettinck, K. (2013). Preparation and rheological characterization of shellac oleogels and oleogel-based emulsions. *Journal of Colloid and Interface Science*, 411, 114–121.
- Pernetti, M., van Malssen, K. E., Flöter, E., & Bot, A. (2007). Structuring edible oils by alternatives to crystalline fat. *Current Opinion in Colloid & Interface Science*, 84, 989-1000.
- Plamen, K., Khanh, L. C. A., Alice, D., Halima, R., Silvia, R., Carla, V., . . . Fabrice, P. (2015).

- Organogels for cosmetic and dermo-cosmetic applications – classification, preparation and characterization of organogel formulations - PART 1. *Household and Personal Care Today*, 10(3), 15-19.
- Popa, M., Glevitzky, I., Dumitrele, G. A., Glevitzky, M., & Popa, D. (2017). Study on peroxide values for different oils and factors affecting the quality of sunflower oil. *Scientific Papers. Series E. Land Reclamation, Earth Observation & Surveying, Environmental Engineering*, 6, 137-140.
- Puengtham, J., Aryasuk, K., Kittiratanapiboon, K., Jeyashoke, N., & Krisnangkura, K. (2008). Extraction Purification and Characterization of Policosanol from Thai Rice Bran Wax. *KMUTT Research and Development Journal*, 31(2), 305-317.
- Rendon, A., Rodriguez, M. D., Lopez, M., Garcia, H., Cajigas, A., Mas, R., & Fernandez, I. (1992). *Policosanol: a study of its genotoxicity and teratogenicity in rodents*. Paper presented at the Abstracts of 6th International Congress of Toxicology, Rome.
- Ribeiro, A. P. B., Masuchi, M. H., Miyasaki, E. K., Domingues, M. A. F., Stroppa, V. L. Z., de Oliveira, G. M., & Kieckbusch, T. G. (2015). Crystallization modifiers in lipid systems. *Journal of Food Science and Technology*, 52(7), 3925 - 3946.
- Rocha, J. C. B., Lopes, J. D., N., M. M. C., Arellano, D. B., Guerreiro, L. M. R., & Cunha, R. L. d. (2013). Thermal and rheological properties of organogels formed by sugarcane or candelilla wax in soybean oil. *Food Research International*, 50, 318–323.
- Rogers, M. A., Wright, A. J., & Marangoni, A. G. (2011). Ceramide organogels. In A. G. Marangoni, & Garti, N. (Ed.), *Edible Organogels: structure and health implications* (pp. 221-234): Academic Press and AOCS Press.
- Rousseau, D. (2000). Fat crystals and emulsion stability - a review. *Food Research International*, 33, 3-14.
- Rousseau, D., Ghosh, S., & Park, H. (2009). Comparison of the dispersed phase coalescence mechanisms in different tablespreads. *Journal of Food Science*, 74, E1 - E7.
- Rousseau, D., Khan, R. S., Zilnik, L., & Hodge, S. M. (2003). Dispersed phase destabilization in tablespreads. *Journal of the American Chemical Society*, 75,

1111–1118.

- Sahoo, S., Kumar, N., Bhattacharya, C., Sagiri, S. S., Jain, K., Pal, K., . . . Nayak, B. (2011). Organogels: Properties and applications in drug delivery. *Designed Monomers and Polymers*, 14, 95–108.
- Salunkhe, D. K., Chavan, J. K., Adsule, R. N., & Kadam, S. S. (1992). *Rice in world oilseeds: chemistry, technology and utilization*. New York: Van Nostrand Reinhold.
- Sato, K. (2001). Crystallization behaviour of fats and lipids: a review. *Chemical Engineering Science*, 56, 2255–2265.
- Saunders, R. M. (1985). Rice bran: composition and potential food sources. *Food Reviews International*, 1, 465–495.
- Schank, H. M., van Malssem, K. F., Morgado-Alves, S., Kalnin, D., & van der Linden, E. (2007). Crystal network for edible oil organogels: possibilities and limitations of the fatty acid and fatty alcohol system. *Food Research International*, 40, 1185–1193.
- Sonwai, S., Kaphueakngam, P., & Flood, A. (2012). Blending of mango kernel fat and palm oil mid-fraction to obtain cocoa butter equivalent. *Journal of Food Science and Technology*, 51(10), 2357–2369.
- Srisaipet, A., Yasamoot, D., & Somsri, S. (2016). Development of microwave energy to the fast extraction of policosanol from beeswax. *International Journal of Applied Chemistry*, 12(1), 39–44.
- Suzuki, M., & Hanabusa, K. (2010). Polymer organogelators that make supramolecular organogels through physical crosslinking and self-assembly. *Chemical Society Reviews*, 39(2), 455–463.
- Tada, A., Masuda, A., Sugimoto, N., Yamagata, K., Yamazaki, T., & Tanamoto, K. (2007). Analysis of constituents of ester type gum bases used as natural food additives. *Food Hygiene and Safety Science Journal*, 48, 179–185.
- Tadros, T. F. (2013). Emulsion formation, stability, and rheology. In T. F. Tadros (Ed.), *Emulsion formation and stability* (pp. 1–75): Wiley-VCH.
- Tambe, D. E., & Sharma, M. M. (1994). Factors controlling the stability of colloid-stabilized emulsions. II. A model for the rheological properties of colloid-laden

- interfaces. *Journal of Colloid and Interface Science*, 162, 1–10.
- Tavernier, I., Doan, C. D., de Wallea, D. V., Danthinec, S., Rimauxd, T., & Dewettincka, K. (2017). Sequential crystallization of high and low melting waxes to improve oil structuring in wax-based oleogels. *The Royal Society of Chemistry*, 7, 12113–12125.
- Terech, P., Pasquier, D., Bordas, V., & Rossat, C. (2000). Rheological properties and structural correlations in molecular organogels. *Langmuir*, 16, 4485-4494.
- Terech, P., & Weiss, R. G. (1997). Low molecular mass gelators of organic liquids and the properties of their gels. *Chemical Reviews*, 97(3133-3159).
- Tian, Y., & Acevedo, N. C. (2018). Kinetic study on photostability of retinyl palmitate entrapped in policosanol oleogels. *Food Chemistry*, 255, 252–259.
- Toro-Vazquez, J. F., Charó-Alonso, M. A., Pérez-Martínez, J. D., & Morales-Rueda, J. A. (2011). Candelilla wax as an organogelator for vegetable oils -an alternative to develop trans-free products for the food industry. In A. G. G. Marangoni, N. (Ed.), *Edible Organogels: Structure and Health Implications* (pp. 119-148): Academic Press and AOCS Press.
- Toro-Vazquez, J. F., Morales-Rueda, J. A., Dibildox-Alvarado, E., Charó-Alonso, M., Alonzo-Macias, M., & González-Chávez, M. M. (2007). Thermal and textural properties of organogels developed by candelilla wax in safflower oil. *Journal of the American Oil Chemists' Society*, 84(11), 989-1000.
- Toro-Vazquez, J. F., R., M.-P., onzález-Chávez, M. M., Sánchez-Becerril, M., Ornelas-Paz, J. J., & Pérez-Martínez, J. D. (2013). Physical properties of organogels and water in oil emulsions structured by mixtures of candelilla wax and monoglycerides. *Food Research*, 54, 1360–1368.
- U.S. Food and Drug Administration. (2016). Retrieved from <https://www.accessdata.fda.gov/scripts/cdrh/cfdocs/cfCFR/CFRSearch.cfm?fr=4172.890>
- Ushikubo, F. Y., & Cunha, R. L. (2014). Stability mechanisms of liquid water-in-oil emulsions. *Food Hydrocolloids*, 34, 145-153.
- Vali, S. R., Ju, Y.-H., Kaimal, T. N. B., & Chern, Y.-T. (2005). A process for the preparation of food-grade rice bran wax and the determination of its composition. *Journal*

of the American Oil Chemists' Society, 82, 57-64.

- Valoppi, F., Calligaris, S., & Marangoni, A. G. (2017). Structure and physical properties of oleogels containing peanut oil and saturated fatty alcohols. *European Journal of Lipid Science and Technology*, 119, 1600252.
- Varady, K. A., Wang, Y., & Jones, P. J. H. (2003). Role of policosanols in the prevention and treatment of cardiovascular disease. *Nutrition Reviews*, 61, 376-383.
- Vintiloiu, A., & Leroux, J. C. (2008). Organogels and their use in drug delivery - A review. *Journal of Controlled Release*, 125(3), 179-192.
- Walstra, P. (1987). In J. M. Blanshard, & Lillford, P. (Ed.), *Food structure and behaviour* (pp. 67-85). Orlando, florida: academic press.
- Walstra, P., Kloek, W., & van Vliet, T. (2001). *Crystallization processes in fats and lipid system*. New York: Marcel Dekker.
- Wang, M. F., Lian, H. Z., Mao, L., Zhou, J. P., Gong, H. J., Qian, B. Y., . . . L., J. (2007). Comparison of various extraction methods for policosanol from rice bran wax and establishment of chromatographic fingerprint of policosanol. *Journal of Agricultural and Food Chemistry*, 55, 5552-5558.
- Wang, T. (2002). Antioxidant activity of phytosterols, oryzanol, and other phytosterol conjugates. *Journal of the American Oil Chemists' Society*, 79(12), 1201-1206.
- Warth, A. H. (1956). *The chemistry and technology of waxes*. New York Reinhold Publishing Corporation.
- Wąsowicz, E., Gramza, A., Heś, M., Jeleń, H. H., Korczak, J., Malecka, M., . . . Zawirska-Wojtasiak, R. (2004). Oxidation of lipids in food. *Polish Journal of Food and Nutrition Sciences*, 13(54), 87-100.
- Weiss, R. G., & Terech, P. (2006). *Introduction: In Molecular gels materials with self-assembled fibrillar networks*. Netherlands: Springer.
- Yılmaz, E., & Öğütçü, M. (2014a). Comparative analysis of olive oil organogels containing beeswax and sunflower wax with breakfast margarine. *Journal of Food Science*, 79, E1732-E1738.
- Yılmaz, E., & Öğütçü, M. (2014b). Properties and stability of hazelnut oil organogels with beeswax and monoglyceride. *Journal of the American Oil Chemists' Society*, 91,

1007–1017.

Yilmaz, E., & Öğütçü, M. (2015). The texture, sensory properties and stability of cookies prepared with wax oleogels. *Food Functional*, 6, 1194-1204.

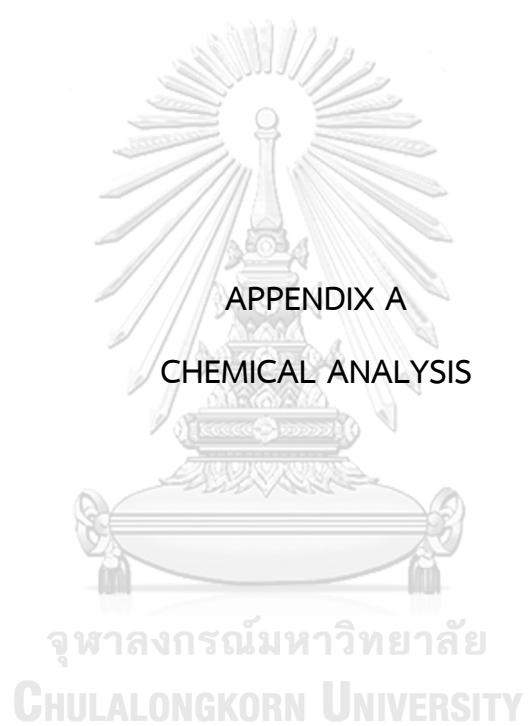
Zetzl, A. K., & Marangoni, A. G. (2011). Novel strategies for nanostructuring liquid oils into functional fats. In A. G. Marangoni, & Garti, N. (Ed.), *Edible Organogels: Structure and Health Implications* (pp. 19-47): Academic Press and AOCS Press.





APPENDICES

จุฬาลงกรณ์มหาวิทยาลัย
CHULALONGKORN UNIVERSITY



APPENDIX A1 Free fatty acids (FFA)

(AOCS Official Method Ca5a-40, 2012)

Reagents

1. Neutralized alcohol
2. 1% phenolphthalein indicator
3. 0.1 N NaOH

Procedure

1. Weigh approximately 7.05 g of sample into the 250 mL Erlenmeyer flask
2. Heat the sample at 80°C until sample melted
2. Add 50 mL of neutralized alcohol and 2 mL of 1% phenolphthalein indicator
3. Titrate it with 0.1 N NaOH until a pale pink is apparent
4. Record the volume of NaOH for titrate the sample and calculate with equation

$$\% \text{free fatty acid as oleic} = \frac{\text{mL of NaOH} \times N \times 28.2}{\text{g of weight sample}}$$

Note: N = NaOH concentrate

APPENDIX A2 Saponification number (SN)

(AOCS Official Method Cd 3-25, 2012)

Reagents

1. 0.5 N Alcoholic Potassium hydroxide (KOH)
2. 1% phenolphthalein indicator
3. 0.5 N Hydrochloric Acid (HCl)

Procedure

1. Weigh approximately 2 g of sample into the 500 mL round boil joint flasks
2. Add 40 mL of 0.5 N Alcoholic KOH
3. Reflux at 75-80°C for 2 hour
4. Titrate while hot sample with 0.5 N HCl and phenolphthalein indicator until a pale pink is apparent
5. Record the volume of HCl for titrate the sample and calculate with equation

$$\text{Saponification Value} = \frac{\text{mL of HCl for titrate blank} - \text{mL of HCl for titrate sample} \times 28.05}{\text{g of weight sample}}$$

APPENDIX A3 Iodine value (IV)

(AOCS Official Method Cd1-25, 2012)

Reagents

1. Cyclohexane - Acetic acid solution (1:1)
2. Wijs solution
3. 10% potassium iodide (KI)
4. 0.1 N sodium thiosulfate ($\text{Na}_2\text{S}_2\text{O}_3$)
5. 1% starch solution indicator

Procedure

1. Weigh approximately 1 g of sample into the 250 mL Erlenmeyer flask
2. Heat the sample at 80°C until sample melted
3. Add 15 mL of cyclohexane-acetic acid solution and swirl until the sample dissolved
4. Add 25 mL of Wijs solution and swirl, and then place in dark for 30 min
5. Add 10 mL of 10% KI and 100 mL distilled water and shake to mixed
6. Titrate it with 0.1 N $\text{Na}_2\text{S}_2\text{O}_3$ until a pale yellow is apparent then add 1 mL of starch solution indicator and titrate again until blue is disappear
7. Record the volume of $\text{Na}_2\text{S}_2\text{O}_3$ for titrate the sample and calculate with equation

$$\text{Iodine Value} = \frac{(B - S) \times N \times 12.69}{\text{g of weight sample}}$$

NoteB = mL of $\text{Na}_2\text{S}_2\text{O}_3$ for titrate blankS = mL of $\text{Na}_2\text{S}_2\text{O}_3$ for titrate sampleN = $\text{Na}_2\text{S}_2\text{O}_3$ concentrate

APPENDIX A4 peroxide value (PV)
(AOCS Official Method Cd 8-53, 2012)

Reagents

1. Acetic acid – Chloroform solution (1.5 : 1)
2. Saturated potassium iodide (KI)
3. 0.1 N Sodium thiosulfate ($\text{Na}_2\text{S}_2\text{O}_3$)
4. 1% starch solution indicator

Procedure

1. Weight 5.00 (± 0.05) g of sample into the 250 mL glass stoppered Erlenmeyer flask
2. Add 30 mL of acetic acid – chloroform solution and swirl the flask until the sample dissolved
3. Add 0.5 mL of Saturated KI solution and shake, and stopper the flask and swirl the mixture for 1 min
4. Add 30 mL of distilled water and shake
5. Add 1 mL of 4. 1% starch solution as indicator
6. Titrate it with 0.1 N $\text{Na}_2\text{S}_2\text{O}_3$ until the blue gray colour disappears
7. Record the volume of $\text{Na}_2\text{S}_2\text{O}_3$ for titrate the sample and calculate with equation

$$\text{Peroxide Value} = \frac{(S - B) \times N \times 1000}{\text{g of weight sample}}$$

- Note**
- S = mL of $\text{Na}_2\text{S}_2\text{O}_3$ for titrate sample
 - B = mL of $\text{Na}_2\text{S}_2\text{O}_3$ for titrate blank
 - N = $\text{Na}_2\text{S}_2\text{O}_3$ concentrate

APPENDIX A5 Thiobarbituric acid reactive substances value (TBARS)

(Modified from: Biege & Aust, 1978)

Reagents

TBARS solution (0.375% w/v of Thiobarbituric acid (TBA) and 15% w/v of Trichloroacetic Acid (TCA))

Procedure

1. Weight approximately 1 g of sample into the screw cap test tube
2. Add 10 mL of TBARS solution and vortex until mixed together
3. Boil the test tube sample for 10 min and then cool in cold water for 2 min
4. Centrifuge the sample at 5,500 rpm for 5 min
5. Bring clearly mixture to measure the absorbance at 532 nm and TBARS solution as a blank
6. Record the absorbance and calculate TBARS with equation

$$\text{TBARS value} = 2.77 \times \text{Abs. at 532}$$



Appendix B1 Colour of RO and BRXO during storage for 90 days at 4°C and 30°C

	0 days	30 days	60 days	90 days
L*				
RO4C	38.14 ^{bA} ± 0.21	37.60 ^{cBC} ± 0.03	37.69 ^{cB} ± 0.02	37.40 ^{cC} ± 0.24
RO30C	38.14 ^{bA} ± 0.21	33.15 ^{dB} ± 0.37	29.75 ^{dC} ± 0.20	25.26 ^{dD} ± 1.58
BRXO4C	46.33 ^{aAB} ± 0.53	46.56 ^{aA} ± 1.74	46.89 ^{aA} ± 0.21	45.17 ^{aB} ± 0.50
BRXO30C	46.33 ^{aA} ± 0.53	43.39 ^{bB} ± 1.44	42.39 ^{bB} ± 1.89	40.44 ^{bC} ± 0.28
a*				
RO4C	-0.73 ^{bD} ± 0.07	-0.47 ^{cC} ± 0.05	1.53 ^{aB} ± 0.03	2.10 ^{bA} ± 0.09
RO30C	-0.73 ^{bD} ± 0.07	-0.25 ^{bC} ± 0.03	0.79 ^{cB} ± 0.04	1.59 ^{cA} ± 0.03
BRXO4C	0.16 ^{aD} ± 0.02	0.62 ^{aC} ± 0.04	0.77 ^{cB} ± 0.06	2.21 ^{bA} ± 0.19
BRXO30C	0.16 ^{aD} ± 0.02	0.61 ^{aC} ± 0.05	1.11 ^{bB} ± 0.07	2.52 ^{aA} ± 0.18
b*				
RO4C	19.55 ^{bA} ± 0.03	13.17 ^{dB} ± 0.36	11.43 ^{dC} ± 0.13	10.39 ^{dD} ± 0.25
RO30C	19.55 ^{bA} ± 0.03	18.59 ^{aB} ± 0.25	17.67 ^{aC} ± 0.30	14.54 ^{aD} ± 0.28
BRXO4C	16.26 ^{aAB} ± 0.72	17.05 ^{bA} ± 0.18	15.93 ^{bB} ± 1.38	13.63 ^{bC} ± 0.39
BRXO30C	16.26 ^{aA} ± 0.72	15.74 ^{cA} ± 0.74	14.69 ^{cB} ± 0.89	12.32 ^{cC} ± 0.99

RO4C: Rice bran oils stored at 4 °C; RO30C: Rice bran oils stored at 30 °C; BRXO4C: Bleached rice bran wax organogels stored at 4 °C; and BRXO30C: Bleached rice bran wax organogels stored at 30 °C.

^{a,b,c,d} Different letters show significant differences within each column for each property ($p < 0.05$).

^{A,B,C,D} Different letters show significant differences within each row for each property ($p < 0.05$).

Appendix B2 Colour of E and EO during storage for 90 days at 4°C and 30°C

	0 days	30 days	60 days	90 days
L*				
E4C	54.52 ^{bA} ± 1.89	53.57 ^{bA} ± 1.92	49.46 ^{bB} ± 0.91	48.22 ^{bB} ± 0.97
E30C	54.52 ^{bA} ± 1.89	43.63 ^{cB} ± 0.61	33.62 ^{cC} ± 1.63	32.59 ^{cC} ± 0.44
EO4C	59.59 ^{aA} ± 0.53	59.80 ^{aA} ± 0.63	59.43 ^{aA} ± 0.25	59.47 ^{aA} ± 0.22
EO30C	59.59 ^{aAB} ± 0.53	59.63 ^{aAB} ± 0.87	58.89 ^{aB} ± 0.42	59.62 ^{aA} ± 0.36
a*				
E4C	-2.78 ^{bC} ± 0.07	-2.81 ^{dC} ± 0.08	-1.71 ^{dB} ± 0.04	-0.14 ^{dA} ± 0.01
E30C	-2.78 ^{bD} ± 0.07	-1.72 ^{cC} ± 0.03	0.11 ^{cB} ± 0.04	0.35 ^{cA} ± 0.02
EO4C	0.32 ^{aC} ± 0.01	0.36 ^{bC} ± 0.02	0.85 ^{bB} ± 0.03	3.30 ^{bA} ± 0.10
EO30C	0.32 ^{aD} ± 0.01	0.94 ^{aC} ± 0.06	1.57 ^{aB} ± 0.05	3.65 ^{aA} ± 0.12
b*				
E4C	8.35 ^{bB} ± 0.33	9.02 ^{bA} ± 0.52	7.21 ^{bC} ± 0.59	6.87 ^{cC} ± 0.41
E30C	8.35 ^{bA} ± 0.33	6.99 ^{cB} ± 0.41	2.29 ^{cC} ± 0.12	2.33 ^{dC} ± 0.11
EO4C	20.17 ^{aA} ± 0.07	20.24 ^{aA} ± 0.07	18.23 ^{aB} ± 0.03	16.74 ^{bC} ± 0.21
EO30C	20.17 ^{aA} ± 0.07	20.06 ^{aA} ± 0.09	18.52 ^{aB} ± 0.29	17.57 ^{aC} ± 0.35

E4C: Emulsion without BRXO addition stored at 4°C; E30C: Emulsion without BRXO addition stored at 30°C; EO4C: Emulsion prepared from BRXO and stored at 4°C and EO30C: Emulsion prepared from BRXO and stored at 30°C.

^{a,b,c,d} Different letters show significant differences within each column for each property ($p < 0.05$).

^{A,B,C,D} Different letters show significant differences within each row for each property ($p < 0.05$).

Appendix B3 Textural properties of BRXO during storage for 90 days at 4°C and 30°C

	0 days	30 days	60 days	90 days
Firmness (g)				
BRXO4C	175.77 ^{aC} ± 10.74	232.68 ^{aB} ± 14.18	259.58 ^{aA} ± 18.28	250.15 ^{aAB} ± 14.50
BRXO30C	54.75 ^{bB} ± 3.12	69.03 ^{bA} ± 2.26	67.56 ^{bA} ± 5.91	66.42 ^{bA} ± 5.31
Hardness (g.sec)				
BRXO4C	1384.36 ^{aC} ± 73.28	1765.13 ^{aB} ± 64.69	1756.63 ^{aB} ± 109.13	1926.71 ^{aA} ± 00.27
BRXO30C	368.90 ^{bB} ± 21.40	429.37 ^{bA} ± 13.55	428.60 ^{bA} ± 37.45	415.32 ^{bA} ± 36.12
Stickiness (g.sec)				
BRXO4C	-83.13 ^{bA} ± 3.37	-126.21 ^{bB} ± 9.75	-157.76 ^{bC} ± 8.44	-163.06 ^{bC} ± 13.24
BRXO30C	-18.60 ^{aA} ± 1.09	-22.04 ^{aB} ± 1.20	-22.54 ^{aB} ± 1.75	-22.83 ^{aB} ± 1.76

BRXO4C: Bleached rice bran wax organogels stored at 4°C; and BRXO30C: Bleached rice bran wax organogels stored at 30°C.

^{a,b,c,d} Different letters show significant differences within each column for each property ($p < 0.05$).

^{A,B,C,D} Different letters show significant differences within each row for each property ($p < 0.05$).

Appendix B4 Textural properties of EO during storage for 90 days at 4°C and 30°C

	0 days	30 days	60 days	90 days
Firmness (g)				
EO4C	74.87 ^{aC} ± 6.69	135.32 ^{aB} ± 18.79	181.47 ^{aA} ± 12.12	141.18 ^{aB} ± 21.11
EO30C	17.57 ^{bA} ± 0.86	10.87 ^{bC} ± 0.95	12.59 ^{bB} ± 1.12	10.02 ^{bC} ± 0.90
Hardness (g.sec)				
EO4C	517.73 ^{aC} ± 46.74	934.67 ^{aB} ± 36.53	1244.58 ^{aA} ± 91.63	937.53 ^{aB} ± 50.65
EO30C	93.08 ^{bA} ± 6.10	74.80 ^{bB} ± 5.53	87.26 ^{bA} ± 6.80	63.44 ^{bC} ± 3.56
Stickiness (g.sec)				
EO4C	-33.89 ^{bA} ± 3.58	-50.36 ^{bB} ± 4.02	-66.22 ^{bB} ± 4.41	-51.99 ^{bC} ± 3.36
EO30C	-12.46 ^{aC} ± 1.62	-6.34 ^{aAB} ± 0.36	-7.34 ^{aB} ± 0.50	-6.07 ^{aA} ± 0.68

EO4C: Emulsion prepared from BRXO and stored at 4°C and EO30C: Emulsion prepared from BRXO and stored at 30°C.

^{a,b,c,d} Different letters show significant differences within each column for each property ($p < 0.05$).

^{A,B,C,D} Different letters show significant differences within each row for each property ($p < 0.05$).

Appendix B5 PV and TBARS of RO and BRXO during storage for 90 days at 4°C and 30°C

	0 days	30 days	60 days	90 days
PV (mEq/kg of sample)				
RO4C	1.99 ^{bc} ± 0.07	5.49 ^{dB} ± 0.47	7.22 ^{dB} ± 0.58	1.17 ^{CA} ± 0.11
RO30C	1.99 ^{bc} ± 0.07	6.08 ^{bc} ± 0.07	7.88 ^{bb} ± 0.55	1.55 ^{BA} ± 0.10
BRXO4C	3.82 ^{ab} ± 0.14	4.21 ^{CA} ± 0.36	4.38 ^{CA} ± 0.33	0.44 ^{CA} ± 0.04
BRXO30C	3.82 ^{ab} ± 0.14	4.95 ^{ac} ± 0.50	5.88 ^{ab} ± 0.43	0.62 ^{AA} ± 0.05
TBARS (mg MDA/kg of sample)				
RO4C	0.16 ^{aD} ± 0.01	0.42 ^{aC} ± 0.02	0.46 ^{ab} ± 0.04	0.56 ^{AA} ± 0.02
RO30C	0.16 ^{aC} ± 0.01	0.24 ^{bb} ± 0.02	0.25 ^{bb} ± 0.01	0.44 ^{BA} ± 0.04
BRXO 4C	0.13 ^{bd} ± 0.00	0.15 ^{CC} ± 0.01	0.16 ^{cb} ± 0.01	0.28 ^{CA} ± 0.01
BRXO30C	0.13 ^{bc} ± 0.00	0.13 ^{dc} ± 0.01	0.15 ^{cb} ± 0.00	0.20 ^{dA} ± 0.02

RO4C: Rice bran oils stored at 4°C; RO30C: Rice bran oils stored at 30°C; BRXO4C: Bleached rice bran wax organogels stored at 4°C; and BRXO30C: Bleached rice bran wax organogels stored at 30°C.

^{a,b,c,d} Different letters show significant differences within each column for each property ($p < 0.05$).

^{A,B,C,D} Different letters show significant differences within each row for each property ($p < 0.05$).

Appendix B6 PV and TBARS of E and EO during storage for 90 days at 4°C and 30°C

	0 days	30 days	60 days	90 days
PV (mEq/kg of sample)				
E4C	0.99 ^{aD} ± 0.04	2.80 ^{bB} ± 0.12	3.06 ^{bA} ± 0.24	1.25 ^{bC} ± 0.10
E30C	0.99 ^{aD} ± 0.04	5.89 ^{aA} ± 0.24	5.27 ^{aB} ± 0.46	2.29 ^{aC} ± 0.21
EO 4C	0.96 ^{aC} ± 0.02	1.02 ^{dB} ± 0.01	1.09 ^{cA} ± 0.06	0.22 ^{dD} ± 0.08
EO30C	0.96 ^{aC} ± 0.02	1.99 ^{cA} ± 0.09	1.22 ^{cB} ± 0.07	0.40 ^{cD} ± 0.06
TBARS (mg MDA/kg of sample)				
E4C	0.11 ^{cD} ± 0.01	0.22 ^{bC} ± 0.02	0.37 ^{bB} ± 0.01	0.80 ^{aA} ± 0.01
E30C	0.12 ^{bD} ± 0.00	0.34 ^{aC} ± 0.00	0.56 ^{aB} ± 0.03	0.83 ^{aA} ± 0.01
EO 4C	0.13 ^{aB} ± 0.01	0.15 ^{dB} ± 0.01	0.17 ^{dB} ± 0.01	0.29 ^{cA} ± 0.01
EO30C	0.12 ^{bD} ± 0.00	0.19 ^{cC} ± 0.01	0.23 ^{cB} ± 0.01	0.39 ^{bA} ± 0.02

E4C: Emulsion without BRXO addition stored at 4°C; E30C: Emulsion without BRXO addition stored at 30°C; EO4C: Emulsion prepared from BRXO and stored at 4°C and EO30C: Emulsion prepared from BRXO and stored at 30°C.

^{a,b,c,d} Different letters show significant differences within each column for each property ($p < 0.05$).

^{A,B,C,D} Different letters show significant differences within each row for each property ($p < 0.05$).

Appendix B7 Colour of PCO during storage for 90 days at 4°C and 30°C

	0 days	30 days	60 days	90 days
L*				
PCO4C	56.67 ^{aA} ± 0.50	55.79 ^{aAB} ± 3.23	54.69 ^{aB} ± 0.04	51.82 ^{aC} ± 0.62
PCO30C	56.87 ^{aA} ± 0.50	53.48 ^{aB} ± 2.66	54.77 ^{aB} ± 0.20	49.79 ^{bC} ± 0.58
a*				
PCO4C	-1.88 ^{aD} ± 0.11	-1.81 ^{aC} ± 0.04	1.71 ^{bB} ± 0.03	1.50 ^{bA} ± 0.04
PCO30C	-1.88 ^{aD} ± 0.11	-1.76 ^{aC} ± 0.09	1.51 ^{aB} ± 0.05	1.19 ^{aA} ± 0.05
b*				
PCO4C	18.95 ^{aC} ± 0.91	18.53 ^{aBC} ± 0.89	19.65 ^{aAB} ± 0.77	19.94 ^{aA} ± 0.22
PCO30C	18.95 ^{aB} ± 0.91	18.35 ^{aB} ± 0.90	20.04 ^{aA} ± 0.97	20.06 ^{aA} ± 0.17

PCO4C: Policosanol organogels stored at 4°C and PCO30C: Policosanol organogels stored at 30°C.

^{a,b,c,d} Different letters show significant differences within each column for each property ($p < 0.05$).

^{A,B,C,D} Different letters show significant differences within each row for each property ($p < 0.05$).

Appendix B8 Colour of PCE and PCM during storage for 90 days at 4°C and 30°C

	0 days	30 days	60 days	90 days
L*				
PCE4C	77.58 ^{aA} ± 0.04	76.87 ^{aB} ± 1.16	77.10 ^{aAB} ± 0.03	75.23 ^{bC} ± 0.06
PCE30C	77.58 ^{aA} ± 0.04	75.93 ^{bB} ± 0.23	72.47 ^{dC} ± 0.57	70.47 ^{dD} ± 0.29
PCM4C	77.25 ^{aA} ± 0.19	75.67 ^{bcC} ± 0.06	75.71 ^{cC} ± 0.11	76.66 ^{aB} ± 0.03
PCM30C	77.25 ^{aA} ± 0.19	75.24 ^{cc} ± 0.31	76.62 ^{bB} ± 0.08	76.49 ^{aB} ± 0.16
a*				
PCE4C	-0.87 ^{aB} ± 0.01	-0.85 ^{cA} ± 0.02	-0.98 ^{cc} ± 0.03	-1.15 ^{dD} ± 0.01
PCE30C	-0.87 ^{aA} ± 0.01	-0.99 ^{aB} ± 0.03	-1.14 ^{dC} ± 0.03	-1.26 ^{dD} ± 0.09
PCM4C	-0.43 ^{bA} ± 0.01	-0.47 ^{bB} ± 0.02	-0.60 ^{bC} ± 0.01	-0.66 ^{bD} ± 0.02
PCM30C	-0.43 ^{bA} ± 0.01	-0.47 ^{bB} ± 0.03	-0.56 ^{aC} ± 0.01	-0.58 ^{aD} ± 0.02
b*				
PCE4C	12.42 ^{bC} ± 0.09	13.49 ^{aB} ± 0.78	13.58 ^{cB} ± 0.01	16.10 ^{aA} ± 0.04
PCE30C	12.42 ^{bC} ± 0.09	12.98 ^{bB} ± 0.59	13.75 ^{dA} ± 0.04	13.51 ^{dA} ± 0.41
PCM4C	12.86 ^{aC} ± 0.05	15.56 ^{aB} ± 0.26	13.45 ^{bB} ± 0.01	13.94 ^{cA} ± 0.01
PCM30C	12.86 ^{aD} ± 0.05	13.51 ^{aB} ± 0.33	13.09 ^{aC} ± 0.02	14.15 ^{bA} ± 0.04

PCE4C: Emulsion prepared from PCO and stored at 4°C and PCE30C: Emulsion prepared from PCO and stored at 30°C. PCM4C: Emulsion prepared from PCO mixed BRXO stored at 4°C and PCM30C: Emulsion prepared from PCO mixed BRXO stored at 30°C.

^{a,b,c,d} Different letters show significant differences within each column for each property ($p < 0.05$).

^{A,B,C,D} Different letters show significant differences within each row for each property ($p < 0.05$).

Appendix B9 Textural properties of PCO during storage for 90 days at 4°C and 30°C

	0 days	30 days	60 days	90 days
Firmness (g)				
PCO4C	63.41 ^{aD} ± 3.70	88.03 ^{aC} ± 5.19	119.30 ^{aB} ± 7.13	139.96 ^{aA} ± 7.01
PCO30C	63.41 ^{aB} ± 3.70	67.04 ^{bB} ± 3.67	68.75 ^{bB} ± 5.13	80.51 ^{bA} ± 7.72
Hardness (g.sec)				
PCO4C	405.64 ^{aD} ± 31.22	638.61 ^{aC} ± 30.18	774.10 ^{aB} ± 35.89	964.59 ^{aA} ± 68.74
PCO30C	405.64 ^{aC} ± 31.22	453.10 ^{bB} ± 31.78	477.45 ^{bAB} ± 17.08	492.29 ^{bD} ± 17.62
Stickiness (g.sec)				
PCO4C	-42.38 ^{aD} ± 2.97	-52.94 ^{aC} ± 5.15	-65.66 ^{aB} ± 5.00	-80.52 ^{aA} ± 6.94
PCO30C	-42.38 ^{aA} ± 2.97	-49.16 ^{aB} ± 3.57	-57.28 ^{bC} ± 4.11	-62.85 ^{bD} ± 5.09

PCO4C: Policosanol organogels stored at 4°C and PCO30C: Policosanol organogels stored at 30°C.

^{a,b,c,d} Different letters show significant differences within each column for each property ($p < 0.05$).

^{A,B,C,D} Different letters show significant differences within each row for each property ($p < 0.05$).

Appendix B10 Textural properties of PCE and PCM during storage for 90 days at 4°C and 30°C

	0 days	30 days	60 days	90 days
Firmness (g)				
PCE4C	327.25 ^{aD} ± 17.71	483.94 ^{aC} ± 39.47	523.13 ^{abB} ± 21.58	630.00 ^{aA} ± 30.59
PCE30C	327.25 ^{aD} ± 17.71	429.15 ^{bC} ± 19.90	464.46 ^{bB} ± 16.21	504.43 ^{bA} ± 39.72
PCM4C	340.94 ^{aD} ± 25.55	475.93 ^{aC} ± 24.63	548.95 ^{abB} ± 32.13	662.20 ^{aA} ± 42.02
PCM30C	340.94 ^{aD} ± 25.55	356.18 ^{bC} ± 22.13	499.64 ^{bCA} ± 43.12	522.49 ^{bA} ± 48.58
Hardness (g.sec)				
PCE4C	2065.79 ^{aD} ± 85.72	2535.73 ^{aC} ± 183.93	2975.33 ^{abB} ± 199.69	3619.65 ^{aA} ± 132.80
PCE30C	2065.79 ^{aC} ± 85.72	2261.76 ^{bB} ± 92.32	2743.11 ^{dA} ± 146.45	2850.10 ^{dA} ± 126.84
PCM4C	1659.38 ^{bD} ± 104.14	2015.15 ^{cC} ± 152.03	2792.38 ^{bB} ± 131.11	3334.75 ^{bA} ± 184.84
PCM30C	1659.38 ^{bC} ± 104.14	1737.71 ^{dC} ± 132.47	2099.40 ^{bB} ± 142.64	2390.35 ^{cA} ± 198.03
Stickiness (g.sec)				
PCE4C	-146.83 ^{bA} ± 5.14	-190.58 ^{bB} ± 11.55	-240.89 ^{cC} ± 11.09	-272.36 ^{dD} ± 32.96
PCE30C	-146.83 ^{bA} ± 5.14	-144.46 ^{bA} ± 7.00	-163.44 ^{bB} ± 12.27	-181.31 ^{abC} ± 17.07
PCM4C	-107.01 ^{aA} ± 7.95	-140.74 ^{bA} ± 12.54	-159.24 ^{bC} ± 7.04	-198.58 ^{bD} ± 12.62
PCM30C	-107.01 ^{aA} ± 7.95	-118.35 ^{abB} ± 7.86	-148.65 ^{aC} ± 8.49	-174.78 ^{aD} ± 13.28

PCE4C: Emulsion prepared from PCO and stored at 4°C and PCE30C: Emulsion prepared from PCO and stored at 30°C. PCM4C: Emulsion prepared from PCO mixed BRXO stored at 4°C and PCM30C: Emulsion prepared from PCO mixed BRXO stored at 30°C.

^{a,b,c,d} Different letters show significant differences within each column for each property ($p < 0.05$).

^{A,B,C,D} Different letters show significant differences within each row for each property ($p < 0.05$).

Appendix B11 PV and TBARS of PCO during storage for 90 days at 4°C and 30°C

	0 days	30 days	60 days	90 days
PV (mEq/kg of sample)				
PCO4C	2.12 ^{aD} ± 0.09	2.37 ^{bC} ± 0.12	3.29 ^{bA} ± 0.22	3.01 ^{bB} ± 0.14
PCO30C	2.12 ^{aD} ± 0.09	4.71 ^{aC} ± 0.29	5.44 ^{aB} ± 0.28	7.75 ^{aA} ± 0.17
TBARS (mg MDA/kg of sample)				
PCO4C	0.04 ^{aD} ± 0.00	0.09 ^{bC} ± 0.00	0.11 ^{bB} ± 0.01	0.13 ^{bA} ± 0.01
PCO30C	0.04 ^{aD} ± 0.00	0.12 ^{aC} ± 0.01	0.15 ^{aB} ± 0.01	0.18 ^{aA} ± 0.01

PCO4C: Policosanol organogels stored at 4 C and PCO30C: Policosanol organogels stored at 30 C.

^{a,b,c,d} Different letters show significant differences within each column for each property ($p < 0.05$).

^{A,B,C,D} Different letters show significant differences within each row for each property ($p < 0.05$).



Appendix B12 PV and TBARS of PCE and PCM during storage for 90 days at 4°C and 30°C

	0 days	30 days	60 days	90 days
PV (mEq/kg of sample)				
PCE4C	2.18 ^{bc} ± 0.12	2.39 ^{db} ± 0.11	2.42 ^{db} ± 0.15	3.15 ^{ca} ± 0.18
PCE30C	2.18 ^{bd} ± 0.12	4.31 ^{bc} ± 0.19	5.50 ^{bb} ± 0.28	6.64 ^{ba} ± 0.49
PCM4C	2.52 ^{ab} ± 0.22	2.92 ^{ca} ± 0.20	3.02 ^{ca} ± 0.25	2.83 ^{ca} ± 0.14
PCM30C	2.52 ^{ad} ± 0.22	4.54 ^{ac} ± 0.27	6.53 ^{ab} ± 0.27	7.44 ^{aa} ± 0.26
TBARS (mg MDA/kg of sample)				
PCE4C	0.15 ^{ad} ± 0.01	0.24 ^{bc} ± 0.01	0.30 ^{bb} ± 0.02	0.38 ^{ca} ± 0.03
PCE30C	0.15 ^{ad} ± 0.01	0.28 ^{ac} ± 0.02	0.32 ^{ab} ± 0.01	0.51 ^{aa} ± 0.02
PCM4C	0.14 ^{ad} ± 0.01	0.22 ^{cb} ± 0.01	0.21 ^{cb} ± 0.01	0.25 ^{da} ± 0.01
PCM30C	0.14 ^{ad} ± 0.01	0.28 ^{ac} ± 0.01	0.32 ^{ab} ± 0.01	0.41 ^{ba} ± 0.02

PCE4C: Emulsion prepared from PCO and stored at 4°C and PCE30C: Emulsion prepared from PCO and stored at 30°C. PCM4C: Emulsion prepared from PCO mixed BRXO stored at 4°C and PCM30C: Emulsion prepared from PCO mixed BRXO stored at 30°C.

^{a,b,c,d} Different letters show significant differences within each column for each property ($p < 0.05$).

^{A,B,C,D} Different letters show significant differences within each row for each property ($p < 0.05$).

VITA

NAME Miss Sawanya Pandolsook

DATE OF BIRTH 21 March 1983

PLACE OF BIRTH Bangkok, Thailand

INSTITUTIONS ATTENDED 2005: Bachelor of Science degree in Food Technology, School of Agricultural Technology, Walailak University.
2007: Master of Science degree in Food Science, Agro-Industry Faculty, King Mongkut's Institute of Technology Ladkrabang (KMITL).

PUBLICATION Pandolsook, S., & Kupongsak, S. (2017). Influence of bleached rice bran wax on the physicochemical properties of organogels and water-in-oil emulsions. *Journal of Food Engineering*, 214, 182-192.
Pandolsook, S., & Kupongsak, S. (2018). Storage stability of bleached rice bran wax organogels and water-in-oil emulsions. *Journal of Food Measurement and Characterization*. DOI : 10.1007/s11694-018-9957-3.